NAVAL POSTGRADUATE SCHOOL

Monterey, California

THESIS

PRESSURE MEASUREMENTS ON A PROPOSED
OPTICAL WINDOW FAIRING FOR THE ALTUS II
UNMANNED AIR VEHICLE

by

Scott C. Ferris

September 1999

Thesis Advisor: Richard M. Howard

Approved for public release; distribution is unlimited.

19991222 068

REPORT DOCUMENTATION PAGE		Form Approved OMB No. 0704-0188
1. AGENCY USE ONLY *(Leave blank)*	**2. REPORT DATE** September 1999	**3. REPORT TYPE AND DATES COVERED** Master's Thesis
4. TITLE AND SUBTITLE PRESSURE MEASUREMENTS ON A PROPOSED OPTICAL WINDOW FAIRING FOR THE ALTUS II UNMANNED AIR VEHICLE		**5. FUNDING NUMBERS**
6. AUTHOR(S) Ferris, Scott C.		
7. PERFORMING ORGANIZATION NAME(S) AND ADDRESS(ES) Naval Postgraduate School Monterey, CA 93943-5000		**8. PERFORMING ORGANIZATION REPORT NUMBER**
9. SPONSORING / MONITORING AGENCY NAME(S) AND ADDRESS(ES) Sandia National Laboritories Livermore, CA		**10. SPONSORING/MONITORING AGENCY REPORT NUMBER**
11. SUPPLEMENTARY NOTES The views expressed in this thesis are those of the author and do not reflect the official policy or position of the Department of Defense or the U.S. Government.		
12a. DISTRIBUTION / AVAILABILITY STATEMENT Approved for public release; distribution is unlimited.		**12b. DISTRIBUTION CODE**

13. ABSTRACT

Low-speed wind tunnel tests were conducted to determine surface pressure measurements on a proposed aerodynamic fairing for the Altus II UAV. These tests were conducted at various angle-of-attack and sideslip positions to determine the effect on the surface pressures for the optical window portion of the fairing. Of particular interests were the pressure contour field located over the optical window region and the total force exerted on this area. Scaled-up loads (lbf) as calculated on the window ran from 1.0 to 1.6 times the freestream dynamic pressure (psf). Pressure measurements were also taken on the upper fuselage of the Altus II UAV model to determine the location of the peak suction area. These measurements provided the data to optimize the placement of external vents on the full-scale version of the airframe.

14. SUBJECT TERMS Altus II UAV, Ultra-Violet Telescope, Fairing			**15. NUMBER OF PAGES** 85
			16. PRICE CODE
17. SECURITY CLASSIFICATION OF REPORT Unclassified	**1. SECURITY CLASSIFICATION OF THIS PAGE** Unclassified	**19. SECURITY CLASSIFICATION OF ABSTRACT** Unclassified	**20. LIMITATION OF ABSTRACT** UL

NSN 7540-01-280-5500

Standard Form 298 (Rev. 2-89)
Prescribed by ANSI Std 239-18

i

PRESSURE MEASUREMENTS ON A PROPOSED OPTICAL WINDOW FAIRING FOR THE ALTUS II UNMANNED AIR VEHICLE

Scott C. Ferris
Lieutenant Commander, United States Navy
B.S., University of Missouri – Rolla, 1987

Submitted in partial fulfillment of the
requirements for the degree of

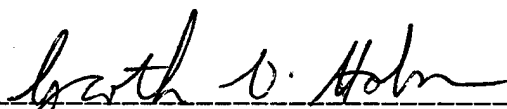**MASTER OF SCIENCE IN AERONAUTICAL ENGINEERING**

from the

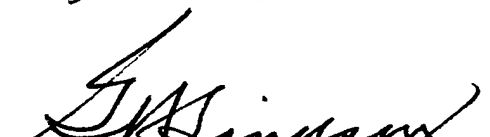**NAVAL POSTGRADUATE SCHOOL**
September 1999

Author: _____
/Scott C. Ferris

Approved by: _____
Richard M. Howard, Thesis Advisor

_____
Garth V. Hobson, Second Reader

_____
Gerald H. Lindsey, Chairman
Department of Aeronautics and Astronautics

ABSTRACT

Low-speed wind tunnel tests were conducted to determine surface pressure measurements on a proposed aerodynamic fairing for the Altus II UAV. These tests were conducted at various angle-of-attack and sideslip positions to determine the effect on the surface pressures for the optical window portion of the fairing. Of particular interests were the pressure contour field located over the optical window region and the total force exerted on this area. Scaled-up loads (lbf) as calculated on the window ran from 1.0 to 1.6 times the freestream dynamic pressure (psf). Pressure measurements were also taken on the upper fuselage of the Altus II UAV model to determine the location of the peak suction area. These measurements provided the data to optimize the placement of external vents on the full-scale version of the airframe.

TABLE OF CONTENTS

LIST OF FIGURES

LIST OF TABLES

LIST OF SYMBOLS, ACRONYMS AND ABBREVIATIONS

AOA	Angle of Attack
cm	Centimeters
C_p	Coefficient of Pressure
GPIB	General Purpose Interface Bus
KTAS	Knots True Airspeed
ℓ	Reynolds Number Reference Length
lbf	Pound - Force
p	Local Static Pressure
p_∞	Freestream Static Pressure
psf	Pounds/Foot^2
psid	pound/inch^2 differential
$q_\infty = \frac{1}{2}\rho V^2$	Freestream Dynamic Pressure
Q-bar	Average Dynamic Pressure
NI	National Instruments
NPS	Naval Postgraduate School
Re	Reynolds Number
Sandia	Sandia National Laboratories
VEG	Valley Engineering Group
VI	Virtual Instrument (*Labview* Software Program)
α	Angle of Attack
β	Sideslip Angle
ΔP	Pressure Difference between Static Ring and Kiel Probe
ρ	Air Density
μ	Air Molecular Viscosity
ν	Air Kinematic Viscosity

ACKNOWLEDGEMENTS

I wish to extend my sincere appreciation to the following individuals for their assistance in making this thesis work possible:

Professor Richard M. Howard

Professor Garth V. Hobson

Lab Technician Donald Meeks

Research Associate Jerry Lentz

Professor Howard provided me with the leadership, guidance and support that kept this project on track from start to finish. Professor Hobson's knowledge of experimental data collection techniques and test equipment setup proved invaluable for this wind tunnel experiment.

Lab Technician Don Meeks is an expert model builder. His craftsmanship, attention to detail and tireless effort resulted in a high-quality wind tunnel model, which was the cornerstone of this entire analysis. Research Assistant Jerry Lentz provided valuable assistance during the early stages of this project. In spite of other commitments, he took the time to help me construct an electrical junction box that was required to interface several elements of the test equipment.

Additionally, I would like to thank the customer support staff of National Instruments for their assistance. Their expertise enabled me to take a dated version of *Labview* and successfully implement it into a data collection process – a very impressive fete conducted by a long-distance telephone call. Also, Valley Engineering Group's engineering drawings proved very valuable during model construction.

This thesis is truly the result of a team effort. I extend my sincere thanks to these individuals, organizations and others that I may have neglected to mention for their assistance in making it all possible.

I. INTRODUCTION

A. BACKGROUND

In 1998, Sandia National Laboratories (Sandia) contracted the Naval Postgraduate School (NPS) to study the pressure field associated with a proposed aerodynamic fairing, designed to fit beneath the forward fuselage section of the Altus II Unmanned Air Vehicle (UAV). The purpose for this analysis arose from the requirement to fit an Ultraviolet (UV) laser remote sensing payload into the forward fuselage section of the Altus II UAV. The dimensions of the UV laser telescope necessitated that a portion of the telescope protrude into the freestream air beneath the originally configured Altus II airframe. To reduce drag and prevent unacceptable levels of telescope vibration, two proposals were developed to design an aerodynamic fairing that would facilitate the installation of this UV telescope. See Figure 1 for an illustration of the Altus II.
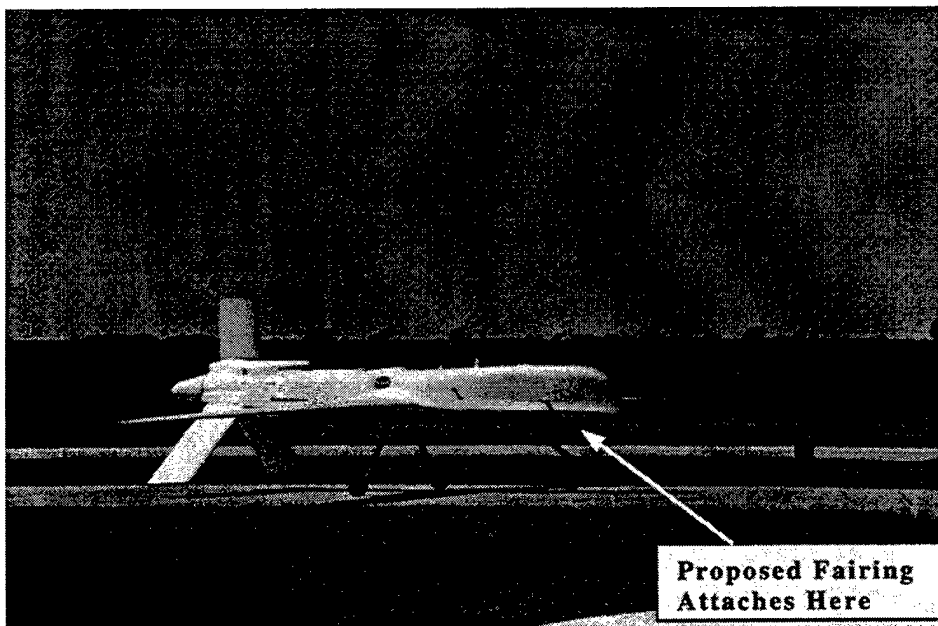
Figure 1. Altus II UAV

1

The first proposal was to design a fairing with an open cavity window, through which the UV telescope would view. This idea had the advantage of minimizing the optical distortion associated with having the telescope view through an optical window. One disadvantage of the open cavity fairing design was that vibrations associated with the open cavity flowfield could generate considerable stress on the telescope. [Ref. 1] This stress would in turn impose nearly continuous strain on the telescope's gimbal system designed to aim and hold it onto the desired target.

The second proposal was to design a fairing with a transparent optical window, through which the UV telescope would view. The engineers at Sandia concluded that a high quality optical window could be designed to sufficiently minimize the distortions in the UV telescope imagery. One advantage of the closed fairing design was that the strains imposed on the telescope's aiming/holding system would be greatly
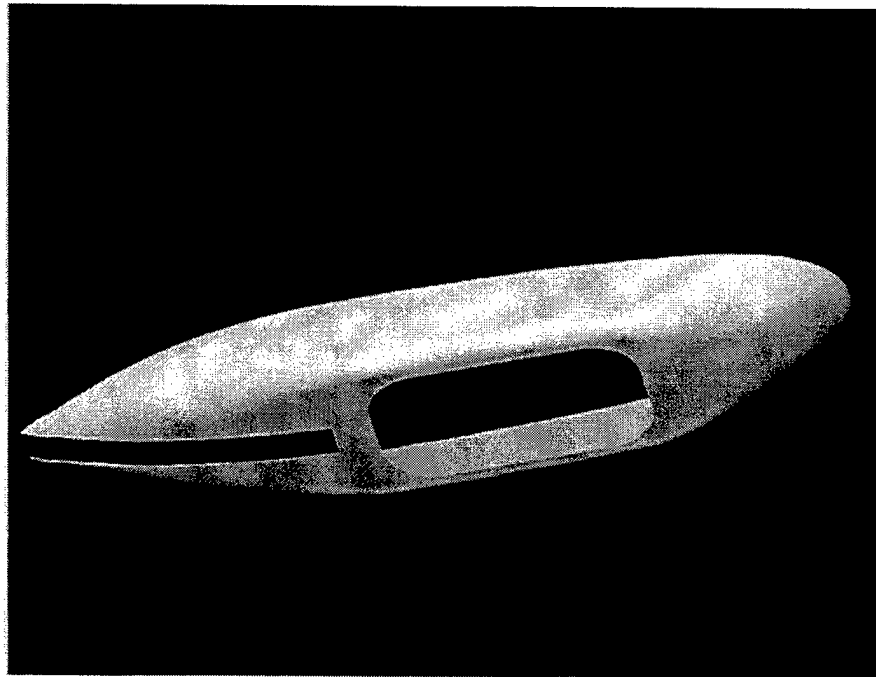
Figure 2. Proposed Aerodynamic Fairing

reduced. When all of these considerations were taken into account, the decision was made to proceed forward with the closed fairing design. Figure 2, provided by Valley Engineering Group (VEG), illustrates the proposed shape of the fairing.

B. PURPOSE

The original purpose of the fairing analysis was to measure the open cavity flow field forces exerted on the proposed gimbaled system used to align and hold the telescope in position. The forces and vibrations imposed on the telescope in the open cavity design would have severely restricted the design of the telescope's aiming/holding system. After the decision was made by Sandia to change to the second proposal for the fairing design, the purpose of analysis changed.

Using the closed fairing with an optical window as the baseline design, the purpose of this analysis was to estimate the pressure-induced forces on the optical window and to estimate the pressure characteristics along the longitudinal centerline axis of the Altus II's upper fuselage. Knowing the approximate force exerted on the window will enable design engineers to fabricate a window possessing minimum weight with acceptable distortion and optical characteristics.

II. TEST EQUIPMENT DESCRIPTION

A. THE MODEL

1. Model Construction

The wind tunnel model used for this analysis was a one-half scale likeness of the forward fuselage section of the Altus II UAV, with the proposed fairing attached. The foundation of the model was cut from a high-quality pine plywood board upon which the upper fuselage and lower fairing surfaces were mounted. To form the shape of these upper fuselage and proposed fairing surfaces as closely as possible to the graphic depiction provided by VEG, cross-sectional ribs were affixed to the baseboard to aid in developing the final surface shapes (Figure 3).
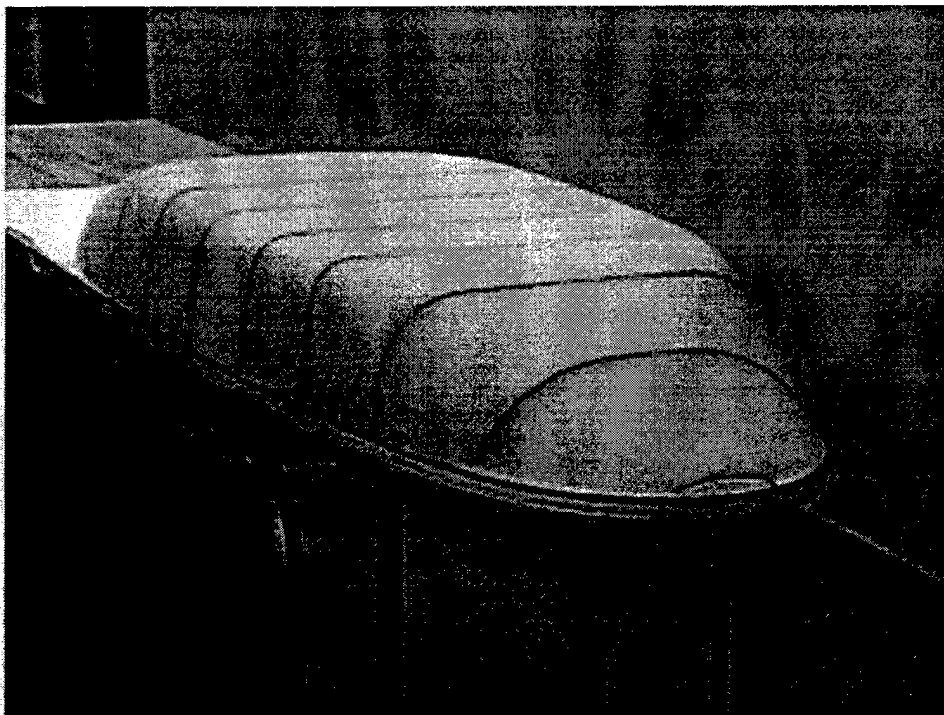
Figure 3. Fairing Shape Before Fiberglass Covering

Blue polystyrene foam, commonly used in fiberglass hand lay-up construction, was inserted between each of the fairing's cross-sectional ribs. The blue foam was then sanded down to the level of the cross-sectional ribs with the contours in the inter-rib regions 'interpolated' by visual observation. Once the blue foam shapes were finished, three layers of fiberglass were applied to the foam core. After the fiberglass set, the foam inside the fairing was removed to facilitate the installation of the pressure ports and the associated *Tygon* tubing. See Figure 4 for the finished fairing.
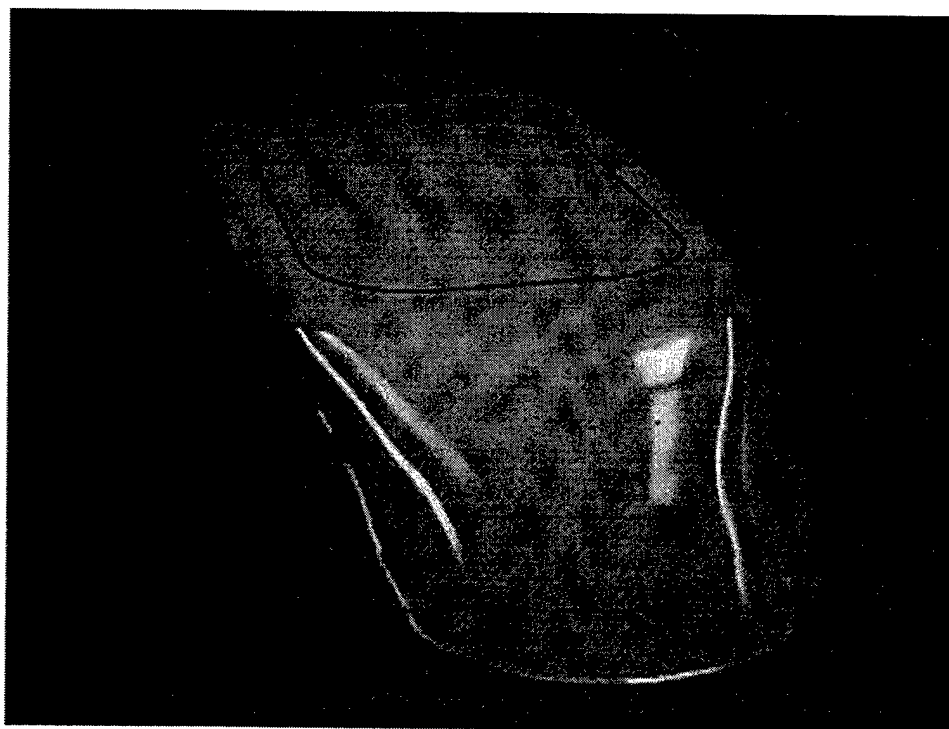
Figure 4. Painted Fiberglass Fairing

2. Model Instrumentation

The principal area of interest on the aerodynamic fairing was that area where the optical window was to be mounted. Consequently, the entire window surface was instrumented with a pattern of pressure ports. To reduce the total number of pressure ports on the fairing, only the right

side of the forward and aft sections was instrumented for pressure measurements. The pressure ports were divided into three sections: the forward section (A Section - 40 ports), the middle section (B Section - 45 ports) and the aft section (C Section - 40 ports). See Figure 5 for details regarding the model port numbers. Dividing the pressure port pattern into these three sections was necessary because the Scanivalve's pressure manifold could only accommodate 48 pressure measurements at one time.
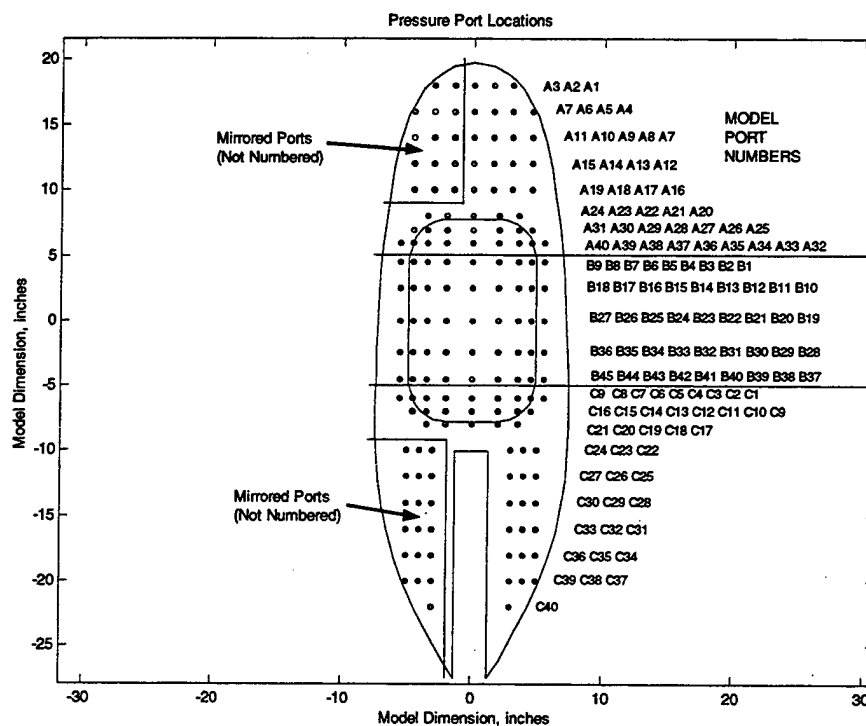
Figure 5. Pressure Port Diagram

Once the holes were drilled for each pressure port, brass fittings were individually glued into every port. Each brass fitting was tailored so that surface flow disruptions on the model were virtually eliminated. Inside the fairing, *Tygon* tubing was attached to each pressure port fitting. Initially, the entire *Tygon* tubing bundle was divided into two smaller bundles to enable the tubing to exit the model and wind tunnel. Once the

7

two bundles were outside the tunnel, they were divided again to reform three tubing bundles. These three bundles corresponded to the three aforementioned pressure port sections on the model: the forward (A), middle (B) and aft (C) sections.

B.   THE WIND TUNNEL

The NPS 3.5' x 5.0' Academic Wind Tunnel (AWT) was used to test the proposed aerodynamic fairing. The vertically oriented closed circuit AWT shown in Figure 6 measures approximately 62.7 feet in length, 33.0 feet in height and 15.0 feet in width with a 14.4 ft^2 (2079 in^2) test section. [Ref. 2] The AWT was originally powered by two 150-hp electric motors that drove two counter-rotating three-bladed variable-pitch fans. As a result of a previous incident involving the fan ingestion of a hand tool, the AWT currently uses only one 150-hp electric motor to drive a single fan. Single motor operation gives the AWT an approximate maximum test speed of 145 KTAS. [Ref. 2]
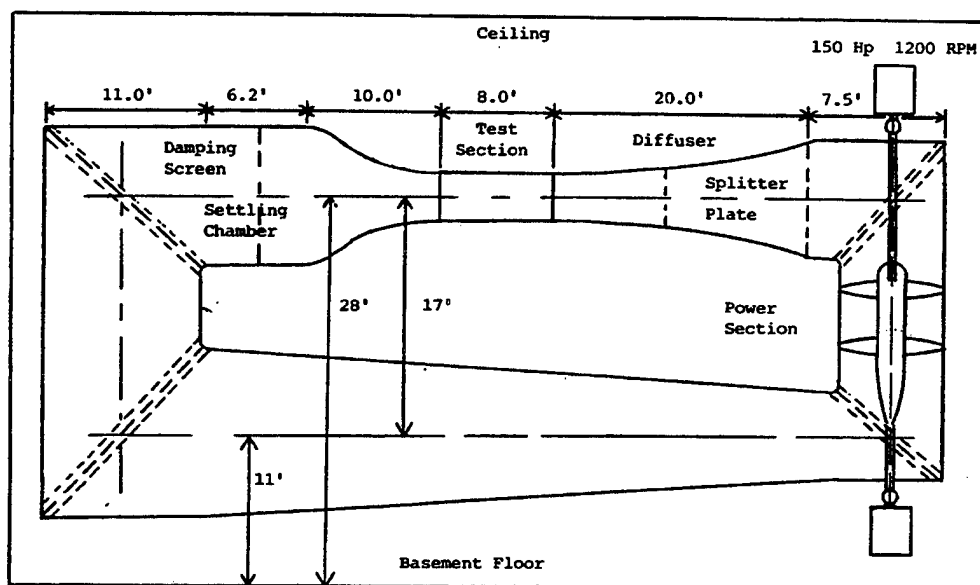
Figure 6. 3.5' x 5.0' Academic Wind Tunnel

The Altus II UAV operates at low subsonic speeds, typically well below 120 knots. For this reason, the AWT is well suited for testing a model of this type of flight vehicle. The frontal cross-sectional area of the Altus UAV model measures approximately 227 square inches, as shown in Figure 7. Based on this cross-sectional area, the blockage equals 10.9%. The model is relatively large for the given test section; the associated blockage effects are discussed in Chapter III Section B. The model scale was chosen to minimize Reynolds number effects.
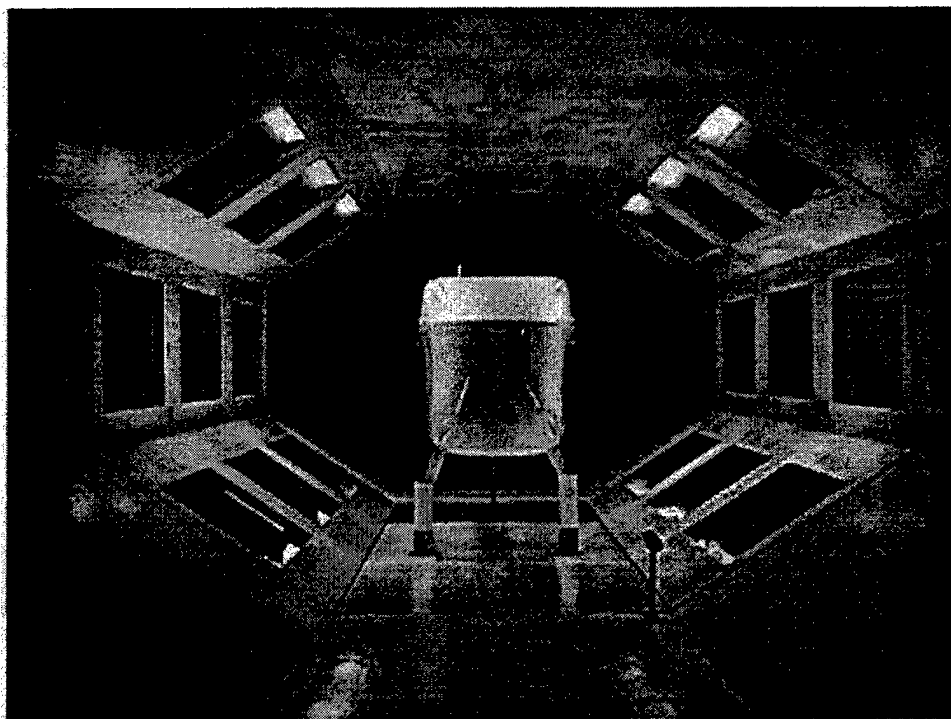
Figure 7. Frontal View of Model in Test Section

C. THE DATA COLLECTION EQUIPMENT

Data collection was accomplished by integrating a Scanivalve pressure measurement device with a PC-based National Instruments *Labview* data acquisition program. See Figure 8 for a schematic diagram of the test equipment set-up.

Junction Box

19 Pin

Scanivalve

5 Pin

26 Pin

GPIB

RS232

Monitor

486 PC

Signal Conditioner

14 Pin

Keyboard

SDIU

CTLR
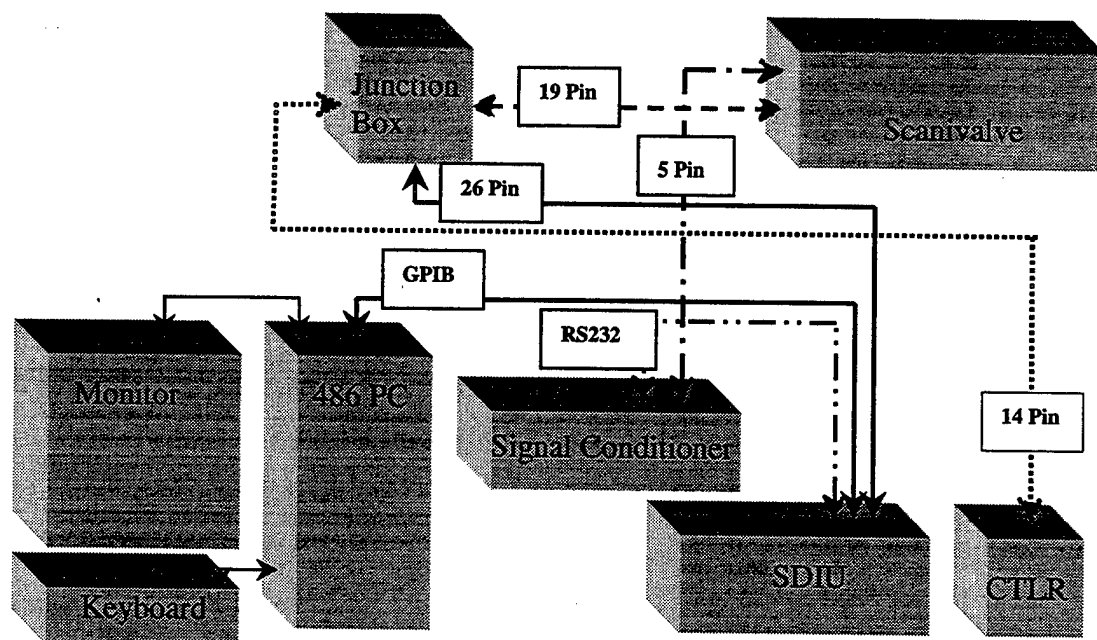
Figure 8. Schematic of Test Equipment Set-up

1.   The Scanivalve

The Scanivalve is a differential pressure measurement device that used a calibrated transducer to measure the difference between a test pressure and a reference pressure (ambient pressure at the Scanivalve's rotary switch). The Scanivalve used in this experiment had a +/- 2.5 psid transducer. It mechanically cycled between and measures pressures from 48 individual ports located on its pressure manifold. Combined with a compatible data acquisition system, the Scanivalve was an effective low-cost means of obtaining low speed wind tunnel pressure measurements.

2.   The Scanivalve Digital Interface Unit (SDIU)

The SDIU was an analog-to-digital converter that converted analog voltage measurements from the *Scanivalve* (corresponding to discrete differential pressure measurements) into digital voltage readings. It also enabled an operator to select individual numbered pressure ports for measurement. Additionally, the SDIU is equipped with a GPIB link which

10

enabled it to be operated remotely by an appropriately configured PC. A 486 PC using NI *Labview* software controlled operated the SDIU.

3. The Scanivalve Solenoid Controller

The Controller provided 28 volt DC electrical power to the Scanivalve unit. It also enabled an operator to manually step through or reset-to-home the Scanivalve's pressure ports. This was one of three units interfaced together with the Junction Box discussed below.

4. The Signal Conditioner

The Signal Conditioner enabled an operator to zero and span the SDIU voltage readings. Additionally, it provided the excitation voltage for the Scanivalve. To calibrate the SDIU, a water manometer was used to calibrate the transducer at 30 cm of H_2O differential pressure.

5. The PC and National Instruments *Labview*

The software program used to drive the experimental equipment and collect the pressure data was taken from LT Greco's thesis work. [Ref. 5] The NI *Labview* VI used for his experiment also employed a Scanivalve to take pressure measurements. The only modification made to the VI was a small addition to the code that enabled the pressure measurement data to be stored on a PC 3.5 inch floppy disk.

6. The Junction Box

A junction box that interfaced the Scanivalve, the SDIU and the Scanivalve Solenoid Controller was fabricated for this experiment. Using design drawings provided by Dr. Hobson, this junction box was constructed to the specifications of another junction box used in the experimental set-up of LT Greco. [Ref. 5] Properly connected to the other experimental apparatus, this junction box facilitated the

PC/SDIU/Scanivalve interface that enabled the pressure measurement system to function as required.

III. RESULTS AND DISCUSSION

A.   TEST PROCEDURE AND RESULTS

After the construction of the wind tunnel model was complete, it was mounted inverted in the test section of the AWT. As shown in Figure 9, the model was supported by two bayonet mounts and one aft-center mount, and was free to pivot about its vertical and lateral axes. The two bayonet mounts were attached to an internal pivoting mechanism that allowed up to five degrees of positive/negative sideslip. The aft-center mount was constructed with a screw-post that allowed up to four degrees of positive/negative AOA.
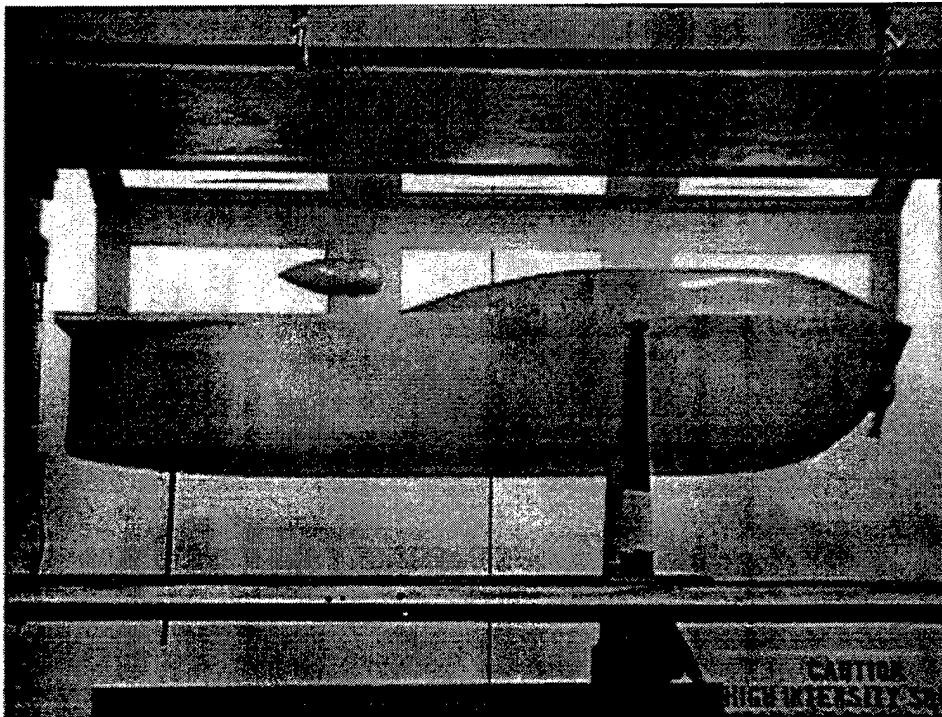
Figure 9. Side View of Model in Test Section

1.   Tunnel Operation Procedure

Several preliminary wind tunnel test runs were conducted to ensure that the model and support structures were robust enough to handle the test velocities. At wind tunnel velocities in excess of $\Delta P = 10$ cm of H_2O pressure (as measured by the H_2O manometer at the AWT Control Panel, shown in Figure 10), model vibration was observed. ΔP measured the difference in pressure between a Kiel probe and a static ring, located just prior to the test section. The conversion from indicated differential pressure (ΔP) at the AWT Control Panel to test section dynamic pressure is discussed in Section B of this chapter.

Two wind tunnel tests were conducted at test section velocities corresponding to $\Delta P = 5$ cm and $\Delta P = 10$ cm H_2O to determine whether Reynolds number significantly affected the pressure measurements.
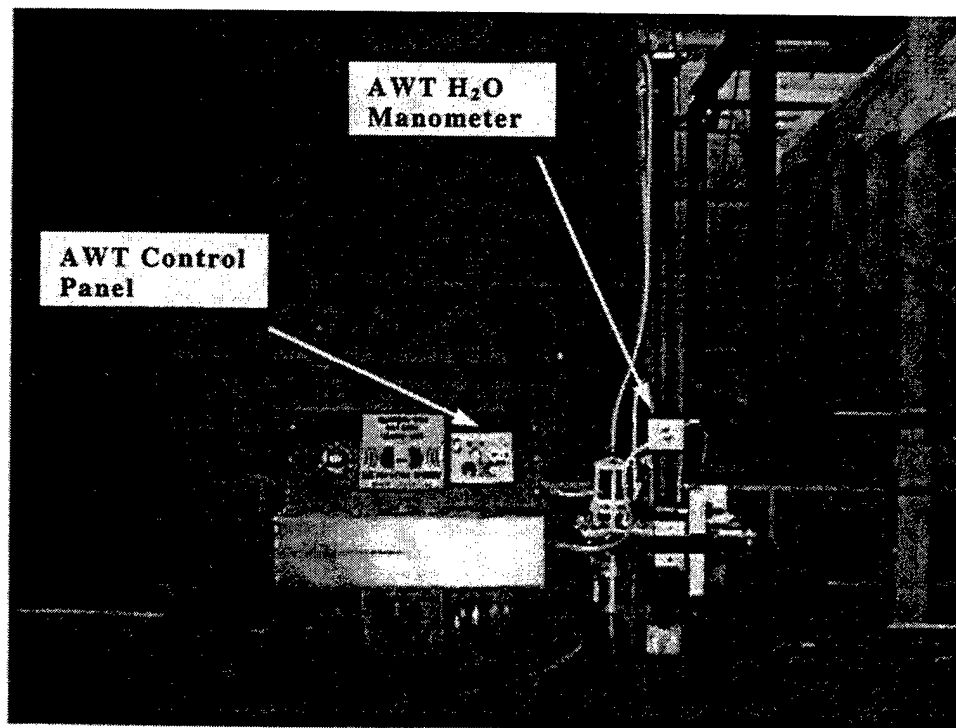
Figure 10. AWT Control Panel and Water Manometer

See Table 1 for conversion between water pressure, pound/foot^2 and airflow velocities.

ΔP (cm H2O)	Q (psf)	Q (psi)	V (feet/sec)	V (KTAS)
5	10.2	0.071	93.0	55.1
10	20.5	0.142	131.5	77.9
15	30.7	0.213	161.0	95.4
20	40.9	0.284	186.0	110.2
25	51.2	0.355	207.9	123.2

Note : density assumed sea-level standard

Table 1. Some Common Conversions for Low-Speed Wind Tunnel Tests

See Appendix A for the tunnel operation checklist used to conduct each test run. In brief, the test equipment was powered up, the SDIU/Scanivalve was calibrated with a stand-alone water manometer, the model was set to the desired AOA/Sideslip (α/β) and the tunnel/test section was inspected for foreign or loose objects. Next, the wind tunnel was powered-up and the flow velocity was steadily increased to ΔP = 10 cm of H_2O pressure. Once the tunnel velocity stabilized, the NI Labview program, which measured and recorded the data taken from the first 48 pressure ports, was enabled. After the initial 48 port measurements were complete, the first 48-port manifold was removed and replaced with the second 48-port manifold while the tunnel maintained its test velocity. This procedure was repeated for each of the three 48-port manifolds until the data for all 125 (40 + 45 + 40) model ports was measured and recorded. Figure 11 illustrates the three 48-port pressure manifolds adjacent to the Scanivalve.

2.   Reynolds Number Effect on C_p

Since it was observed that excessive model vibrations might occur at full Reynolds number testing, the effects of reduced Reynolds number testing was observed. Two test-runs, one at ΔP = 5 cm and another at ΔP = 10 cm H_2O water pressure, were conducted to observe the effects on the
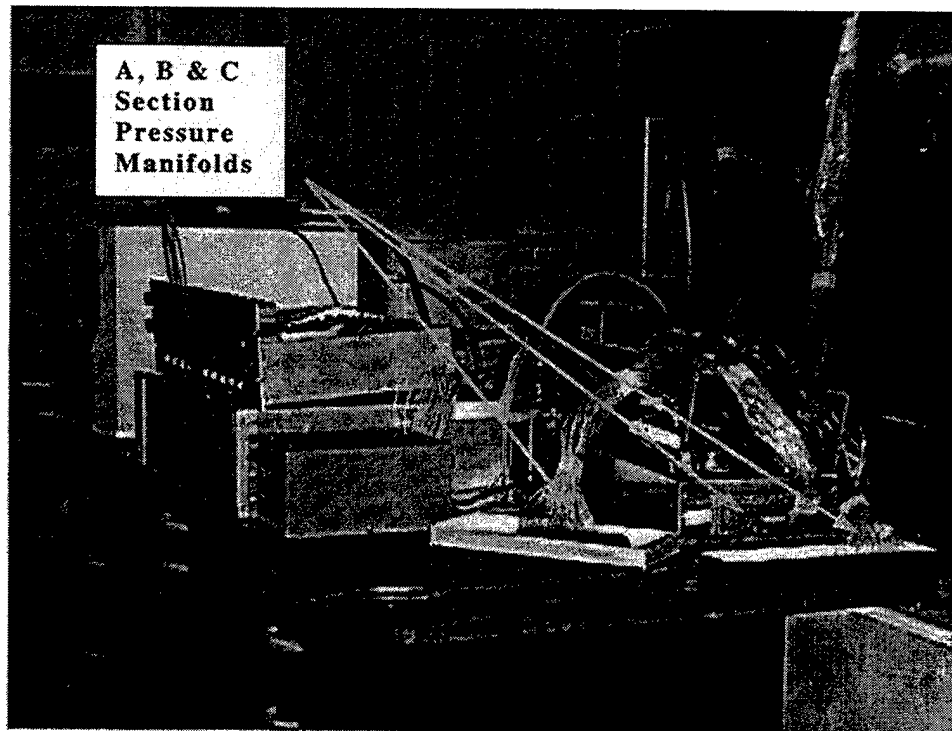
Figure 11. The Three 48-Port Pressure Manifolds

LONGITUDINAL AXIS USED
FOR REYNOLDS NUMBER
EFFECTS ANALYSIS
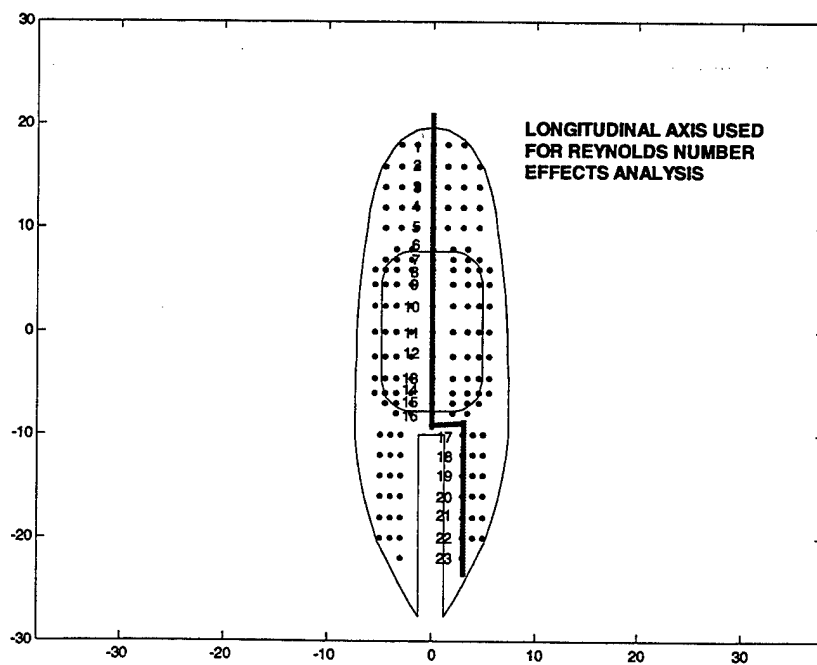
Figure 12. Longitudinal Axis of Fairing for Reynolds Number Effects Tests

pressure measurements taken along the longitudinal axis of the model. See Figure 12 for the longitudinal measurement axis used for these Reynolds number effects tests.

Cp vs Longitudinal Position
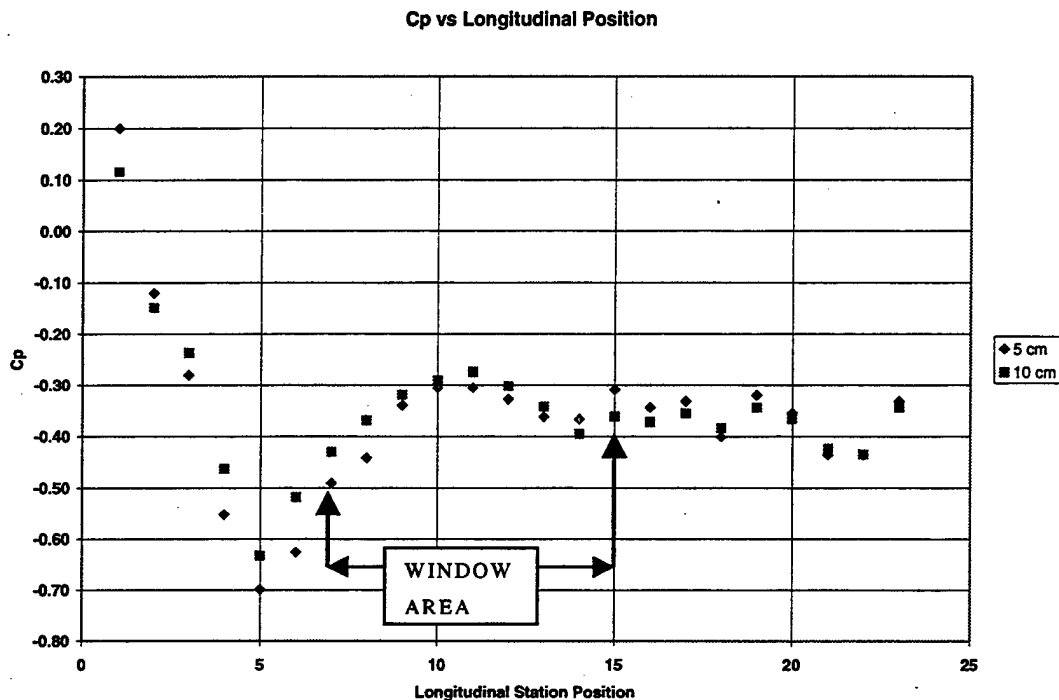
Figure 13. Reynolds Number Effects Test – C_P vs Longitudinal Station Position

Figure 13 illustrates that a reduced Reynolds number has little overall effect on the C_P measurements. The pressure coefficient C_P is given by:

$$C_P = \frac{p - p_\infty}{q_\infty}$$

where p_∞ and q_∞ are freestream ambient pressure and dynamic pressure, respectively. Although some variation in the measurements exists between stations four through eight, the difference in these measured C_P's is negligible for this type of analysis. The overall intent of these C_P measurements is to estimate the average force exerted on the optical

17

window area (longitudinal stations 7–15 in Figure 13). It was decided to run at sub-scale Reynolds number to avoid model aerostructural concerns.

The Reynolds number for the 18 test cases is determined from

$Re = \dfrac{\rho V \ell}{\mu}$, where the absolute viscosity of the air is given by Sutherland's

equation $\mu = 2.27x10^{-8}\left(\dfrac{T^{1.5}}{T+198.6}\right)$ (lbf s/ft²). [Ref. 4] The characteristic

length for the Reynolds number is taken as the model's fairing length, $\ell = 4$ ft. Standard sea-level density ρ is assumed and the test velocity is determined from Q-bar, as discussed in section B sub-section 1 of this chapter. Based on these assumptions, test case Reynolds numbers equaled 3.1 million. Based on a standard 5000-ft altitude flight at 70 KTAS, the actual full-scale Reynolds number equals 6.4 million.

B. WINDOW PRESSURE MEASURMENTS

The first step in obtaining the total force exerted on the optical window was to determine the local pressure coefficient C_p at each port location on the model. One calibration and two corrections were applied to the raw experimental data to obtain the C_p's. The wind tunnel calibration related test section average dynamic pressure Q-bar to measured $_\Delta$P, as displayed on the AWT Control Panel H_2O manometer. The two corrections took into account test section blockage effects due the model size and zero voltage readings from the Scanivalve reference pressure.

1. Data Calibration, Reduction and Corrections

a. Tunnel Q-bar Calibration

In Reference 2, the author calibrated the wind tunnel test section Q-bar. After conducting a pressure survey of the AWT test section, a relation between indicated pressure ($_\Delta$P) and calibrated dynamic

pressure (Q-bar) was determined. Figure 14 illustrates the results from this calibration. The ratio of the calibrated (Q-bar) to the measured ΔP (as read from the AWT water manometer) is a linear function. After the raw pressure data was collected in the Microsoft Excel spreadsheets, this calibration was applied to all of the other pressure measurements.

**Academic Wind Tunnel Calibration
16 October 1992**

y = 0.98831 + 0.00102*Q(psf)
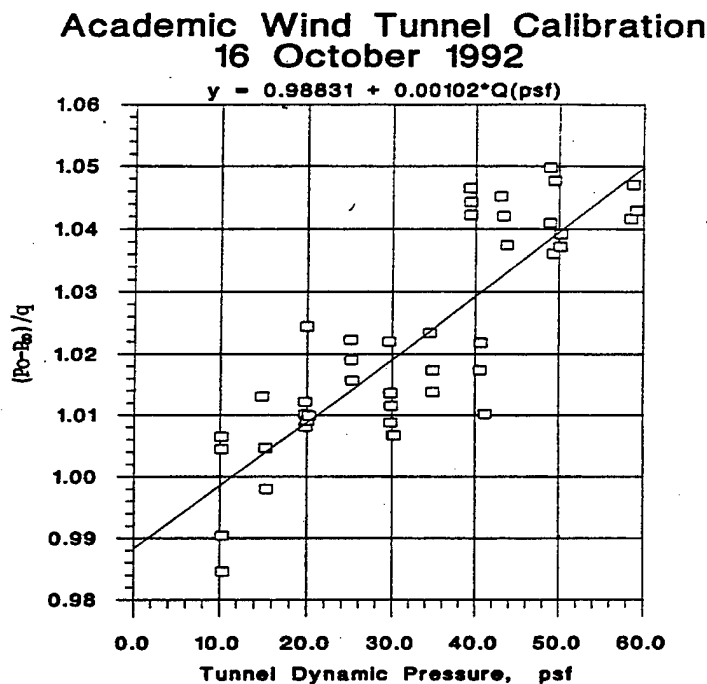
Figure 14. Academic Wind Tunnel Calibration

All of the test cases were conducted at approximately ΔP = 10 cm H_2O (20.5 psf), which after unit conversion and calibration, resulted in Q-bar = 20.7 psf.

b. Test Section Blockage Correction

The second modification to the raw pressure data involved the correction for test section blockage effects. Authors Rae and Pope propose a simple correction factor that applies to models of 'unusual shapes': [Ref. 6]

19

$$\varepsilon = \frac{1}{4} \frac{Model\ Frontal\ Area}{Test\ Section\ Area} \qquad\qquad \varepsilon = \frac{\Delta V}{V_U}$$

ε is the ratio of the velocity change due to blockage over uncorrected velocity. Rae and Pope state that "a maximum ratio of model frontal area to test section cross-sectional area of 7.5% should probably be used, unless errors of several percent can be accepted." [Ref 6] The model blockage in the current tests is 10.9%. Since average pressure forces are the desired result of this analysis, it was decided that correction errors of "several percent" are acceptable.

c. Zero Pressure Differential Correction

When the pressure measurement data was observed, a small inconsistency was noted in the data. Ambient atmospheric pressure was not always measured as zero volts. Scanivalve pressure manifold port #1 was open to the ambient atmosphere, which is also the Scanivalve's reference pressure when taking the other differential pressure measurements. In theory, a properly calibrated Scanivalve/SDIU should always read zero volts for port #1, since any variation in ambient atmospheric pressure would be sensed by both port #1 and the Scanivalve's reference port located near its rotary switch. Since both of these ports measure ambient atmospheric pressure, the measured pressure difference between them should equal exactly zero.

During the various wind tunnels runs, the Scanivalve/SDIU was calibrated with a stand-alone water manometer for each testing session. Each testing session lasted about one hour and measured between six and nine Scanvalve pressure manifolds. Three manifold measurements were required to measure the entire model in one configuration. During calibration, the SDIU was zeroed for ambient pressure and set to approximately -1.78 Volts for 30 cm of H_2O pressure on the manometer. The signal conditioner was used to set this zero and span. Setting the

span (of −1.78 Volts) sometimes slightly shifted the zero pressure reading, so an iterative process of zero and span setting was used to confirm that each reading was stable.

During the test runs a small measurement drift occurred for the ambient atmospheric pressure reading. To correct this problem, the voltage (and corresponding pressure) reading of Scanivalve port #1 was subtracted from all of the other pressure port measurements for each individual test run. This action applied an average correction to the measured data, which removed the error induced by the measurement drift of the Scanivalve's reference pressure.

2.   Pressure Coefficient Profiles on the Fairing

This section contains Figures 15 through 32, which depict the contour plots of the measured C_p's on the aerodynamic fairing. Appendix C contains the MATLAB program code used to convert the Microsoft Excel spreadsheet data into these pictorial C_p representations. Table 2 presents a summary list of the 18 test cases run at the specified values of α and β.

Test Case #	AOA (deg)	Sideslip (deg)	Test Case #	AOA (deg)	Sideslip (deg)
1	0	0	10	-4	-2.5
2	-2	0	11	-4	-5
3	2	0	12	-4	2.5
4	4	0	13	-4	5
5	-4	0	14	4	5
6	0	-2.5	15	4	2.5
7	0	-5	16	4	-2.5
8	0	2.5	17	4	-5
9	0	5	18	0	0

Note: test case #18 conducted with antenna installed

Table 2. List of α and β Test Cases

Included in the discussion of each test case is the pressure-induced force on the window. These force calculations assume a flight condition of 100 KTAS at sea level and are discussed in more detail in the next section.

21
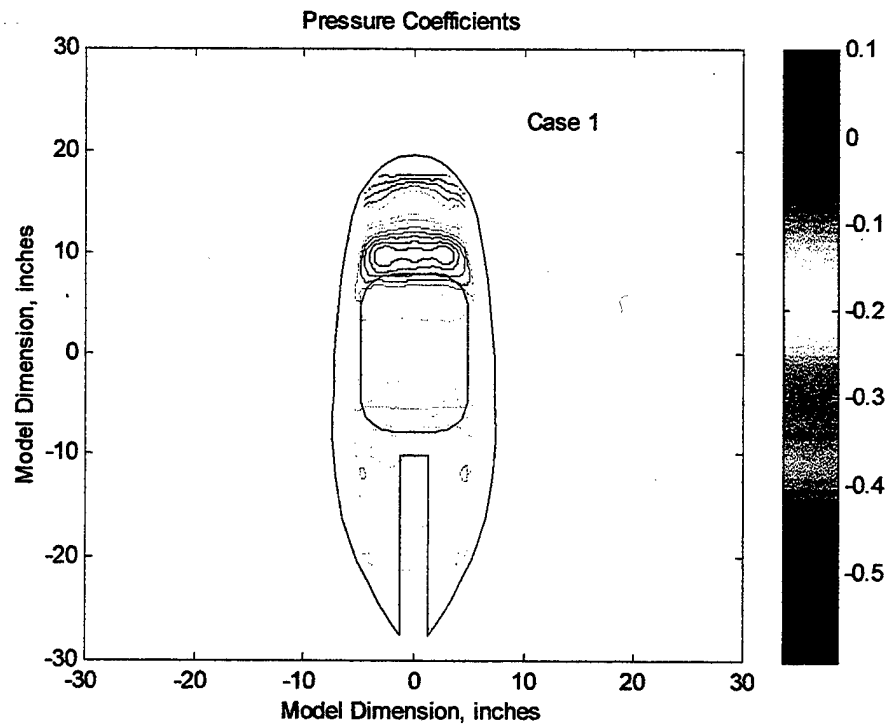
Figure 15. Case 1 - C_P at 0° α and 0° β
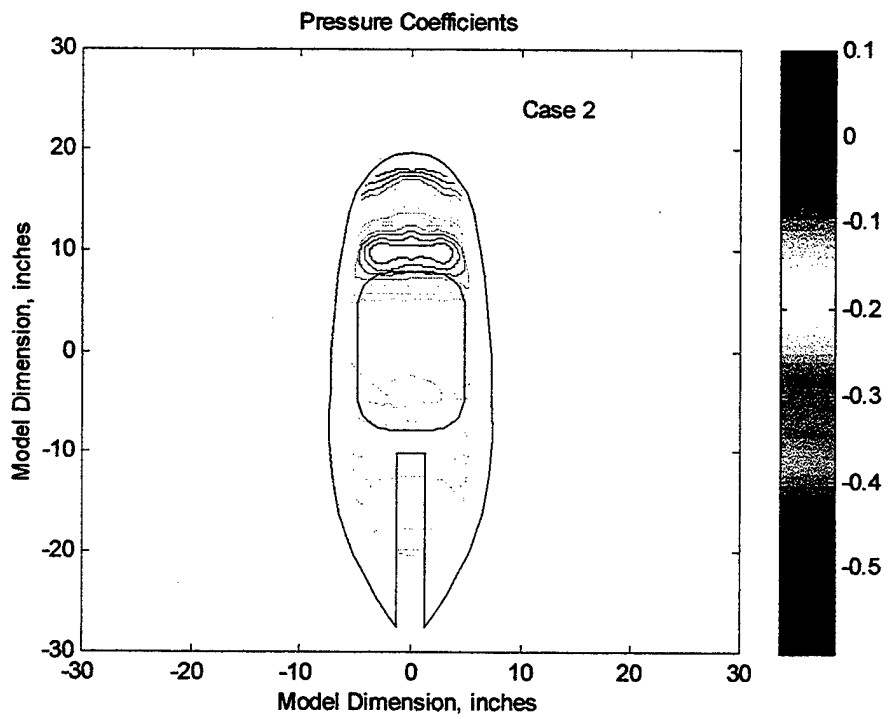
Figure 16. Case 2 - C_P at -2° α and 0° β

22
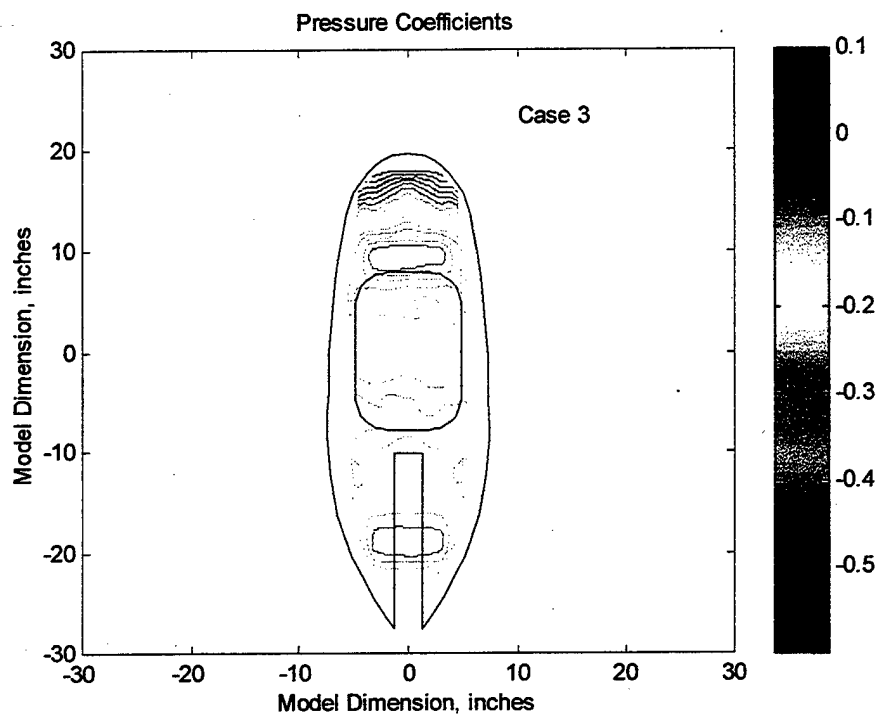
Figure 17. Case 3 - C_P at +2° α and 0° β
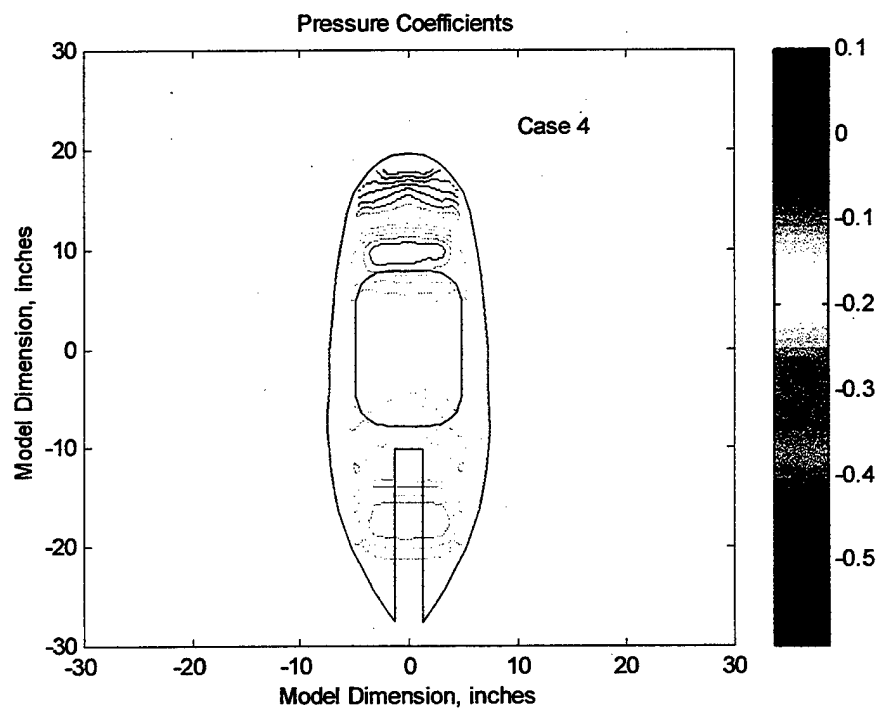
Figure 18. Case 4 - C_P at +4° α and 0° β
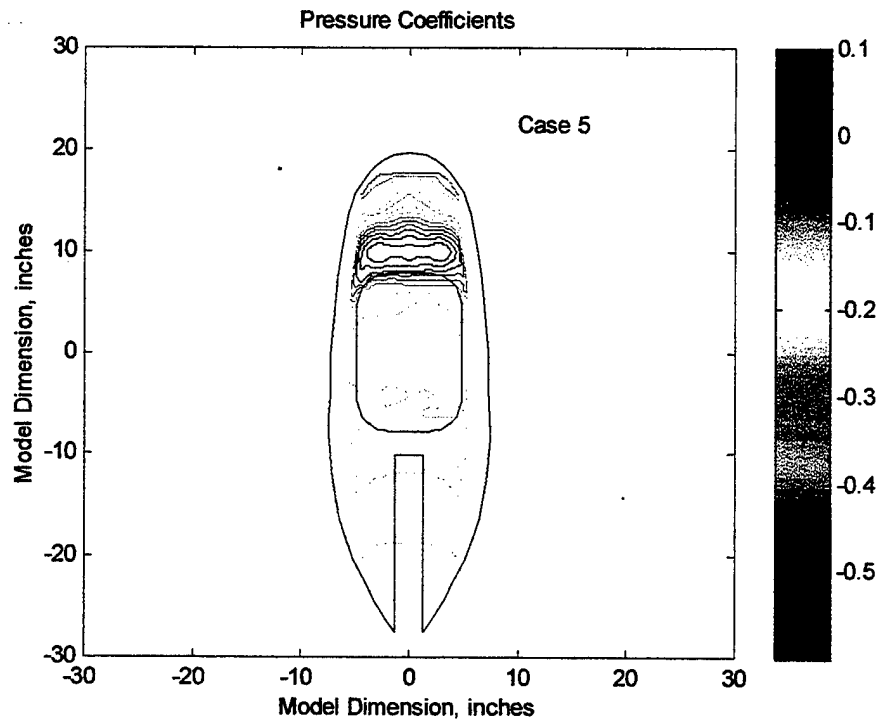
Figure 19. Case 5 - C_P at -4° α and 0° β
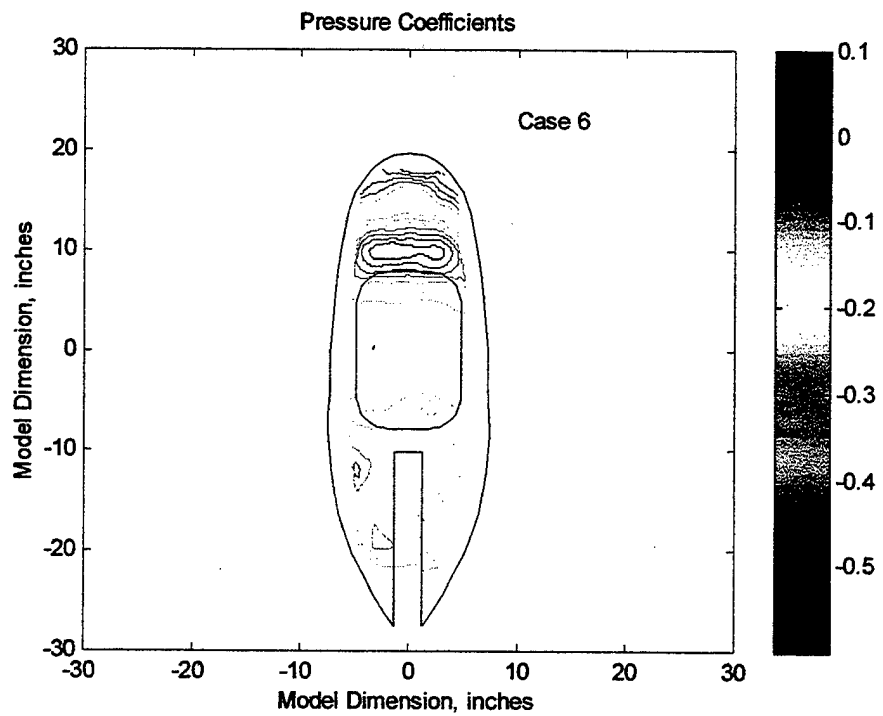
Figure 20. Case 6 - C_P at 0° α and -2.5° β

24
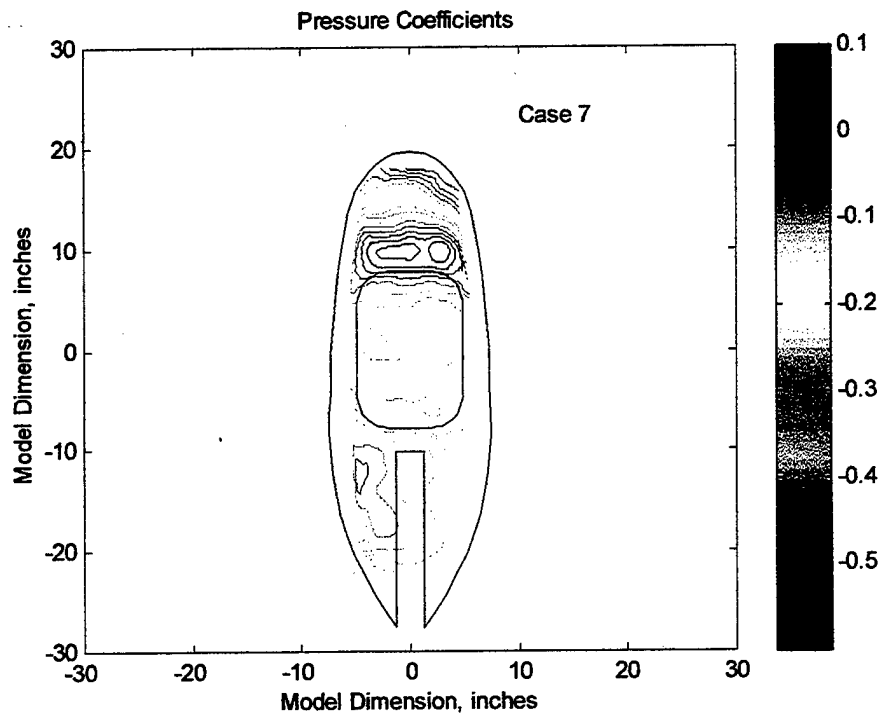
Figure 21. Case 7 - C_P at 0° α and -5° β
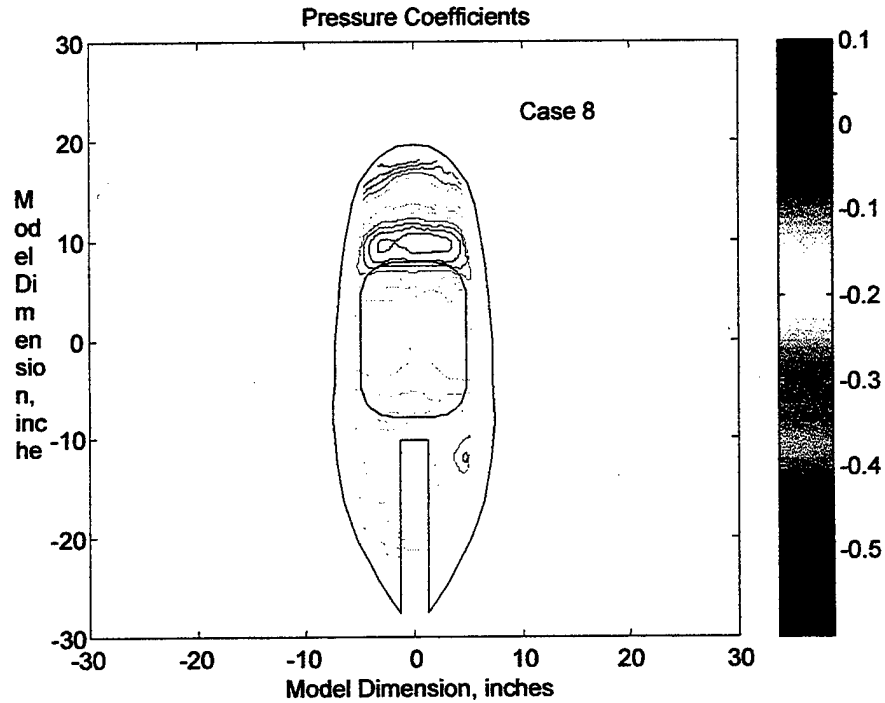
Figure 22. Case 8 - C_P at 0° α and +2.5° β
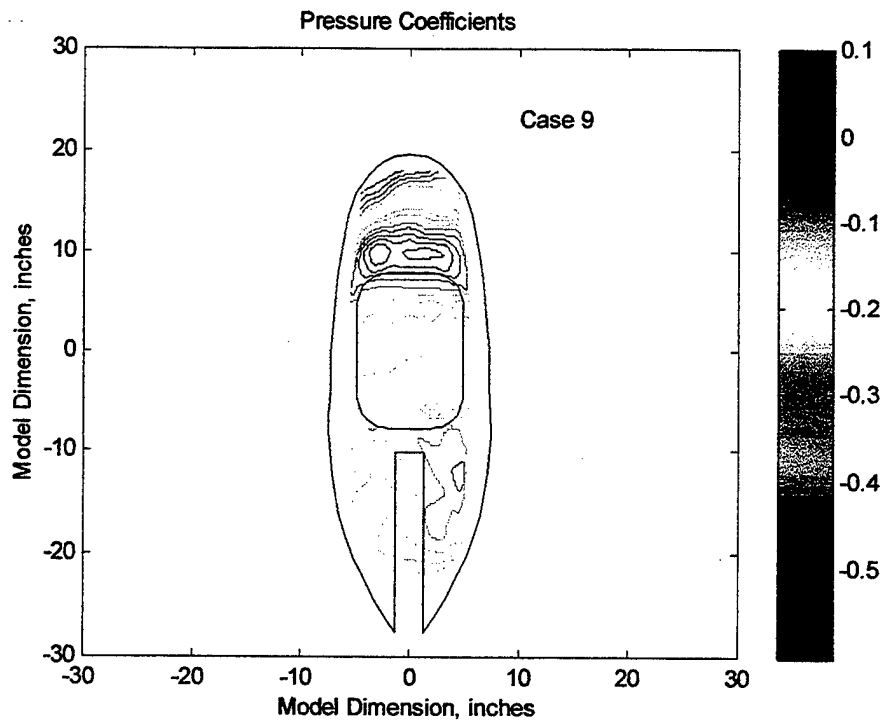
Figure 23. Case 9 - C$_P$ at 0° α and +5° β
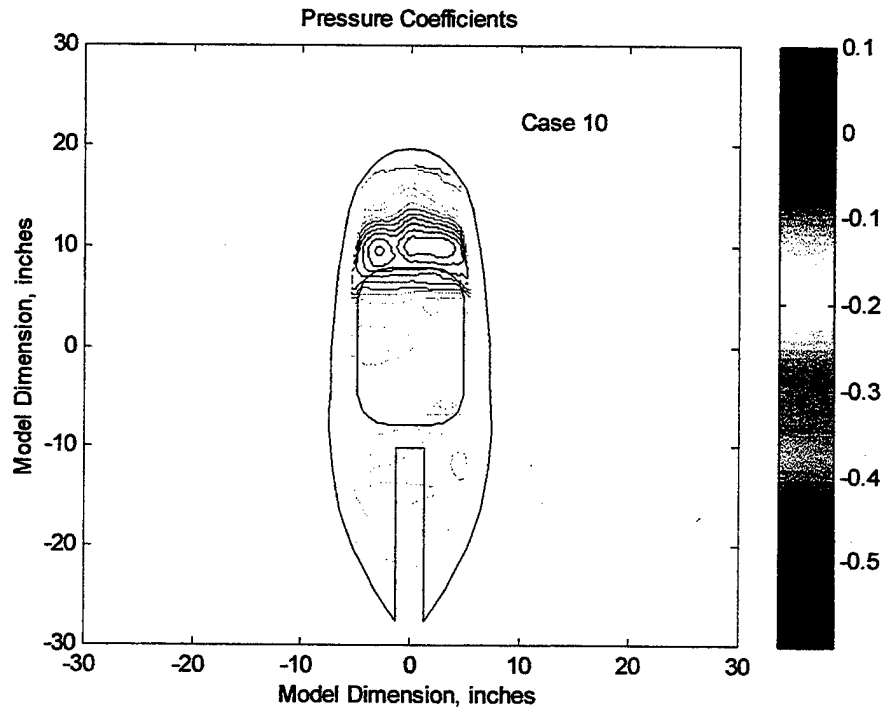
Figure 24. Case 10 - C$_P$ at -4° α and -2.5° β

26
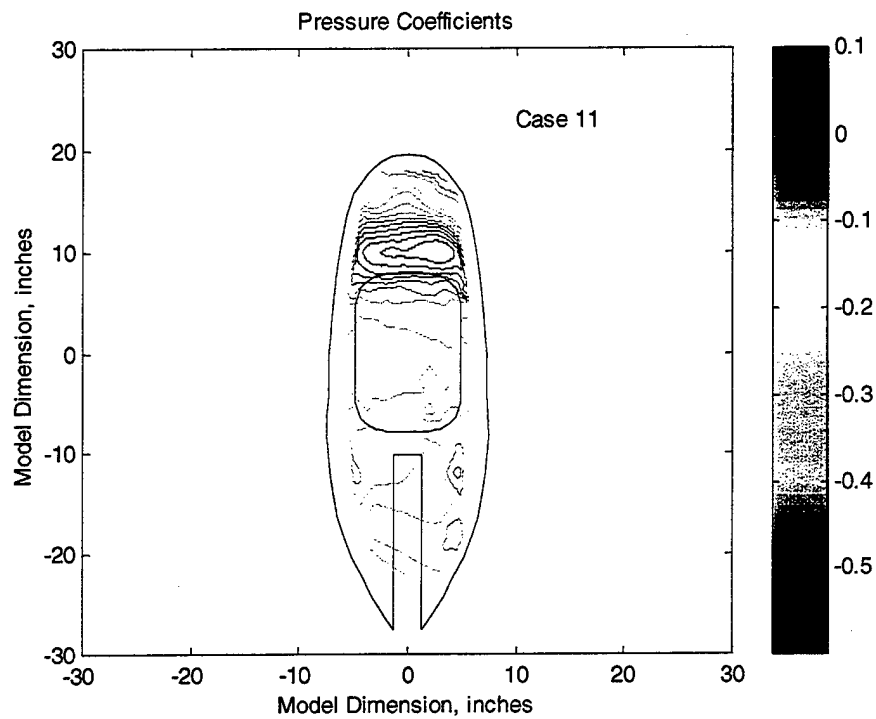
Figure 25. Case 11 - C_P at -4° α and -5° β
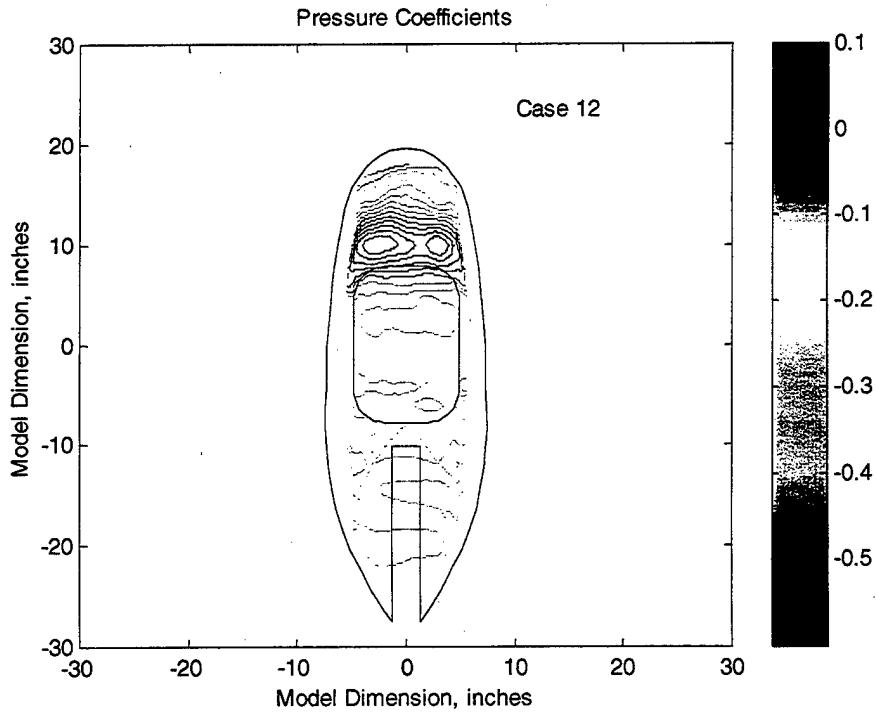
Figure 26. Case 12 - C_P at -4° α and +2.5° β
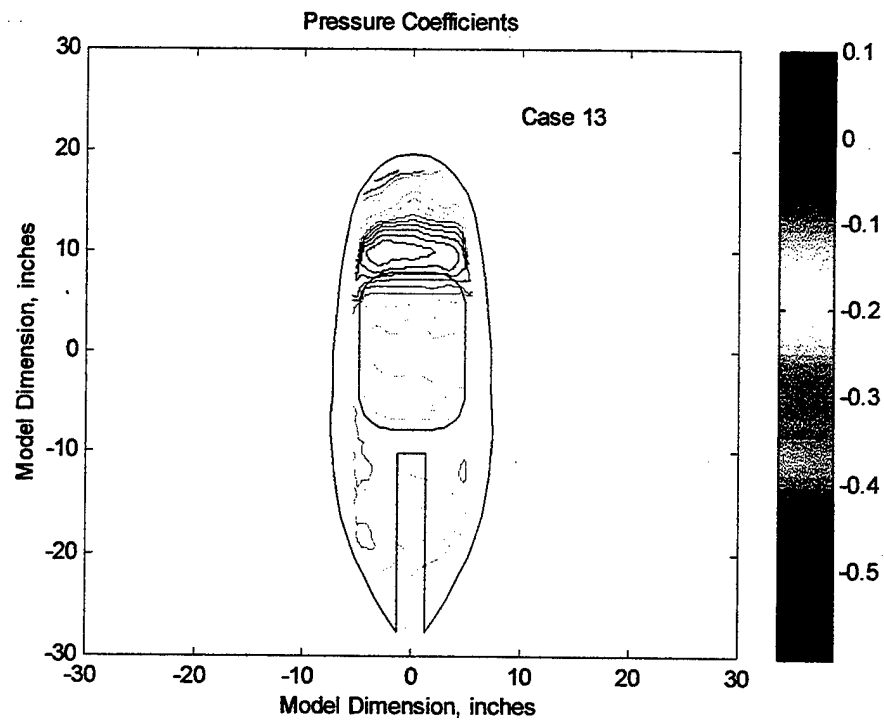
Figure 27. Case 13 - C_P at -4° α and +5° β
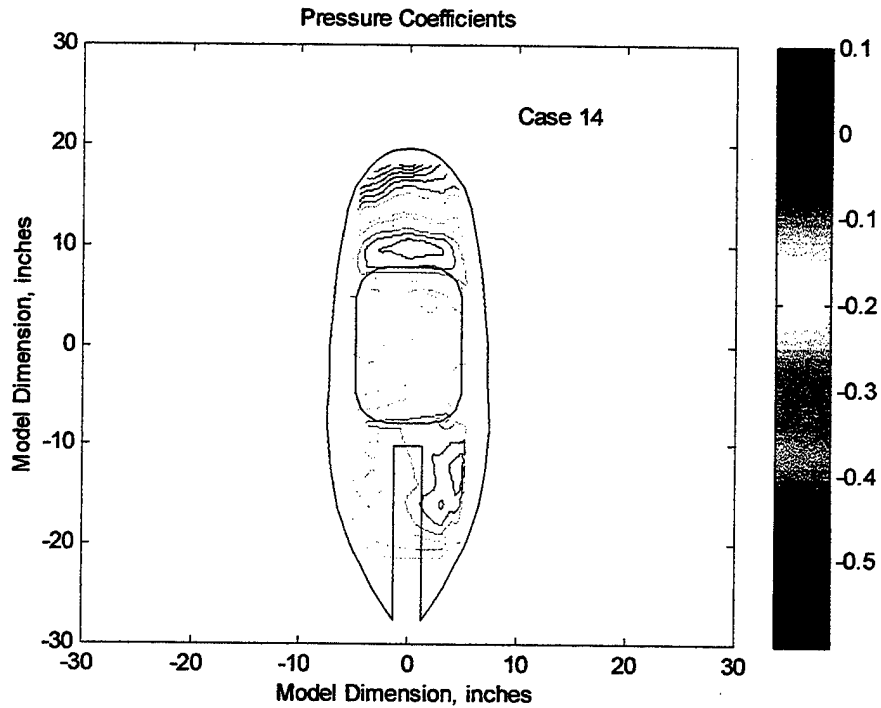
Figure 28. Case 14 - C_P at +4° α and +5° β
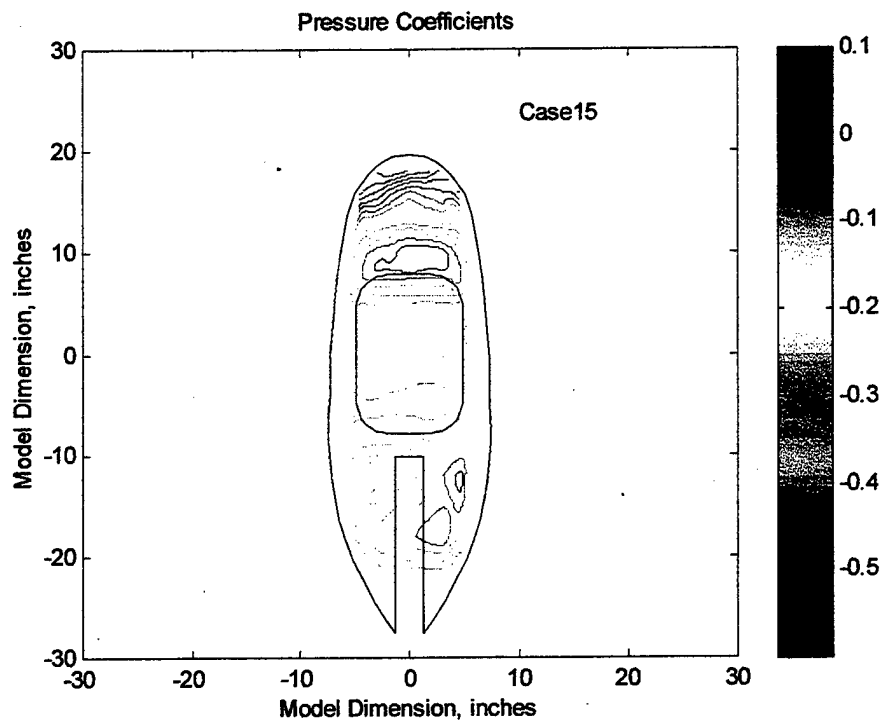
Figure 29. Case 15 - C_P at +4° α and +2.5° β
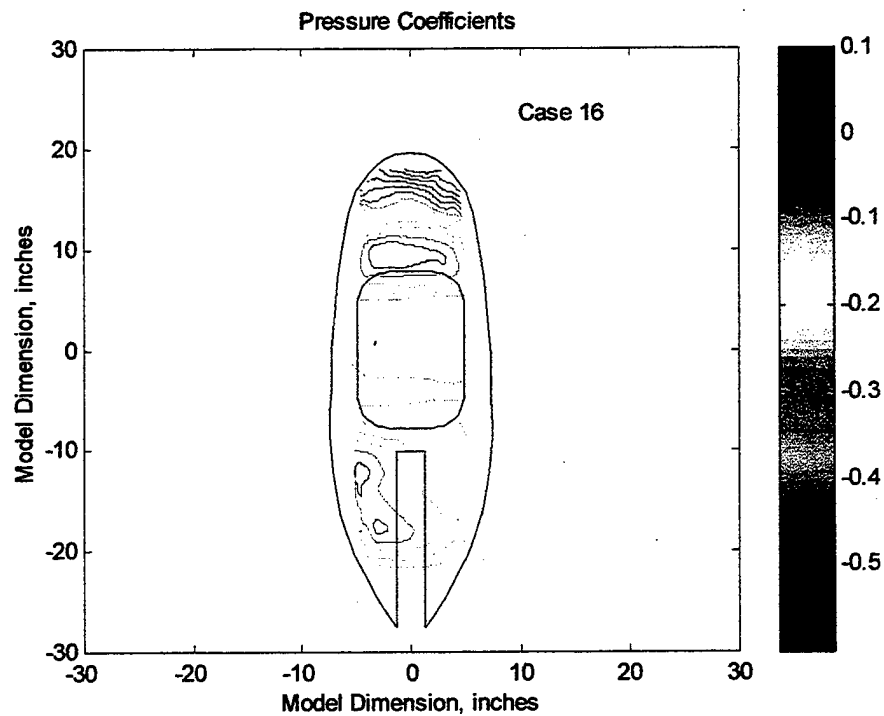
Figure 30. Case 16 - C_P at +4° α and −2.5° β

29
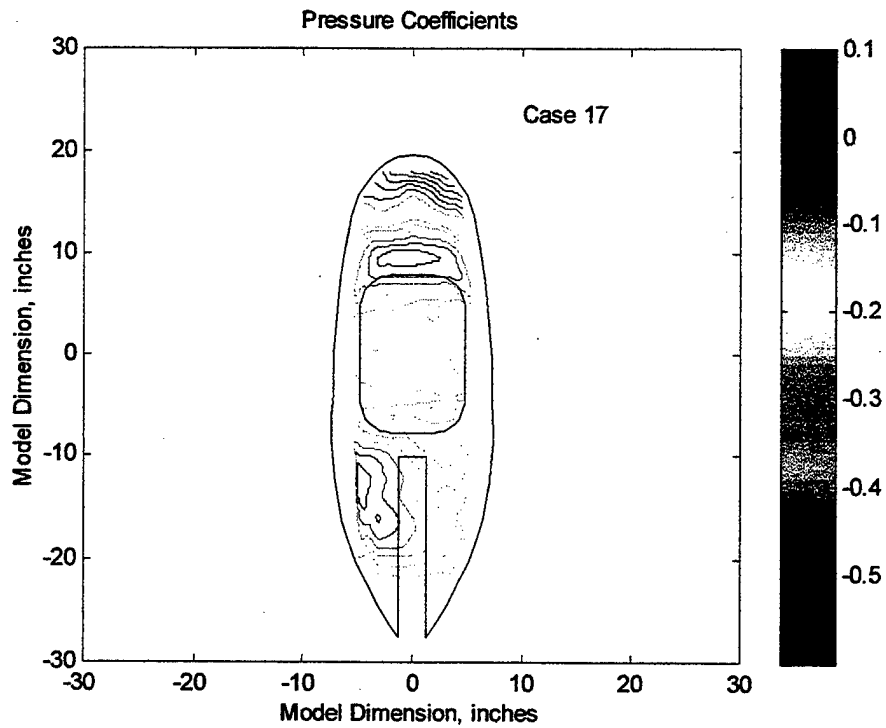
Figure 31. Case 17 - C_P at +4° α and -5° β
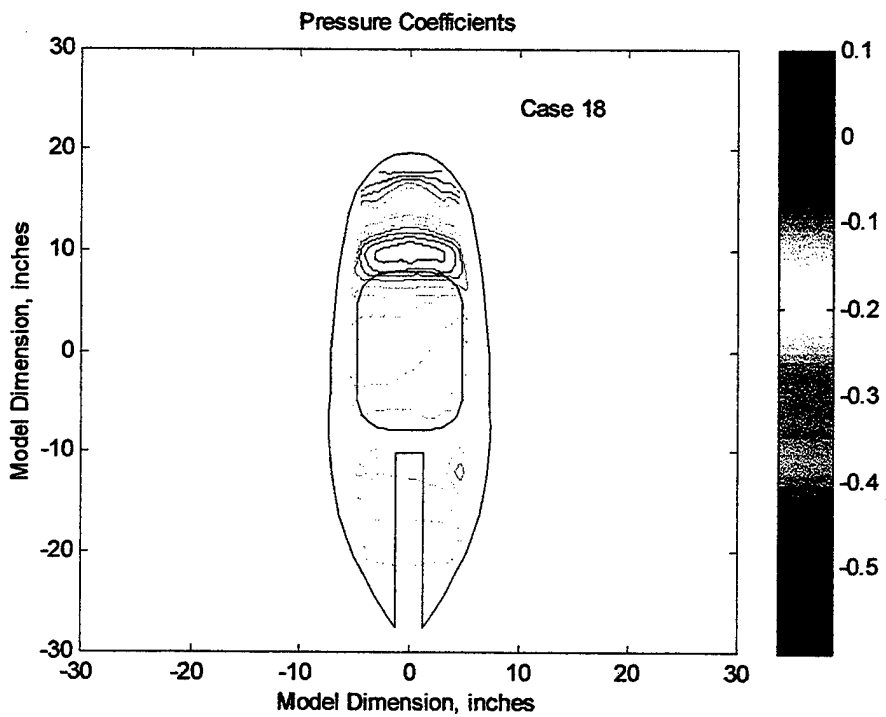
Figure 32. Case 18 - C_P at 0° α and 0° β with Antenna

Figure 15 illustrates the results of the baseline test case, which was conducted at 0° α and 0° β. The stagnation line ($C_P = 1$) occurred near the model leading edge, located well before the pressure measurement area. Consequently, the pressure contours do not depict it. The highest surface pressures were measured immediately aft of the leading-edge area and the lowest surface pressures were located just forward of the window. The window area experienced a relatively constant pressure field of $C_P \approx -0.35$. Additionally, there were two small areas of local low pressure ($C_P \approx -0.5$) located aft of the window in line with the window longitudinal edges. See position (± 5, -10) on Figure 14. The total force on the window for test case 1, extrapolated to full scale for the nominal flight condition described, was 51.3 lbf suction.

Figure 16 illustrates the next test case, which was conducted at -2° α and 0° β. Compared to Figure 15, the leading-edge area of high pressure remained largely unchanged. The local suction region forward of the window was also similar to the previous case, except that the area aft this region experienced a greater *increasing* pressure gradient across the leading edge of the window. After this *increasing* gradient, the remaining window area experienced a relatively constant pressure of $C_P \approx -0.3$. The total force on the window for test case 2 was 40.4 lbf suction.

Figure 17 illustrates test case 3, which was conducted at +2° α and 0° β. The leading-edge area of high pressure was approximately twice as large as the two previous test cases. The *increasing* pressure gradient associated with the local suction region forward of the window was less than the previous two test cases. This case had a $C_P \approx -0.4$, vice a $C_P \approx -0.5$ from the two previous test cases, for this local suction region. The center of the window area experienced a relatively constant pressure of $C_P \approx -0.17$, compared to -0.35 and -0.30 from test cases 1 and 2, respectively. The trailing edge of the window experienced a *decreasing*

31

pressure gradient from $C_P \approx -0.2$ to $C_P \approx -0.35$. The total force on the window for test case 3 was 40.4 lbf suction.

Figure 18 illustrates test case 4, which was conducted at +4° α and 0° β. The leading-edge area of high pressure was similar to test case 3. The local suction region forward of the window was also similar to test case 3, except $C_P \approx -0.43$ instead of $C_P \approx -0.4$. The *increasing* pressure gradient located aft of this suction region was less than test case 3. The center window area experienced a relatively constant pressure of $C_P \approx -0.25$, compared to -0.17 from test case 3. The total force on the window for test case 4 was 37.0 lbf suction.

Figure 19 illustrates test case 5, which was conducted at -4° α and 0° β. The leading-edge area of high pressure ($C_P > 0$) was the smallest yet, as compared to the previous test cases. The local suction region forward of the window was the strongest of the test cases discussed so far with a $C_P \leq -0.5$. The center window area experienced a relatively constant pressure of $C_P \approx -0.35$. There was no significant pressure gradient at the window trailing edge, as in test case 3. The total force on the window for test case 5 was 48.7 lbf suction.

Figure 20 illustrates test case 6, which was conducted at 0° α and -2.5° β. This test case was the first in the series of non-zero sideslip runs. The leading-edge area of high pressure is skewed slightly in the direction of the sideslip. The model was tested upside down, so negative sideslip angles *appear* as relative wind coming from the right. The local suction region located forward of the window is similar to test case 1, but it was skewed slightly due to the -2.5° β. The center window area experienced a relatively constant pressure of $C_P \approx -0.27$. Located at position (-4, -12) on Figure 20, a small local suction region developed due to the -2.5° β. The total force on the window for test case 6 was 41.1 lbf suction.

Figure 21 illustrates test case 7, which was conducted at 0° α and -5° β. This test case was similar to the previous one, except the skew

angle of the leading-edge area of high pressure was more pronounced. The local suction region located forward of the window was also more skewed than test case 6. The center window area experienced a relatively constant pressure of $C_P \approx -0.30$. The leeward local suction region at position (-4,-12) increased in strength, compared to test case 6. The total force on the window for test case 7 was 44.9 lbf suction.

Figure 22 illustrates test case 8, which was conducted at 0° α and +2.5° β. This run was the mirror image of test case 6. The results were similar to test case 6, except that the skew angle of the pressure field was in the opposite direction due to +2.5° β, vice -2.5° β. The total force on the window for test case 8 was 46.2 lbf suction.

Figure 23 illustrates test case 9, which was conducted at 0° α and +5° β. This run was the mirror image of test case 7. The results were similar to test case 7, except that the skew angle of the pressure field was in the opposite direction due to +5° β, vice -5° β. The total force on the window for test case 9 was 50.7 lbf suction.

Figure 24 illustrates test case 10, which was conducted at -4° α and –2.5° β. This test case was the first in the series of ones examining the combination of non-zero α and β. The leading-edge area of high pressure was relatively small (similar to test case 5) and also had the skew angle due to the –2.5° β. The local suction region located in front of the window was strong (similar to test case 5), but was more skewed than test case 6. Apparently, the -4° α in combination with the –2.5° β increased the skew angle effect of the pressure field. The center window area experienced a relatively constant pressure of $C_P \approx -0.34$. The total force on the window for test case 10 was 52.2 lbf suction.

Figure 25 illustrates test case 11, which was conducted at -4° α and –5° β. At the maximum negative α and β, these results were similar to test case 10. The skew angle effect was more pronounced than test case

33

10 due to the $-5°$ β, vice the $-2.5°$ β. Otherwise, the results of test cases 10 and 11 were very similar. The total force on the window for test case 11 was 51.1 lbf suction.

Figure 26 illustrates test case 12, which was conducted at $-4°$ α and $+2.5°$ β. This run was the mirror image of test case 10. The results were similar to test case 10, except that the skew angle of the pressure field was in the opposite direction due to $+2.5°$ β, vice $-2.5°$ β. The total force on the window for test case 12 was 50.5 lbf suction.

Figure 27 illustrates test case 13, which was conducted at $-4°$ α and $+5°$ β. This run was the mirror image of test case 11. The results were similar to test case 11, except that the skew angle of the pressure field was in the opposite direction due to $+5°$ β, vice $-5°$ β. The total force on the window for test case 13 was 53.2 lbf suction.

Figure 28 illustrates test case 14, which was conducted at $+4°$ α and $+5°$ β. The leading-edge area of high pressure was similar to test case 4, except that it was skewed similar to test case 9. The local suction region located in front of the window was similar to test case 4 in strength with $C_P \approx -0.43$. The center window area experienced a relatively constant pressure of $C_P \approx -0.27$. The $+5°$ β caused a local suction region on the leeward surface of the fairing located at position $(+5,-12)$ with a pressure of $C_P \approx -0.44$. The total force on the window for test case 14 was 45.2 lbf suction.

Figure 29 illustrates test case 15, which was conducted at $+4°$ α and $+2.5°$ β. The results of this run were similar to test case 14, except that the skew angle was less pronounced because of the $+2.5°$ β, vice $+5°$ β. The center window area experienced the same relatively constant pressure as test case 14. The total force on the window for test case 15 was 43.8 lbf suction.

Figure 30 illustrates test case 16, which was conducted at +4° α and -2.5° β. This run was the mirror image of test case 15. The results were similar to test case 15, except that the skew angle of the pressure field was in the opposite direction due to -2.5° β, vice +2.5° β. The total force on the window for test case 16 was 40.3 lbf suction.

Figure 31 illustrates test case 17, which was conducted at +4° α and -5° β. This run was the mirror image of test case 14. The results were similar to test case 14, except that the skew angle of the pressure field was in the opposite direction due to -5° β, vice +5° β. The total force on the window for test case 17 was 43.2 lbf suction.

Figure 32 illustrates test case 18, which was conducted at 0° α and -0° β with the external antenna installed. The purpose of this run was to determine what effect, if any, the presence of the external antenna had on the measured surface pressures. When compared to test case 1, which was conducted at the same α and β with no external antenna installed, these two pressure contour patterns were very similar. There did exist a very small asymmetry in the pressure field on the antenna side of the fairing, but this had a minimal effect on the window pressures.

The model antenna was not constructed at the time the first 17 test cases were conducted. Given the results of test case 18, the presence of the external antenna was deemed as insignificant as it relates to the surface pressure measurements on the window. Therefore, the previous 17 test cases were not repeated with the external antenna installed. The total force on the window for test case 18 was 46.9 lbf suction.

In summary, as α increased, the contour lines where suction pressure began ($C_P = 0$) moved aft toward the optical window. When β was non-zero, the asymmetry of the pressure contour patterns on the lee corner of the fairing illustrated a local suction region. This agrees with what one would intuitively expect. For all 18 test cases, relatively

constant pressures were measured across the aft one-third of the fairing. This indicates that the flow was probably separated in this aft region of the fairing.

Recall that only the right side of the forward and aft sections of the model was instrumented for pressure measurements. Left side data was mirrored from the appropriate right side data, as determined by the Sideslip angle β. For $\beta=0$, current test case data was mirrored from the right to the left side. For non-zero β, data from the opposite-sign β test case was mirrored from the right side to the left.

The optical window area experiences relatively constant C_P for every test case configuration. This observation is significant in that it suggests that the position of the optical window is relatively well suited, in terms of minimizing distortions due to large pressure gradients across the surface of the glass. Test cases 1 through 17 were conducted with no external antenna installed on the model. Test case 18 was conducted with the external antenna installed on the model. It was determined that the measured C_P variation due to the presence of the antenna was negligible. Therefore, test case configurations 1 through 17 were not repeated with the antenna installed.

3. Total Pressure Induced Forces on the Fairing Window

To determine a representative total force exerted on the optical window during flight, a flight condition of 100 KTAS at sea level was assumed. Q-bar at this condition equals 33.9 psf. Given this assumption, the calculated C_P at each pressure port on the window was converted to a local pressure and integrated across the area of the window. Summing these local pressures across each of their respective rectangular elemental areas results in the total pressure force on the window. The pressure exerted on the inside surface of the window was assumed to be freestream atmospheric. The dimensions of each rectangular area were determined by

36

equaling dividing the vertical and horizontal distances between each of the pressure ports located in the optical window area.

Test Case #	Window Force	Force/Q-bar	Test Case #	Window Force	Force/Q-bar
1	-51.3	-1.51	10	-52.2	-1.54
2	-40.4	-1.19	11	-51.1	-1.51
3	-40.4	-1.19	12	-50.5	-1.49
4	-37	-1.09	13	-53.2	-1.57
5	-48.7	-1.44	14	-45.2	-1.33
6	-41.1	-1.21	15	-43.8	-1.29
7	-44.9	-1.32	16	-40.3	-1.19
8	-46.2	-1.36	17	-43.2	-1.27
9	-50.7	-1.50	18	-46.9	-1.38

Note: test case #18 conducted with antenna installed

Table 3. Summary of Window Force for the 18 Test Cases

Table 3 depicts the total pressure force exerted on the window (measured in lbf) for each of the 18 test cases. The window force varies from 37 lbf suction for test case 4 and to about 53 lbf suction for test case 13. These total force figures were determined by extrapolating to full-scale. Also provided in Table 3 are the ratios of window force to Q-bar for each test case, so estimates at other freestream dynamic pressures can easily be made.

C. CENTERLINE LONGITUDINAL PRESSURE VARIATION

Sandia requested that pressure measurements also be taken on the upper fuselage section of the wind tunnel model. This information will assist them in their effort to properly position an external NACA vent to provide cooling for the onboard instrumentation. To accomplishment this, 25 pressure ports were installed along the centerline longitudinal axis of the upper fuselage section at two-inch intervals, as measured along the surface. One wind tunnel test run was conducted at zero α/zero β with ΔP = 20.5 psf.

37

Figure 33 illustrates how C_P varies along the upper fuselage of the full-scale airframe. The shape of this curve is similar to that of a typical airfoil section. Stagnation C_P is observed near the leading edge and peak suction occurs approximately ten inches measured longitudinally aft of the leading edge. This information can assist Sandia in optimizing the placement of an external cooling vent. Ideally, this air exhaust vent should be placed in the forward fuselage surface section where suction is maximized. This results in maximum cooling airflow. However, even aft of the suction peak, the pressure remains below its freestream value, providing sources for external venting.

Full Scale Upper Fuselage Cp vs Longitudinal Position
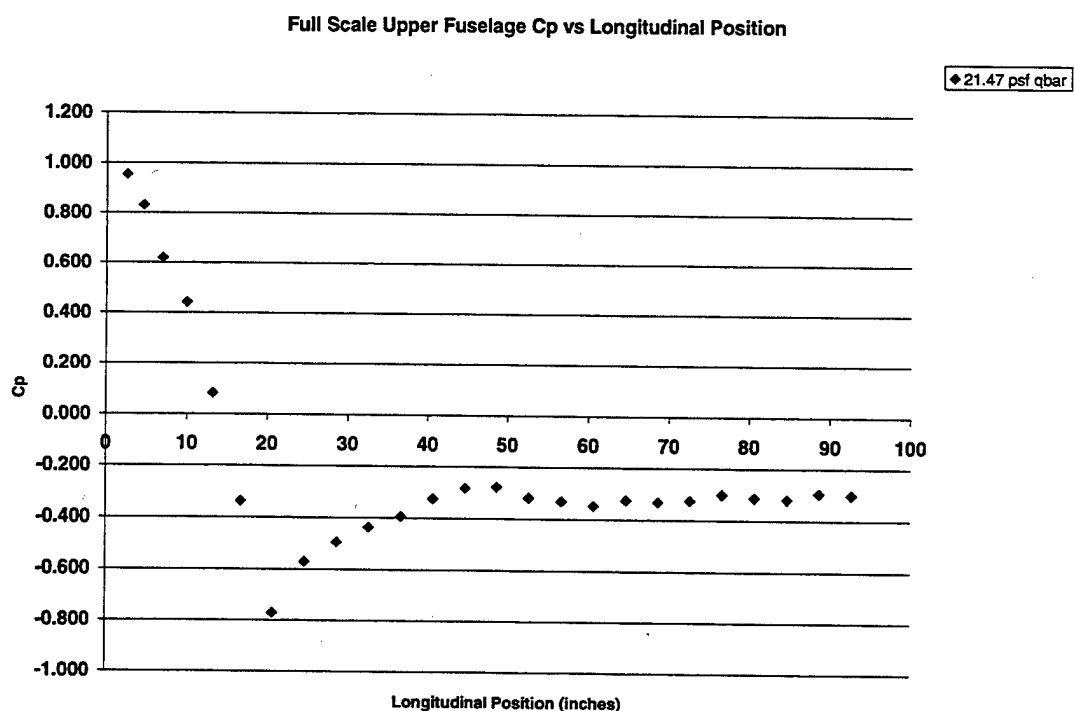
Figure 33. Upper Fuselage C_P vs Longitudinal Position

IV. CONCLUSIONS AND RECOMMENDATIONS

A. CONCLUSIONS

The surface pressures on the proposed aerodynamic fairing for the Altus II UAV have been successfully characterized. Using a half-scale model, a wind tunnel experiment conducted at one-half the Reynolds number experienced in full-scale flight has estimated the surface pressure coefficients. Two wind tunnel test runs were conducted initially to determine that this Reynolds number difference would be expected to have a minimal impact on data accuracy.

Seventeen wind tunnel test runs, conducted at various α and β combinations, illustrated the effect of small attitude changes on the fairing's surface pressures. Of particular interest was the fact that the pressure contours over the fairing's optical window remained relatively constant for these test runs. After measuring these window pressures, integration was performed to determine the estimated total force on the window area. Loads extrapolated to full scale varied from 37 to 53 lbf suction for a reference flight condition of 100 KTAS at sea level. An eighteenth test run determined that an antenna that was not available for the initial runs did not significantly affect the measured data.

Lastly, pressure ports were installed on the upper fuselage of the model to take pressure measurements along its centerline longitudinal axis. These measurements illustrated the position of peak suction and characterized the flow aft of this peak. This information may be used to optimize the installation of external exhaust vents used for payload cooling.

B. RECOMMENDATIONS

This study provides baseline information for Sandia's installation of the full-scale version of the proposed aerodynamic fairing onto the Altus

II UAV. The window forces that were calculated may be used to determine the required glass thickness needed to minimize weight, but also to minimize distortion. The pressure measurements on the upper fuselage may prove useful in optimizing the placement of external cooling vents.

For the Naval Postgraduate School, a more permanent test equipment set-up should be acquired for future AWT testing. Virtually all of the equipment used for this thesis research was borrowed from other research areas. The AWT is an excellent research tool for low speed testing, but it needs dedicated test equipment to realize its full potential.

APPENDIX A.   EXPERIMENTAL PROCEDURE CHECKLIST

This section contains the checklist used to operate the wind tunnel and run each of the 18 test cases. A single test case took approximately 40 minutes to conduct. The following checklist to conduct the wind tunnel experiment is presented below:

1. Ensure the Solenoid Controller, SDIU, Signal Conditioner, PC 486 and AWT Control Panel are turned ON.

2. Set model AOA and Sideslip.

3. Ensure the tunnel and test-section are clear of foreign objects and all access doors properly closed.

4. Calibrate the SDIU/Scanivalve with the stand-alone H_2O manometer. Using the Signal Conditioner, set the zero and span voltages which correspond to zero and 30 cm H_2O pressure. Zero pressure should read zero volts and 30 cm H2O pressure should read about negative 1.8 volts.

5. Select port #45 on the SDIU to ensure sufficient overlap of collected data. Select remote operation mode on the SDIU.

6. On the PC 486, NI *Labview* program starts automatically after bypassing the User Login. Select FILE – OPEN – "Vi.lib" – "SDIU 4-20-99" – "SVWorking". [Ref. 5]

7. Once the "SVWorking" VI is activated, enter the file path for the 3.5-inch floppy disk output data file. Enter "10" in the time delay field. Select ON for "Append to File".

8. At the AWT Control Panel, start the wind tunnel motor.

9. After the AWT motor has stabilized, slowly advance the fan pitch angle and set 10 cm H_2O indicated dynamic pressure on the AWT H_2O manometer.

10. Activate the Iterative run option on the "SVWorking" VI.

11. After "SVWorking" has measured and recorded the data from all 48 ports, stop the VI. Change the pressure manifold on the Scanivalve to the next one. Select local mode on the SDIU, reselect port #46 and return the SDIU to remote mode. Restart the VI to begin measuring and recording pressure data again. Repeat this procedure for each of the three pressure manifolds, for each test case.

12. Use Notepad or another similar ASCII text editor to verify the data recording on the 3.5-inch floppy. Remove overlapping data elements and transfer the edited data into a Microsoft Excel spreadsheet program for further data reduction.

APPENDIX B.   MICROSOFT EXCEL SPREADSHEETS

This section includes the Microsoft Excel spreadsheets used for each of the 18 test cases. Also included is an expanded discussion of how Scanivalve/SDIU voltage measurements are converted to pressure measurements. The last two spreadsheets illustrate how the pressure forces on the optical window are integrated across its area to determine the total exerted force.

For each test case, SDIU voltage readings are imported into the left-most columns of each Excel worksheet. Next, the voltages were converted to pressure measured in pounds/foot^2 using the following relations:

$$Pressure\,(psf) = \frac{30\,cm\,H_2O}{-1.8\,Volts} \times \frac{2116.2\,psf}{1033.68\,cm\,H_2O}$$

The calibration voltage of -1.8 volts corresponding to 30 cm H_2O on the stand-alone manometer varied slightly for each test run, but the basic conversion equation remained the same for all the runs. Recall that the pressure measured in Scanivalve port #1 was subtracted from all of the other 47 ports for all 18 test cases. This was the zero reference correction discussed in Chapter III Section B.

In the last column set, the C_P is determined with the tunnel calibration and blockage correction applied according to the following equation:

$$C_P = \left\{ \frac{p - p_\infty}{[.98831 + .00102 \times (qbar)] \times qbar} \right\} \times \left(\frac{V_2}{V_1} \right)^2, \text{ where } Qbar = p_{total} - p_\infty \text{ and}$$

$$\varepsilon = \frac{V_2 - V_1}{V_1} = \frac{1}{4} \times \frac{Model\,Frontal\,Area}{Test\,Section\,Area}. \text{ So, therefore } \frac{V_2}{V_1} = \varepsilon + 1.$$

The spreadsheets are presented in the following pages.

43

Port #	SDIU(V) +4 A-10cm	SDIU(V) +4 B-10cm	SDIU(V) +4 C-10cm	SDIU(V) -4 A-10cm	SDIU(V) -4 B-10cm	SDIU(V) -4 C-10cm	+4 A Pg-psf	+4 B Pg-psf	+4 C Pg-psf	-4 A Pg-psf	-4 B Pg-psf	-4 C Pg-psf	+4 A-Cp	+4 B-Cp	+4 C-Cp	-4 A-Cp	-4 B-Cp	-4 C-Cp
1	0.00E+00	0.00E+00	0.00E+00	0.00E+00	1.22E-02	3.66E-02	0.00	0.00	0.00	0.45	-0.45	-1.34	0.000	0.000	0.000	0.026	-0.010	-0.053
2	0.00E+00	0.00E+00	0.00E+00	0.00E+00	1.83E-02	3.97E-02	0.00	0.00	0.00	0.11	-0.22	-0.11	0.000	0.000	0.000	0.000	0.000	0.000
3	5.74E-01	5.62E-01	3.83E-01	5.49E-01	5.43E-01	5.07E-01	20.98	20.53	21.31	20.53	20.31	19.86	0.939	0.939	0.939	0.939	0.939	0.939
4	-9.46E-02	1.59E-01	1.80E-01	3.05E-03	2.29E-01	1.98E-01	3.46	-5.80	-6.58	0.33	-7.92	-5.91	0.155	-0.290	-0.290	0.010	-0.352	-0.273
5	-1.46E-01	1.56E-01	1.68E-01	0.00E+00	2.08E-01	1.98E-01	6.36	-5.69	-6.14	0.45	-7.14	-5.91	0.240	-0.260	-0.270	0.015	-0.316	-0.273
6	-1.40E-01	1.37E-01	1.83E-01	0.00E+00	2.26E-01	1.98E-01	5.13	-5.02	-6.69	0.45	-7.81	-5.91	0.230	-0.230	-0.295	0.015	-0.347	-0.273
7	-8.41E-02	1.43E-01	1.65E-01	0.00E+00	2.04E-01	2.01E-01	2.34	-5.24	-6.02	0.45	-7.03	-6.02	0.105	-0.240	-0.265	0.015	-0.311	-0.278
8	-3.66E-02	1.59E-01	1.98E-01	7.02E-02	2.23E-01	2.20E-01	1.34	-5.80	-7.25	-2.12	-7.70	-6.69	0.060	-0.250	-0.319	-0.103	-0.342	-0.310
9	-2.14E-02	1.50E-01	1.77E-01	1.34E-01	2.38E-01	2.32E-01	0.78	-5.47	-6.47	-4.46	-8.26	-7.14	0.035	-0.250	-0.285	-0.210	-0.367	-0.331
10	0.00E+00	1.43E-01	1.68E-01	1.65E-01	2.38E-01	2.26E-01	0.00	-5.24	-6.14	-5.58	-8.14	-6.92	0.000	-0.240	-0.270	-0.262	-0.362	-0.320
11	1.83E-02	1.43E-01	1.68E-01	1.10E-01	2.35E-01	2.35E-01	-0.67	-5.24	-6.14	-3.67	-8.81	-7.25	-0.030	-0.240	-0.270	-0.169	-0.393	-0.336
12	3.05E-02	1.62E-01	1.80E-01	1.56E-01	2.53E-01	2.44E-01	-1.12	-5.91	-6.58	-5.24	-8.37	-7.59	-0.050	-0.270	-0.290	-0.246	-0.372	-0.352
13	5.19E-02	1.50E-01	1.83E-01	2.08E-01	2.41E-01	2.38E-01	-1.90	-5.47	-6.69	-7.14	-7.70	-7.25	-0.085	-0.050	-0.295	-0.334	-0.342	-0.341
14	7.63E-02	1.43E-01	2.04E-01	2.26E-01	2.23E-01	2.35E-01	-2.79	-5.24	-7.48	-7.81	-7.48	-7.14	-0.125	-0.240	-0.329	-0.364	-0.332	-0.336
15	1.25E-01	1.31E-01	1.98E-01	2.44E-01	2.17E-01	2.32E-01	-4.57	-4.80	-7.25	-8.48	-7.36	-7.14	-0.205	-0.219	-0.319	-0.395	-0.327	-0.331
16	1.77E-01	1.37E-01	1.98E-01	3.24E-01	2.14E-01	2.32E-01	-6.47	-5.02	-7.25	-11.38	-7.03	-7.03	-0.290	-0.230	-0.319	-0.529	-0.311	-0.331
17	1.98E-01	1.34E-01	1.92E-01	3.24E-01	2.04E-01	2.29E-01	-7.25	-4.91	-7.03	-11.38	-7.25	-7.48	-0.324	-0.230	-0.309	-0.529	-0.321	-0.346
18	2.08E-01	1.37E-01	1.83E-01	3.51E-01	2.11E-01	2.41E-01	-7.59	-5.02	-6.69	-12.38	-7.25	-7.25	-0.339	-0.225	-0.295	-0.575	-0.321	-0.336
19	2.26E-01	1.37E-01	1.95E-01	3.63E-01	2.11E-01	2.35E-01	-8.26	-5.02	-7.14	-12.83	-7.48	-7.59	-0.369	-0.230	-0.314	-0.595	-0.332	-0.352
20	2.96E-01	1.34E-01	2.04E-01	4.24E-01	2.17E-01	2.44E-01	-10.82	-4.91	-7.48	-15.06	-7.92	-7.48	-0.484	-0.225	-0.329	-0.698	-0.352	-0.346
21	2.99E-01	1.25E-01	2.01E-01	4.09E-01	2.29E-01	2.41E-01	-10.93	-4.57	-7.36	-14.50	-7.70	-7.48	-0.489	-0.209	-0.324	-0.672	-0.342	-0.346
22	3.11E-01	1.34E-01	2.04E-01	4.15E-01	2.23E-01	2.41E-01	-11.38	-4.91	-7.48	-14.73	-7.25	-7.59	-0.509	-0.225	-0.329	-0.682	-0.321	-0.352
23	2.44E-01	1.40E-01	2.08E-01	3.42E-01	2.11E-01	2.44E-01	-8.93	-5.13	-7.59	-12.05	-7.14	-8.14	-0.399	-0.214	-0.334	-0.559	-0.316	-0.362
24	2.56E-01	1.28E-01	2.23E-01	3.42E-01	2.08E-01	2.50E-01	-9.37	-4.69	-8.14	-12.27	-7.25	-7.92	-0.419	-0.235	-0.349	-0.570	-0.321	-0.367
25	2.72E-01	1.40E-01	2.17E-01	3.48E-01	2.11E-01	2.50E-01	-9.93	-5.13	-7.92	-12.27	-7.25	-8.14	-0.444	-0.230	-0.359	-0.570	-0.321	-0.362
26	2.75E-01	1.37E-01	2.23E-01	3.48E-01	2.11E-01	2.53E-01	-10.04	-5.02	-8.14	-12.72	-7.14	-7.48	-0.449	-0.209	-0.329	-0.590	-0.316	-0.388
27	2.69E-01	1.25E-01	2.04E-01	3.60E-01	2.08E-01	2.41E-01	-9.82	-4.57	-7.48	-10.15	-7.14	-8.37	-0.439	-0.214	-0.427	-0.472	-0.316	-0.346
28	2.17E-01	1.28E-01	2.66E-01	2.90E-01	2.08E-01	2.59E-01	-7.92	-4.69	-9.71	-9.93	-7.14	-8.14	-0.354	-0.189	-0.388	-0.462	-0.327	-0.378
29	2.14E-01	1.13E-01	2.84E-01	2.84E-01	2.14E-01	2.41E-01	-7.81	-4.13	-8.81	-9.82	-7.36	-7.48	-0.349	-0.199	-0.354	-0.457	-0.332	-0.346
30	2.11E-01	1.19E-01	2.20E-01	2.20E-01	2.17E-01	2.32E-01	-7.70	-4.35	-8.03	-9.82	-7.48	-7.03	-0.344	-0.235	-0.349	-0.457	-0.321	-0.331
31	2.17E-01	1.40E-01	2.17E-01	2.81E-01	2.11E-01	2.29E-01	-7.92	-5.13	-7.92	-9.71	-7.25	-6.69	-0.354	-0.219	-0.359	-0.452	-0.327	-0.325
32	2.08E-01	1.40E-01	2.23E-01	2.78E-01	2.14E-01	2.17E-01	-7.59	-5.13	-8.14	-10.04	-7.36	-6.58	-0.339	-0.240	-0.324	-0.467	-0.321	-0.310
33	2.14E-01	1.31E-01	2.01E-01	2.87E-01	2.11E-01	2.20E-01	-7.81	-4.80	-7.36	-12.36	-7.25	-6.69	-0.349	-0.219	-0.309	-0.573	-0.327	-0.304
34	2.17E-01	1.43E-01	1.92E-01	3.50E-01	2.14E-01	2.17E-01	-7.92	-5.24	-7.03	-9.71	-7.48	-6.69	-0.314	-0.245	-0.354	-0.452	-0.332	-0.310
35	1.92E-01	1.46E-01	2.20E-01	2.78E-01	2.14E-01	2.20E-01	-7.03	-5.36	-8.03	-8.37	-7.36	-6.58	-0.285	-0.240	-0.433	-0.390	-0.321	-0.310
36	1.74E-01	1.40E-01	2.41E-01	2.41E-01	2.17E-01	2.14E-01	-6.36	-5.13	-9.83	-8.48	-7.25	-6.69	-0.295	-0.235	-0.370	-0.395	-0.332	-0.304
37	1.80E-01	1.31E-01	2.44E-01	2.44E-01	2.11E-01	2.20E-01	-6.58	-4.80	-8.40	-8.59	-7.36	-6.58	-0.300	-0.219	-0.401	-0.400	-0.321	-0.310
38	1.83E-01	1.53E-01	2.47E-01	2.47E-01	2.14E-01	2.17E-01	-6.69	-5.58	-9.12	-8.48	-7.59	-7.03	-0.300	-0.255	-0.451	-0.395	-0.327	-0.304
39	1.83E-01	1.43E-01	2.44E-01	2.44E-01	2.20E-01	2.29E-01	-6.69	-5.24	-10.24	-8.37	-7.81	-6.47	-0.295	-0.240	-0.311	-0.390	-0.337	-0.325
40	1.80E-01	1.56E-01	2.41E-01	2.41E-01	2.26E-01	2.14E-01	-6.58	-5.69	-7.07	-8.48	-7.48	-6.47	-0.285	-0.260	-0.275	-0.395	-0.332	-0.299
41	1.74E-01	1.56E-01	2.44E-01	2.44E-01	2.17E-01	2.14E-01	-6.36	-5.69	-6.25	-8.81	-7.48	-7.70	-0.290	-0.260	-0.368	-0.410	-0.342	-0.299
42	1.77E-01	1.62E-01	2.53E-01	2.53E-01	2.17E-01	2.47E-01	-6.47	-5.91	-8.37	-9.82	-7.70	-7.48	-0.304	-0.270	-0.289	-0.457	-0.342	-0.357
43	1.86E-01	1.62E-01	2.81E-01	2.81E-01	2.23E-01	2.41E-01	-6.81	-5.91	-6.56		-7.70			-0.270			-0.362	-0.346
44		1.68E-01			2.29E-01			-6.14		-7.92				-0.281				
45		1.62E-01			2.17E-01			-5.91		-7.48				-0.270				
46		1.59E-01			2.35E-01			-5.80		-8.14				-0.265				
47		1.56E-01						-5.69						-0.260				
48		1.68E-01						-6.14						-0.281				

Pa = 30.20 in Hg
Ta = 65 deg F

Run Order		
C	T Inf = 63	deg F
B	T Inf = 66	deg F
A	T Inf = 68	deg F
A	T Inf = 67	deg F
B	T Inf = 70	deg F
C	T Inf = 72	deg F

Notes:
1) Schmidler: 30 cm H2O = -1.68 V
2) add 0.6 cm H2O to Schmidter pressure reading
3) Run 1 - 10.3 cm speed; Run 2 - 10.2 cm speed
4) 10 msec data read time delay

Test 520

Port #	SDIU (V) 0 AOA / -2.5 SS A-10cm	B-10cm	C-10cm	SDIU (V) 0 AOA / -5.0 SS A-10cm	B-10cm	C-10cm	0 AOA / -2.5 SS A Pg-psf	B Pg-psf	C Pg-psf	0 AOA / -5.0 SS A Pg-psf	B Pg-psf	C Pg-psf	0 AOA / -2.5 SS A-Cp	B-Cp	C-Cp	0 AOA / -5.0 SS A-Cp	B-Cp	C-Cp
1	0.00E+00	0.00E+00	0.00E+00	0.00E+00	0.00E+00	3.66E-02	0.00	0.00	0.00	0.00	0.00	-1.35	0.000	0.000	0.000	0.000	-0.015	-0.062
2	0.00E+00	0.00E+00	0.00E+00	0.00E+00	6.10E-03	3.05E-03	0.00	0.00	0.00	0.00	0.11	0.11	0.000	0.000	0.000	0.000	0.000	0.000
3	-5.55E-01	-5.66E-01	-5.71E-01	-5.49E-01	-5.71E-01	-5.62E-01	20.55	21.00	21.12	20.32	21.34	22.13	0.939	0.938	0.938	0.939	0.938	0.937
4	-7.02E-02	1.92E-01	1.86E-01	-8.85E-02	2.26E-01	2.26E-01	2.60	-7.11	-6.89	3.27	-8.13	-7.00	0.119	-0.318	-0.306	0.151	-0.364	-0.303
5	-8.55E-02	1.86E-01	1.83E-01	-7.32E-02	2.11E-01	2.23E-01	3.16	-6.89	-6.77	2.71	-7.57	-6.89	0.144	-0.308	-0.301	0.125	-0.339	-0.298
6	-7.63E-02	1.77E-01	1.89E-01	-6.41E-02	1.95E-01	2.17E-01	2.82	-6.55	-7.00	2.37	-7.00	-6.66	0.129	-0.293	-0.311	0.110	-0.314	-0.288
7	-4.88E-02	1.62E-01	1.71E-01	-6.41E-02	1.80E-01	1.86E-01	1.81	-5.98	-6.32	2.37	-8.44	-5.53	0.083	-0.267	-0.281	0.110	-0.289	-0.240
8	-6.10E-03	1.74E-01	1.95E-01	-2.75E-02	2.04E-01	2.35E-01	0.23	-6.44	-7.23	1.02	-7.34	-7.34	0.010	-0.288	-0.321	0.047	-0.329	-0.317
9	5.19E-02	1.74E-01	1.80E-01	4.88E-02	2.04E-01	2.17E-01	-1.92	-6.32	-6.66	-1.81	-7.34	-6.66	-0.088	-0.283	-0.296	-0.083	-0.329	-0.288
10	8.55E-02	1.71E-01	1.80E-01	1.01E-01	2.04E-01	2.20E-01	-3.16	-6.44	-6.66	-3.73	-6.77	-6.77	-0.144	-0.288	-0.296	-0.172	-0.304	-0.293
11	3.66E-02	1.74E-01	1.77E-01	1.83E-02	1.89E-01	2.17E-01	-1.35	-6.55	-6.55	-0.68	-7.11	-6.66	-0.062	-0.288	-0.291	-0.031	-0.319	-0.288
12	8.85E-02	1.77E-01	1.83E-01	9.77E-02	1.98E-01	2.23E-01	-3.27	-6.55	-6.77	-3.61	-7.00	-6.89	-0.150	-0.293	-0.301	-0.167	-0.314	-0.298
13	1.34E-01	1.68E-01	1.92E-01	1.53E-01	1.95E-01	2.29E-01	-4.97	-6.21	-7.11	-5.65	-6.44	-7.11	-0.227	-0.277	-0.316	-0.261	-0.289	-0.308
14	1.59E-01	1.59E-01	2.04E-01	1.65E-01	1.80E-01	2.29E-01	-5.87	-5.87	-7.57	-6.10	-6.21	-7.11	-0.268	-0.262	-0.336	-0.282	-0.279	-0.308
15	1.50E-01	1.62E-01	1.95E-01	1.65E-01	1.74E-01	2.23E-01	-5.53	-5.98	-7.23	-6.10	-6.55	-6.89	-0.253	-0.267	-0.321	-0.282	-0.294	-0.298
16	2.50E-01	1.56E-01	1.98E-01	2.72E-01	1.83E-01	2.26E-01	-9.26	-5.76	-7.34	-10.05	-6.32	-7.00	-0.423	-0.257	-0.326	-0.464	-0.284	-0.303
17	2.62E-01	1.53E-01	1.92E-01	2.81E-01	1.77E-01	2.26E-01	-9.71	-5.65	-7.11	-10.39	-6.77	-7.00	-0.444	-0.252	-0.316	-0.480	-0.304	-0.303
18	2.72E-01	1.53E-01	1.98E-01	2.96E-01	1.89E-01	2.32E-01	-10.05	-5.85	-7.34	-10.95	-6.10	-7.23	-0.459	-0.252	-0.326	-0.506	-0.274	-0.312
19	2.87E-01	1.50E-01	1.98E-01	3.14E-01	1.71E-01	2.35E-01	-10.61	-5.53	-7.34	-11.63	-6.77	-7.34	-0.485	-0.247	-0.326	-0.537	-0.304	-0.317
20	3.54E-01	1.53E-01	2.01E-01	4.03E-01	1.89E-01	2.38E-01	-13.10	-5.65	-7.45	-14.90	-6.55	-7.45	-0.598	-0.252	-0.331	-0.689	-0.294	-0.322
21	3.54E-01	1.62E-01	1.98E-01	3.69E-01	1.83E-01	2.38E-01	-13.10	-5.98	-7.34	-13.66	-7.11	-7.45	-0.598	-0.267	-0.326	-0.631	-0.319	-0.322
22	3.60E-01	1.59E-01	2.20E-01	3.91E-01	1.98E-01	2.41E-01	-13.32	-5.87	-8.13	-14.45	-6.21	-7.57	-0.609	-0.262	-0.361	-0.668	-0.279	-0.327
23	3.02E-01	1.59E-01	2.04E-01	3.42E-01	1.74E-01	2.35E-01	-11.18	-5.87	-7.57	-12.65	-5.87	-7.34	-0.511	-0.262	-0.336	-0.584	-0.264	-0.317
24	3.11E-01	1.46E-01	2.14E-01	3.36E-01	1.65E-01	2.44E-01	-11.52	-5.42	-7.90	-12.42	-6.21	-7.68	-0.526	-0.242	-0.351	-0.574	-0.279	-0.332
25	2.87E-01	1.56E-01	2.14E-01	3.36E-01	1.74E-01	2.59E-01	-10.61	-5.76	-7.90	-12.42	-6.10	-8.24	-0.485	-0.257	-0.351	-0.574	-0.274	-0.356
26	2.96E-01	1.46E-01	2.17E-01	3.39E-01	1.71E-01	2.50E-01	-10.95	-5.42	-8.02	-12.53	-5.87	-7.90	-0.500	-0.242	-0.356	-0.579	-0.264	-0.341
27	3.05E-01	1.40E-01	1.86E-01	3.27E-01	1.65E-01	2.38E-01	-11.29	-5.19	-6.89	-12.08	-6.10	-7.45	-0.516	-0.232	-0.306	-0.558	-0.264	-0.322
28	2.56E-01	1.40E-01	2.44E-01	2.90E-01	1.65E-01	2.75E-01	-9.48	-5.19	-9.03	-10.73	-5.87	-8.81	-0.433	-0.232	-0.401	-0.496	-0.264	-0.380
29	2.41E-01	1.50E-01	2.35E-01	2.78E-01	1.71E-01	2.59E-01	-8.92	-5.53	-8.69	-10.28	-6.10	-8.24	-0.408	-0.247	-0.386	-0.475	-0.274	-0.356
30	2.41E-01	1.43E-01	1.89E-01	2.59E-01	1.77E-01	2.35E-01	-9.60	-5.31	-7.00	-9.60	-6.32	-7.34	-0.408	-0.237	-0.311	-0.443	-0.284	-0.317
31	2.44E-01	1.53E-01	1.86E-01	2.75E-01	1.83E-01	2.38E-01	-9.03	-5.65	-6.89	-10.16	-6.55	-7.45	-0.413	-0.252	-0.306	-0.470	-0.294	-0.322
32	2.47E-01	1.56E-01	2.01E-01	2.62E-01	1.74E-01	2.26E-01	-9.15	-5.76	-7.45	-9.71	-7.23	-7.00	-0.418	-0.257	-0.331	-0.449	-0.324	-0.303
33	2.44E-01	1.43E-01	1.80E-01	2.66E-01	1.80E-01	2.20E-01	-9.03	-5.31	-6.66	-9.82	-7.11	-6.77	-0.413	-0.237	-0.296	-0.454	-0.319	-0.293
34	2.59E-01	1.56E-01	1.83E-01	2.78E-01	1.83E-01	2.23E-01	-9.60	-5.76	-6.77	-10.28	-6.66	-6.89	-0.438	-0.257	-0.301	-0.475	-0.299	-0.298
35	2.47E-01	1.56E-01	1.95E-01	2.90E-01	1.80E-01	2.32E-01	-9.15	-5.76	-7.23	-10.73	-6.77	-7.23	-0.418	-0.257	-0.321	-0.496	-0.304	-0.312
36	2.08E-01	1.53E-01	1.77E-01	2.41E-01	1.83E-01	2.23E-01	-7.68	-5.65	-6.55	-8.92	-7.23	-6.89	-0.351	-0.252	-0.291	-0.412	-0.324	-0.298
37	2.04E-01	1.53E-01	1.89E-01	2.35E-01	1.83E-01	2.32E-01	-7.57	-5.65	-7.00	-8.69	-7.34	-7.23	-0.346	-0.252	-0.311	-0.402	-0.329	-0.312
38	2.17E-01	1.62E-01	2.04E-01	2.29E-01	1.83E-01	2.38E-01	-8.02	-5.98	-7.57	-8.47	-7.45	-7.45	-0.366	-0.267	-0.336	-0.391	-0.334	-0.322
39	2.11E-01	1.59E-01	2.04E-01	2.32E-01	1.86E-01	2.38E-01	-7.79	-5.87	-7.57	-8.58	-6.66	-7.45	-0.356	-0.262	-0.336	-0.396	-0.299	-0.322
40	2.08E-01	1.71E-01	1.43E-01	2.32E-01	2.01E-01	2.11E-01	-7.68	-6.32	-5.31	-8.58	-7.00		-0.351	-0.283	-0.236	-0.396	-0.324	-0.279
41	2.04E-01	1.59E-01	1.56E-01	2.23E-01	1.98E-01	2.08E-01	-7.57	-5.87	-5.76	-8.24	-7.45		-0.346	-0.262	-0.256	-0.381	-0.319	-0.274
42	2.08E-01	1.71E-01	2.26E-01	2.35E-01	1.89E-01	2.35E-01	-7.68	-6.32	-8.36	-8.69	-6.77		-0.351	-0.283	-0.371	-0.402	-0.304	-0.317
43	2.17E-01	1.80E-01	1.65E-01	2.35E-01	2.01E-01	2.11E-01	-8.02	-6.66	-6.10	-8.69	-7.23		-0.366	-0.298	-0.271	-0.402	-0.324	-0.279
44		1.77E-01			2.04E-01			-6.55			-7.34			-0.293			-0.329	
45		1.74E-01			2.06E-01			-6.44			-7.45			-0.288			-0.334	
46		1.65E-01			1.86E-01			-6.10			-6.66			-0.272			-0.299	
47		1.74E-01			1.95E-01			-6.44			-7.00			-0.288			-0.314	
48		1.74E-01			2.08E-01			-6.44			-7.45			-0.288			-0.334	

Pa = 30.20 In Hg
Ta = 65 deg F

Run Order			
C	T Inf =	63	deg F
B	T Inf =	65	deg F
A	T Inf =	68	deg F
A	T Inf =	68	deg F
B	T Inf =	70	deg F
C	T Inf =	72	deg F

Notes:
1) Schmidler: 30 cm H2O = -1.66 V
2) add 0.6 cm H2O to Schmidler pressure reading
3) Run 1 - 10.2 cm speed; Run 2 - 10.6 cm speed
4) 10 msec data read time delay

Test 524

Manifold Port #	SDIU (V) 0 AOA / -2.5 SS			SDIU (V) 0 AOA / +5.0 SS			0 AOA / -2.5 SS			0 AOA / +5.0 SS			0 AOA / -2.5 SS			0 AOA / +5.0 SS		
	A -10 cm	B -10 cm	C -10 cm	A -10 cm	B -10 cm	C -10 cm	A Pg-psf	B Pg-psf	C Pg-psf	A Pg-psf	B Pg-psf	C Pg-psf	A - Cp	B - Cp	C - Cp	A - Cp	B - Cp	C - Cp
1	6.71E-02	2.16E-02	6.71E-02	6.71E-02	8.86E-02	7.63E-02	-1.13	3.18	-2.25	-1.13	2.97	2.56	0.028	-0.271	-0.326	-0.025	-0.259	-0.299
2	5.19E-02	4.88E-02	4.88E-02	5.19E-02	5.19E-02	6.80E-02	0.61	1.54	0.61	0.51	1.13	0.61	0.079	-0.281	-0.366	0.054	-0.299	-0.313
3	5.68E-01	6.17E-01	5.28E-01	5.31E-01	5.31E-01	5.28E-01	21.30	21.43	19.07	20.08	20.79	20.28	0.116	-0.313	-0.341	0.084	-0.338	-0.333
4	3.36E-02	2.29E-01	2.53E-01	6.71E-02	2.17E-01	2.44E-01	1.13	-4.51	-6.25	-4.30	-4.30	-5.63	0.042	-0.271	-0.376	-0.039	-0.289	-0.269
5	0.00E+00	2.35E-01	2.78E-01	1.83E-02	2.41E-01	2.53E-01	2.25	-4.71	-7.07	1.64	-5.12	-5.84	-0.032	-0.304	-0.361	-0.118	-0.343	-0.377
6	-2.44E-02	2.56E-01	2.78E-01	0.00E+00	2.66E-01	2.66E-01	3.07	-5.43	-7.07	2.25	-5.94	-6.35	-0.092	-0.313	-0.366	-0.148	-0.357	-0.387
7	2.44E-02	2.29E-01	2.62E-01	7.63E-02	2.35E-01	2.26E-01	1.43	-4.51	-6.56	-0.31	-4.92	-5.02	-0.143	-0.313	-0.366	-0.172	-0.347	-0.377
8	7.32E-02	2.50E-01	2.84E-01	1.25E-01	2.69E-01	2.93E-01	-0.20	-5.22	-7.27	-1.95	-6.04	-7.27	-0.171	-0.331	-0.391	-0.216	-0.416	-0.406
9	1.13E-01	2.56E-01	2.75E-01	1.43E-01	2.78E-01	2.99E-01	-1.54	-5.43	-6.96	-2.56	-6.35	-7.48	-0.171	-0.322	-0.398	-0.271	-0.372	-0.411
10	1.46E-01	2.56E-01	2.78E-01	1.59E-01	2.72E-01	2.93E-01	-2.66	-5.43	-7.07	-3.07	-6.15	-7.27	-0.231	-0.294	-0.388	-0.285	-0.343	-0.421
11	1.65E-01	2.56E-01	2.78E-01	2.04E-01	2.84E-01	2.93E-01	-3.28	-5.43	-7.07	-4.61	-6.56	-7.89	-0.268	-0.290	-0.396	-0.418	-0.343	-0.408
12	1.65E-01	2.69E-01	2.93E-01	1.86E-01	2.87E-01	3.11E-01	-3.28	-5.84	-7.58	-3.99	-7.58	-7.99	-0.338	-0.294	-0.381	-0.448	-0.333	-0.396
13	2.04E-01	2.62E-01	2.96E-01	2.20E-01	2.69E-01	3.14E-01	-4.61	-5.63	-7.68	-5.12	-6.66	-7.99	-0.435	-0.271	-0.386	-0.453	-0.313	-0.401
14	2.29E-01	2.44E-01	2.90E-01	2.29E-01	2.62E-01	3.20E-01	-5.43	-5.02	-7.48	-6.04	-6.04	-8.19	-0.435	-0.290	-0.396	-0.517	-0.323	-0.401
15	2.75E-01	2.44E-01	2.96E-01	3.11E-01	2.50E-01	3.11E-01	-6.96	-4.92	-7.68	-8.19	-5.84	-7.99	-0.476	-0.290	-0.376	-0.522	-0.308	-0.431
16	3.39E-01	2.44E-01	2.87E-01	3.30E-01	2.56E-01	3.05E-01	-9.12	-5.02	-7.37	-8.81	-5.84	-7.68	-0.527	-0.281	-0.406	-0.635	-0.382	-0.416
17	3.39E-01	2.90E-01	2.90E-01	3.33E-01	2.47E-01	3.05E-01	-9.12	-4.51	-7.48	-8.91	-5.63	-7.78	-0.610	-0.285	-0.416	-0.654	-0.328	-0.428
18	3.66E-01	2.41E-01	2.96E-01	3.72E-01	2.59E-01	3.08E-01	-10.04	-4.92	-7.68	-10.24	-5.63	-7.78	-0.638	-0.304	-0.418	-0.650	-0.357	-0.426
19	4.00E-01	2.35E-01	2.84E-01	3.75E-01	2.93E-01	3.17E-01	-11.16	-4.71	-7.27	-10.34	-5.33	-8.40	-0.555	-0.276	-0.411	-0.586	-0.333	-0.431
20	4.55E-01	2.38E-01	3.02E-01	4.46E-01	2.78E-01	3.27E-01	-13.01	-5.22	-7.89	-12.70	-5.74	-8.30	-0.546	-0.276	-0.401	-0.566	-0.333	-0.445
21	4.73E-01	2.50E-01	3.08E-01	4.58E-01	2.62E-01	3.24E-01	-13.02	-4.81	-8.09	-13.01	-6.86	-8.09	-0.546	-0.290	-0.450	-0.571	-0.323	-0.460
22	4.18E-01	2.38E-01	3.05E-01	4.55E-01	2.56E-01	3.24E-01	-13.72	-5.22	-7.99	-11.68	-5.84	-8.40	-0.541	-0.262	-0.425	-0.566	-0.318	-0.436
23	4.12E-01	2.32E-01	3.30E-01	4.15E-01	2.53E-01	3.45E-01	-13.78	-4.81	-8.09	-13.11	-6.86	-8.40	-0.559	-0.287	-0.420	-0.595	-0.303	-0.509
24	4.12E-01	2.41E-01	2.99E-01	4.06E-01	2.44E-01	3.27E-01	-11.57	-4.61	-8.81	-13.01	-6.35	-8.71	-0.486	-0.258	-0.495	-0.512	-0.308	-0.485
25	4.12E-01	2.23E-01	2.41E-01	4.06E-01	2.50E-01	3.36E-01	-11.67	-4.92	-8.30	-11.68	-5.84	-8.09	-0.453	-0.271	-0.460	-0.472	-0.333	-0.450
26	4.09E-01	2.26E-01	3.14E-01	4.03E-01	2.62E-01	3.30E-01	-11.47	-4.61	-8.30	-11.27	-5.63	-8.30	-0.449	-0.271	-0.406	-0.467	-0.352	-0.450
27	4.21E-01	2.20E-01	3.11E-01	4.21E-01	2.66E-01	3.75E-01	-11.88	-4.30	-8.19	-11.27	-5.53	-8.50	-0.458	-0.290	-0.416	-0.477	-0.338	-0.455
28	3.72E-01	2.29E-01	3.36E-01	3.69E-01	2.69E-01	3.60E-01	-10.24	-4.40	-9.01	-11.88	-5.22	10.04	-0.458	-0.285	-0.406	-0.482	-0.343	-0.426
29	3.51E-01	2.41E-01	3.14E-01	3.54E-01	2.72E-01	3.39E-01	-9.53	-4.20	-8.19	10.14	-5.33	-8.81	-0.458	-0.299	-0.406	-0.512	-0.333	-0.377
30	3.48E-01	2.38E-01	3.08E-01	3.45E-01	2.59E-01	3.42E-01	-9.42	-4.51	-8.30	-9.63	-5.43	-8.81	-0.467	-0.299	-0.356	-0.443	-0.347	-0.426
31	3.54E-01	2.41E-01	3.02E-01	3.42E-01	2.59E-01	3.24E-01	-0.83	-4.92	-7.89	-9.32	-5.74	-9.12	-0.416	-0.304	-0.411	-0.418	-0.328	-0.465
32	3.54E-01	2.47E-01	3.08E-01	3.51E-01	2.84E-01	2.93E-01	-8.71	-4.81	-8.09	-9.22	-6.25	-8.81	-0.375	-0.290	-0.430	-0.423	-0.328	-0.343
33	3.60E-01	2.50E-01	2.72E-01	3.69E-01	2.81E-01	3.24E-01	-7.78	-4.81	-7.89	-9.42	-5.94	-8.91	-0.379	-0.290	-0.361	-0.418	-0.328	-0.357
34	3.27E-01	2.41E-01	3.05E-01	3.27E-01	2.72E-01	3.48E-01	-7.89	-5.12	-6.86	-9.53	-6.04	-8.30	-0.393	-0.290	-0.391	-0.423	-0.362	-0.450
35	3.27E-01	2.41E-01	2.50E-01	3.11E-01	2.84E-01	2.72E-01	-8.19	-5.22	-8.40	-10.14	-6.15	-8.30	-0.398	-0.294	-0.445	-0.408	-0.362	-0.269
36	2.99E-01	2.41E-01	2.41E-01	3.14E-01	2.78E-01	2.81E-01	-7.99	-4.92	-8.40	-8.71	-5.74	-9.12	-0.384	-0.304	-0.287	-0.418	-0.372	-0.269
37	3.02E-01	2.44E-01	2.75E-01	3.11E-01	2.59E-01	2.26E-01	-8.30	-4.92	-6.96	-8.19	-5.74	-8.56	-0.398	-0.308	-0.322	-0.347	-0.347	-0.367
38	3.11E-01	2.50E-01	2.93E-01	3.14E-01	2.78E-01	2.87E-01	-8.19	-4.92	-7.58	-8.30	-6.66	-6.88	-0.375	-0.308	-0.435	-0.472	-0.367	-0.254
39	3.14E-01	2.53E-01	3.27E-01	3.05E-01	2.75E-01	3.02E-01	-8.30	-5.02	-8.71	-8.30	-6.45	-8.81	-0.412	-0.313	-0.391	-0.423	-0.347	-0.357
40	3.05E-01	2.56E-01	2.29E-01	3.11E-01		9.16E-02	-7.99	-5.33	-6.43	-7.99	-6.66	-5.02	-0.384	-0.294	-0.445	-0.408	-0.362	-0.269
41	3.14E-01	2.53E-01	3.11E-01	3.14E-01		8.24E-02	-8.30	-5.33	-8.15	-8.19	-6.15	-5.02	-0.398	-0.304	-0.287	-0.418	-0.372	-0.269
42	2.99E-01	2.56E-01	3.20E-01	3.45E-01		8.24E-02	-7.78	-5.43	-8.50	-8.30	-6.15	-7.07	-0.398	-0.308	-0.322	-0.418	-0.347	-0.367
43	3.24E-01	2.56E-01	2.38E-01	9.16E-02		7.93E-02	-8.60	-5.43	-5.74	-9.32	-6.25	-4.71	-0.375	-0.308	-0.435	-0.423	-0.347	-0.254
44	9.16E-02	2.66E-01	8.55E-02	7.93E-02		7.93E-02		-5.74			-6.35		-0.327	-0.313	-0.391	-0.357	-0.357	
45	7.63E-02	2.56E-01	6.71E-02	7.93E-02				-5.43			-6.35			-0.313	-0.430		-0.357	
46	7.02E-02	2.59E-01	6.71E-02	7.32E-02				-5.43			-6.25			-0.313			-0.352	
47	7.02E-02	2.59E-01	7.02E-02	7.32E-02				-5.53			-6.25			-0.317			-0.352	
48	6.71E-02	2.66E-01	6.71E-02					-5.74			-7.17			-0.327			-0.396	

Pa = 30.14 in Hg
Ta = 64 deg F

Run Order		
B	T inf =	68 deg F
C	T inf =	70 deg F
A	T inf =	71 deg F
A	T inf =	72 deg F
B	T inf =	73 deg F
C	T inf =	74 deg F

Notes:
1) Schmidter: 30 cm H2O = -1.83 V
2) add 0.8 cm H2O to Schmidter pressure reading
3) Run 1 - 10.5 cm speed; Run 2 - 10.1 cm speed
4) 10 msec data read time delay

Test 526

Manifold Port #	SDIU (V) -4 AOA / 2.5 SS			SDIU (V) -4 AOA / -5.0 SS			-4 AOA / 2.5 SS			-4 AOA / -5.0 SS			-4 AOA / 2.5 SS			-4 AOA / -5.0 SS		
	A-10cm	B-10cm	C-10cm	A-10cm	B-10cm	C-10cm	A Pg-psi	B Pg-psi	C Pg-psi	A Pg-psi	B Pg-psi	C Pg-psi	A-Cp	B-Cp	C-Cp	A-Cp	B-Cp	C-Cp
1	0.00E+00	1.33E-02	4.27E-02	6.41E-01	7.63E-02	5.80E-02	0.00	-0.64	0.45	2.24	2.66	2.02	0.000	-0.035	0.094	0.034	0.183	0.130
2	2.11E-02	1.53E-02	4.27E-02	4.88E-02	4.66E-02	3.07E-02	0.75	0.11	0.53	0.53	1.06	0.64	0.000	0.000	0.000	0.000	0.000	0.000
3	6.04E-01	6.02E-01	5.44E-01	5.89E-01	5.07E-01	5.13E-01	21.09	20.23	20.66	20.55	20.34	19.92	0.939	0.939	0.939	0.939	0.940	0.940
4	4.27E-02	2.56E-01	2.38E-01	0.00E+00	2.59E-01	1.98E-01	-4.27E-02	-8.31	-8.82	1.49	-8.39	-4.90	0.034	-0.393	-0.343	0.080	-0.364	-0.270
5	-3.66E-02	2.23E-01	2.26E-01	2.75E-02	2.53E-01	2.78E-01	1.28	-7.14	-8.39	1.28	-8.18	-7.67	0.025	-0.348	-0.323	0.035	-0.353	-0.405
6	-6.10E-03	2.29E-01	2.17E-01	6.10E-01	2.69E-01	2.69E-01	0.21	-7.35	-6.07	0.11	-8.71	-7.35	-0.025	-0.348	-0.308	-0.020	-0.379	-0.390
7	-1.53E-02	1.86E-01	2.26E-01	4.58E-02	2.50E-01	2.32E-01	0.53	-5.86	-6.39	0.84	-6.07	-6.07	-0.010	-0.278	-0.353	0.005	-0.348	-0.327
8	3.97E-02	2.38E-01	2.44E-01	8.24E-01	2.62E-01	2.59E-01	-1.38	-7.67	-7.03	-0.64	-6.50	-7.03	-0.098	-0.363	-0.353	-0.055	-0.369	-0.374
9	1.16E-01	2.47E-01	2.44E-01	1.71E-01	2.66E-01	2.62E-01	-4.05	-7.99	-7.03	-3.73	-6.60	-7.14	-0.221	-0.378	-0.358	-0.200	-0.374	-0.379
10	1.65E-01	2.47E-01	2.47E-01	2.17E-01	2.59E-01	2.38E-01	-5.75	-7.67	-7.14	-5.32	-6.39	-6.28	-0.300	-0.378	-0.358	-0.275	-0.364	-0.338
11	1.19E-01	2.38E-01	2.47E-01	1.46E-01	2.53E-01	2.50E-01	-4.15	-7.67	-7.03	-2.88	-6.18	-6.71	-0.226	-0.363	-0.358	-0.160	-0.353	-0.358
12	1.71E-01	2.50E-01	2.44E-01	2.01E-01	2.66E-01	2.72E-01	-5.96	-8.09	-7.03	-4.79	-6.60	-7.45	-0.310	-0.383	-0.353	-0.250	-0.374	-0.395
13	2.23E-01	2.59E-01	2.82E-01	2.53E-01	2.99E-01	2.75E-01	-7.77	-8.41	-7.67	-8.60	-7.77	-7.77	-0.393	-0.398	-0.393	-0.335	-0.431	-0.400
14	2.50E-01	2.35E-01	2.59E-01	2.69E-01	2.56E-01	2.81E-01	-8.73	-7.56	-7.56	-7.35	-6.28	-7.56	-0.438	-0.358	-0.378	-0.375	-0.343	-0.410
15	2.56E-01	2.23E-01	2.23E-01	2.78E-01	2.47E-01	2.75E-01	-8.95	-7.14	-7.03	-7.45	-5.96	-6.71	-0.447	-0.338	-0.353	-0.585	-0.343	-0.400
16	3.36E-01	2.23E-01	2.44E-01	4.06E-01	2.47E-01	2.50E-01	-11.71	-7.14	-7.46	-11.93	-5.96	-6.71	-0.575	-0.338	-0.353	-0.605	-0.338	-0.358
17	3.57E-01	2.17E-01	2.53E-01	4.18E-01	2.44E-01	2.63E-01	-12.46	-6.92	-7.35	-12.35	-5.88	-6.82	-0.610	-0.328	-0.368	-0.665	-0.332	-0.364
18	3.72E-01	2.17E-01	2.47E-01	4.06E-01	2.41E-01	2.62E-01	-12.99	-6.82	-7.14	-11.93	-5.75	-7.14	-0.634	-0.328	-0.358	-0.585	-0.332	-0.379
19	4.00E-01	2.14E-01	2.56E-01	4.55E-01	2.29E-01	2.59E-01	-13.95	-6.82	-7.46	-13.63	-5.32	-7.03	-0.678	-0.323	-0.373	-0.744	-0.312	-0.374
20	4.55E-01	2.14E-01	2.56E-01	5.04E-01	2.35E-01	2.78E-01	-15.87	-6.82	-7.46	-15.34	-5.54	-7.67	-0.767	-0.323	-0.373	-0.725	-0.322	-0.405
21	4.39E-01	2.23E-01	2.59E-01	4.91E-01	2.50E-01	2.69E-01	-15.34	-7.14	-7.56	-14.91	-6.07	-7.35	-0.742	-0.338	-0.378	-0.700	-0.348	-0.390
22	4.49E-01	2.38E-01	2.53E-01	4.76E-01	2.53E-01	2.69E-01	-15.66	-7.67	-7.35	-14.38	-6.39	-7.35	-0.757	-0.363	-0.368	-0.620	-0.364	-0.390
23	3.88E-01	2.20E-01	2.62E-01	4.27E-01	2.44E-01	2.69E-01	-13.53	-7.03	-7.67	-12.67	-5.88	-7.35	-0.659	-0.333	-0.383	-0.605	-0.338	-0.390
24	3.78E-01	2.14E-01	2.66E-01	4.18E-01	2.41E-01	2.75E-01	-13.21	-6.82	-7.77	-12.35	-5.76	-7.56	-0.644	-0.328	-0.388	-0.639	-0.327	-0.400
25	3.75E-01	2.17E-01	2.38E-01	4.12E-01	2.38E-01	3.05E-01	-13.10	-6.92	-8.09	-12.14	-5.64	-8.63	-0.639	-0.328	-0.403	-0.659	-0.343	-0.452
26	3.88E-01	2.11E-01	2.78E-01	4.15E-01	2.20E-01	2.84E-01	-13.53	-6.71	-8.20	-12.25	-5.01	-7.88	-0.659	-0.318	-0.408	-0.664	-0.306	-0.415
27	3.91E-01	2.04E-01	2.47E-01	4.09E-01	2.26E-01	2.62E-01	-13.63	-6.50	-7.14	-12.03	-5.22	-7.14	-0.664	-0.308	-0.358	-0.590	-0.296	-0.379
28	3.57E-01	2.11E-01	2.17E-01	3.78E-01	2.14E-01	3.17E-01	-12.46	-6.71	-8.95	-10.97	-4.79	-9.05	-0.610	-0.318	-0.442	-0.540	-0.286	-0.473
29	3.45E-01	2.04E-01	2.93E-01	3.42E-01	2.17E-01	3.17E-01	-12.03	-6.50	-8.73	-9.89	-4.90	-9.05	-0.590	-0.308	-0.432	-0.480	-0.291	-0.473
30	3.14E-01	2.11E-01	2.53E-01	3.51E-01	2.23E-01	2.62E-01	-10.97	-6.71	-7.35	-10.01	-5.11	-7.14	-0.541	-0.318	-0.368	-0.495	-0.301	-0.379
31	3.24E-01	2.35E-01	2.66E-01	3.33E-01	2.56E-01	2.93E-01	-11.28	-7.56	-7.77	-10.37	-6.28	-8.20	-0.556	-0.358	-0.388	-0.465	-0.358	-0.431
32	3.30E-01	2.17E-01	2.50E-01	3.57E-01	2.50E-01	2.56E-01	-11.50	-6.92	-7.24	-10.22	-6.07	-6.92	-0.565	-0.328	-0.363	-0.505	-0.348	-0.369
33	3.33E-01	2.14E-01	2.47E-01	3.48E-01	2.35E-01	2.47E-01	-11.61	-6.82	-6.39	-9.90	-5.54	-6.60	-0.570	-0.323	-0.323	-0.490	-0.322	-0.353
34	3.33E-01	2.26E-01	2.38E-01	3.51E-01	2.47E-01	2.87E-01	-11.61	-7.24	-8.82	-10.01	-5.96	-7.99	-0.570	-0.343	-0.343	-0.495	-0.343	-0.421
35	3.39E-01	2.23E-01	2.35E-01	4.06E-01	2.35E-01	2.78E-01	-11.82	-7.14	-7.14	-11.93	-5.54	-7.67	-0.580	-0.338	-0.358	-0.585	-0.322	-0.405
36	2.93E-01	2.20E-01	2.32E-01	3.33E-01	2.38E-01	2.59E-01	-10.22	-7.03	-8.60	-9.37	-5.64	-7.03	-0.506	-0.333	-0.333	-0.465	-0.327	-0.374
37	2.84E-01	2.14E-01	2.56E-01	3.08E-01	2.23E-01	2.99E-01	-9.90	-6.82	-7.46	-9.27	-5.11	-8.41	-0.492	-0.318	-0.373	-0.425	-0.301	-0.441
38	2.90E-01	2.17E-01	2.53E-01	3.30E-01	2.35E-01	3.11E-01	-10.12	-6.92	-7.35	-9.27	-6.28	-8.84	-0.501	-0.328	-0.368	-0.460	-0.322	-0.462
39	2.75E-01	2.44E-01	2.47E-01	3.11E-01	2.59E-01	2.75E-01	-9.58	-7.68	-7.14	-8.63	-6.07	-7.56	-0.477	-0.373	-0.358	-0.430	-0.322	-0.400
40	2.81E-01	2.29E-01	2.29E-01	2.96E-01	2.59E-01	2.59E-01	-9.90	-7.68	-6.50	-8.09	-6.39	-7.99	-0.492	-0.348	-0.328	-0.405	-0.364	-0.374
41	2.84E-01	2.29E-01	2.47E-01	3.11E-01	2.59E-01	2.87E-01	-9.80	-7.14	-7.14	-8.63	-6.39	-7.99	-0.487	-0.348	-0.358	-0.430	-0.384	-0.421
42	2.78E-01	2.72E-01	2.72E-01	2.99E-01	2.50E-01	2.90E-01	-9.69	-7.24	-7.99	-8.20	-6.07	-8.09	-0.482	-0.343	-0.398	-0.410	-0.348	-0.426
43	2.90E-01	2.26E-01	2.53E-01	3.14E-01	2.44E-01	2.62E-01	-10.12	-7.24	-7.35	-8.73	-5.86	-7.14	-0.501	-0.363	-0.368	-0.435	-0.338	-0.379
44	6.10E-02	7.32E-02	7.32E-02	8.85E-02	2.47E-01	7.93E-02	-7.35				-5.98			-0.348			-0.343	
45	4.27E-02	2.29E-01	5.80E-02	7.32E-02	2.41E-01	6.41E-02	-7.35				-5.75			-0.348			-0.332	
46	5.80E-02	2.29E-01	5.80E-02	7.02E-02	2.41E-01	6.10E-02	-7.14				-5.75			-0.338			-0.332	
47	3.66E-02	2.23E-01	5.80E-02	7.02E-02	2.38E-01	2.90E-02	-7.14				-5.64			-0.338			-0.327	
48	3.66E-02	2.38E-01	5.80E-02	6.71E-01	2.47E-01	5.80E-02	-7.67				-5.96			-0.363			-0.343	

Pa = 30.14 in Hg
Ta = 62 degF

Run Order		
A	T inf = 61	deg F
B	T inf = 64	deg F
C	T inf = 66	deg F
C	T inf = 63	deg F
B	T inf = 64	deg F
A	T inf = 70	deg F

Notes:
1) Schmidter: 30 cm H2O = -1.76 V
2) add 0.8 cm H2O to Schmidter pressure reading
3) Run 1 - 10.2 cm speed; Run 2 - 10.0 cm speed
4) 10 msec data read time delay

49

Test 527

Manifold Port #	SDIU (V) -4 AOA/+2.5 SS			SDIU (V) -4 AOA/+5.0 SS			-4 AOA/+2.5 SS			-4 AOA/+5.0 SS			-4 AOA/+2.5 SS			-4 AOA/+5.0 SS		
	A-10 cm	B-10 cm	C-10 cm	A-10 cm	B-10 cm	C-10 cm	A Pg-psf	B Pg-psf	C Pg-psf	A Pg-psf	B Pg-psf	C Pg-psf	A-Cp	B-Cp	C-Cp	A-Cp	B-Cp	C-Cp
(ref)	-3.05E-03	0.00E+00	-2.97E-02	5.19E-02	6.41E-02	3.97E-02	0.00	0.00	-1.38	-1.80	-2.22	-1.38	-0.025	-0.020	0.064	-0.115	-0.105	-0.079
(ref)	-2.14E-02	-1.22E-02	-2.75E-02	3.66E-02	3.36E-02	3.34E-02	0.42	0.42	0.42	0.53	1.08	0.21	0.000	0.000	0.000	0.000	0.000	0.000
(ref)	-6.01E-01	-5.92E-01	-5.55E-01	-5.13E-01	-5.28E-01	-5.13E-01	20.54	20.54	20.54	19.59	20.54	19.17	0.939	0.939	0.939	0.940	0.940	0.940
1	3.05E-03	1.99E-01	1.59E-01	8.85E-02	1.98E-01	1.86E-01	-0.21	-6.88	-4.13	-1.27	-4.66	-5.09	-0.040	-0.341	-0.211	-0.089	-0.276	-0.263
2	-8.10E-03	1.95E-01	2.26E-01	5.80E-02	2.56E-01	2.41E-01	0.11	-6.78	-6.46	-0.21	-6.67	-6.99	-0.025	-0.336	-0.320	-0.037	-0.373	-0.357
3	-1.22E-02	1.92E-01	2.26E-01	3.36E-02	2.53E-01	2.44E-01	0.32	-8.67	-8.48	0.64	-6.57	-7.10	-0.015	-0.331	-0.320	0.005	-0.368	-0.362
4	6.10E-03	1.71E-01	2.04E-01	8.24E-02	2.32E-01	2.29E-01	-0.32	-5.83	-5.72	-1.06	-5.82	-6.57	-0.044	-0.297	-0.285	-0.078	-0.332	-0.336
5	6.41E-02	2.01E-01	2.32E-01	1.46E-01	2.62E-01	2.53E-01	-2.33	-6.99	-6.67	-3.29	-6.88	-7.41	-0.138	-0.346	-0.329	-0.188	-0.383	-0.378
6	1.19E-01	2.01E-01	2.41E-01	1.83E-01	2.69E-01	2.59E-01	-4.24	-6.99	-6.99	-4.55	-7.09	-7.31	-0.227	-0.361	-0.344	-0.251	-0.393	-0.373
7	1.43E-01	2.11E-01	2.41E-01	1.98E-01	2.65E-01	2.59E-01	-5.08	-7.31	-8.88	-5.08	-7.20	-7.62	-0.267	-0.356	-0.339	-0.277	-0.398	-0.389
8	1.28E-01	2.08E-01	2.35E-01	2.01E-01	2.72E-01	2.69E-01	-4.55	-7.20	-6.78	-5.19	-7.20	-7.94	-0.242	-0.356	-0.334	-0.282	-0.398	-0.405
9	1.40E-01	2.38E-01	2.66E-01	2.17E-01	3.08E-01	2.90E-01	-4.98	-8.26	-7.84	-5.72	-8.47	-8.68	-0.262	-0.405	-0.384	-0.308	-0.460	-0.441
10	1.86E-01	1.98E-01	2.41E-01	1.80E-01	2.62E-01	2.66E-01	-6.67	-6.88	-6.99	-6.57	-6.88	-7.84	-0.336	-0.341	-0.344	-0.350	-0.383	-0.399
11	2.01E-01	1.80E-01	2.44E-01	2.72E-01	2.35E-01	2.66E-01	-7.09	-6.25	-7.10	-7.62	-5.93	-7.84	-0.361	-0.311	-0.349	-0.402	-0.337	-0.399
12	2.38E-01	1.68E-01	2.41E-01	3.14E-01	2.41E-01	2.62E-01	-8.37	-5.82	-6.99	-8.11	-6.14	-7.73	-0.420	-0.292	-0.344	-0.475	-0.347	-0.394
13	1.80E-01	1.74E-01	3.51E-01	3.51E-01	2.41E-01	2.62E-01	-10.70	-6.04	-6.99	-10.38	-6.14	-7.73	-0.529	-0.302	-0.344	-0.538	-0.322	-0.394
14	1.68E-01	1.71E-01	1.80E-01	3.63E-01	2.26E-01	2.62E-01	-10.70	-5.93	-6.99	-10.80	-5.61	-8.28	-0.529	-0.297	-0.344	-0.559	-0.322	-0.394
15	3.05E-01	1.71E-01	2.50E-01	3.91E-01	2.41E-01	2.78E-01	-11.12	-6.25	-7.31	-11.75	-5.93	-8.26	-0.549	-0.311	-0.359	-0.606	-0.337	-0.420
16	3.17E-01	1.68E-01	2.53E-01	3.97E-01	2.35E-01	2.78E-01	-12.18	-5.82	-7.41	-11.97	-6.14	-7.84	-0.598	-0.292	-0.364	-0.616	-0.337	-0.420
17	3.48E-01	1.89E-01	2.47E-01	4.36E-01	2.56E-01	2.69E-01	-14.72	-8.57	-7.20	-13.34	-6.67	-7.84	-0.717	-0.400	-0.354	-0.684	-0.424	-0.405
18	4.21E-01	2.35E-01	2.47E-01	4.49E-01	2.87E-01	2.59E-01	-13.55	-8.15	-7.20	-13.77	-7.73	-7.62	-0.662	-0.356	-0.369	-0.705	-0.337	-0.426
19	3.88E-01	2.08E-01	2.56E-01	4.58E-01	2.35E-01	2.81E-01	-14.30	-7.20	-7.52	-14.08	-5.93	-7.94	-0.697	-0.369	-0.388	-0.721	-0.322	-0.389
20	4.09E-01	1.95E-01	2.50E-01	4.12E-01	2.26E-01	2.84E-01	-11.97	-6.78	-7.31	-12.50	-5.61	-7.94	-0.588	-0.331	-0.364	-0.643	-0.312	-0.405
21	3.42E-01	1.92E-01	2.69E-01	3.97E-01	2.20E-01	2.84E-01	-11.33	-6.67	-7.31	-11.97	-5.40	-8.47	-0.559	-0.341	-0.364	-0.616	-0.327	-0.431
22	3.24E-01	1.98E-01	2.56E-01	4.09E-01	2.29E-01	2.78E-01	-11.65	-6.88	-7.41	-11.97	-5.72	-8.26	-0.573	-0.341	-0.369	-0.637	-0.327	-0.420
23	3.33E-01	1.98E-01	2.53E-01	4.21E-01	2.29E-01	2.72E-01	-12.18	-6.88	-7.52	-12.39	-5.51	-8.05	-0.598	-0.336	-0.339	-0.658	-0.317	-0.420
24	3.48E-01	1.98E-01	2.38E-01	3.57E-01	2.29E-01	3.02E-01	-12.60	-6.78	-8.28	-12.81	-5.72	-9.11	-0.618	-0.341	-0.403	-0.637	-0.327	-0.405
25	3.60E-01	1.98E-01	2.78E-01	3.42E-01	2.44E-01	2.72E-01	-10.06	-6.88	-8.15	-10.59	-6.25	-8.05	-0.499	-0.381	-0.398	-0.549	-0.352	-0.462
26	2.87E-01	1.98E-01	2.75E-01	3.51E-01	2.69E-01	2.72E-01	-9.74	-6.88	-8.15	-10.06	-6.25	-8.05	-0.484	-0.381	-0.369	-0.522	-0.393	-0.410
27	2.78E-01	2.23E-01	2.56E-01	3.51E-01	2.29E-01	2.53E-01	-9.21	-7.73	-6.99	-10.38	-5.72	-7.41	-0.460	-0.381	-0.344	-0.470	-0.393	-0.410
28	2.62E-01	2.04E-01	2.41E-01	3.63E-01	2.29E-01	2.50E-01	-9.85	-7.09	-6.99	-10.38	-5.82	-7.62	-0.489	-0.351	-0.325	-0.538	-0.327	-0.378
29	2.81E-01	1.95E-01	2.20E-01	3.69E-01	2.32E-01	2.23E-01	-9.64	-8.88	-6.57	-10.80	-5.93	-6.35	-0.480	-0.341	-0.290	-0.538	-0.332	-0.389
30	2.75E-01	1.98E-01	2.29E-01	3.17E-01	2.35E-01	2.47E-01	-10.91	-7.20	-5.82	-11.01	-6.14	-7.84	-0.539	-0.346	-0.325	-0.569	-0.337	-0.373
31	3.11E-01	2.08E-01	2.08E-01	3.02E-01	2.14E-01	2.14E-01	-9.00	-6.99	-5.93	-8.68	-6.04	-6.04	-0.450	-0.366	-0.305	-0.481	-0.337	-0.373
32	2.56E-01	2.11E-01	2.23E-01	3.05E-01	2.56E-01	2.26E-01	-7.94	-7.20	-6.35	-8.68	-6.67	-6.48	-0.400	-0.356	-0.315	-0.454	-0.337	-0.368
33	2.26E-01	2.47E-01	2.75E-01	3.05E-01	2.58E-01	2.35E-01	-8.15	-7.41	-6.14	-9.00	-7.31	-7.84	-0.410	-0.366	-0.295	-0.470	-0.347	-0.310
34	2.35E-01	1.86E-01	1.80E-01	3.05E-01	2.41E-01	2.01E-01	-8.26	-8.05	-5.00	-8.79	-6.14	-4.87	-0.415	-0.395	-0.354	-0.454	-0.404	-0.331
35	2.41E-01	2.23E-01	2.04E-01	3.02E-01	2.32E-01	2.29E-01	-8.47	-7.73	-5.72	-8.68	-6.14	-5.61	-0.425	-0.381	-0.256	-0.460	-0.347	-0.399
36	2.32E-01	2.11E-01	2.72E-01	3.17E-01	2.32E-01	1.95E-01	-8.28	-7.31	-8.05	-8.68	-5.82	-6.57	-0.415	-0.361	-0.285	-0.454	-0.373	-0.252
37	2.44E-01	2.14E-01	2.32E-01	3.66E-01	2.41E-01	1.95E-01	-8.15	-7.41	-6.67	-9.21	-5.82	-5.40	-0.410	-0.366	-0.393	-0.481	-0.332	-0.289
38	2.90E-01	2.20E-01	6.41E-02	7.63E-02	2.47E-01	6.41E-02	-8.58	-7.62		-10.91	-6.35		-0.430	-0.376	-0.329	-0.564	-0.347	-0.338
39	0.00E+00	2.20E-01	4.58E-02	5.80E-02	2.41E-01	4.58E-02	-10.17	-7.52			-6.14		-0.504	-0.371			-0.358	-0.278
40	0.00E+00	2.17E-01	4.58E-02	5.80E-02	2.41E-01	4.58E-02		-7.52			-6.35			-0.391			-0.358	
41	0.00E+00	2.29E-01	4.27E-02	5.80E-02	2.69E-01	4.58E-02		-7.94			-7.09			-0.405			-0.393	
42	0.00E+00	2.38E-01	3.97E-01	5.80E-02	2.87E-01	4.88E-02		-8.26			-7.73						-0.424	

Pa = 30.19 In Hg
Ta = 63 deg F

Run Order

A	T Inf =	62	deg F
B	T Inf =	64	deg F
C	T Inf =	66	deg F
C	T Inf =	66	deg F
B	T Inf =	68	deg F
A	T Inf =	70	deg F

Notes:
1) Schmidler: 30 cm H2O = -1.77 V
2) add 0.8 cm H2O to Schmidler pressure reading
3) Run 1 - 10.1 cm speed; Run 2 - 10.1 cm speed
4) 10 msec data read time delay

50

Test 530_1

Manifold Port #	SDIU (V) +4 AOA/+5 SS A-10 cm	B-10 cm	C-10 cm	SDIU (V) +4 AOA/+2.5 SS A-10 cm	B-10 cm	C-10 cm	+4 AOA/+5 SS A Pσ-psi	B Pσ-psi	C Pσ-psi	+4 AOA/+2.5 SS A Pσ-psi	B Pσ-psi	C Pσ-psi	+4 AOA/+5 SS A-Cp	B-Cp	C-Cp	+4 AOA/+2.5 SS A-Cp	B-Cp	C-Cp
1	0.00E+00	2.14E-02	1.53E-02	2.44E-02	4.88E-03	2.44E-02	0.00	-0.74	0.53	0.85	1.69	0.85	0.063	0.144	0.068	0.003	0.072	0.054
2	3.05E-03	0.00E+00	0.00E+00	0.00E+00	1.22E-02	9.16E-03	0.11	0.74	0.53	0.42	1.27	0.03	0.000	0.000	0.000	0.000	0.000	0.000
3	-5.40E-01	-5.56E-01	-5.31E-01	-5.40E-01	-5.46E-01	-5.43E-01	18.74	20.01	18.96	19.38	20.85	19.70	0.940	0.940	0.940	0.941	0.940	0.941
4	-3.97E-02	1.37E-01	1.89E-01	-5.80E-02	1.19E-01	1.46E-01	1.38	-4.02	-6.04	2.86	-2.44	-4.24	0.121	-0.180	-0.234	0.064	-0.232	-0.335
5	-9.77E-03	1.95E-01	1.95E-01	-1.01E-01	1.77E-01	1.98E-01	3.39	-6.04	-6.25	4.34	-4.45	-6.04	0.194	-0.277	-0.322	0.166	-0.331	-0.346
6	-1.56E-01	1.80E-01	2.17E-01	-1.19E-01	1.74E-01	2.17E-01	5.40	-5.51	-6.99	4.98	-4.34	-6.67	0.228	-0.272	-0.353	0.267	-0.305	-0.384
7	0.00E+00	1.22E-01	1.92E-01	-3.66E-02	1.59E-01	1.92E-01	0.00	-3.49	-7.20	2.12	-3.81	-5.82	0.084	-0.247	-0.312	-0.005	-0.207	-0.341
8	0.00E+00	1.68E-01	2.26E-01	0.00E+00	1.80E-01	2.14E-01	0.00	-5.08	-7.31	0.85	-4.55	-6.57	0.021	-0.283	-0.348	-0.005	-0.284	-0.400
9	1.53E-02	1.77E-01	2.11E-01	1.22E-02	1.80E-01	2.17E-01	0.00	-5.40	-6.78	0.42	-4.55	-6.67	0.000	-0.283	-0.353	-0.005	-0.300	-0.373
10	5.49E-02	1.65E-01	1.98E-01	3.05E-02	1.80E-01	2.08E-01	-0.53	-5.19	-6.46	-0.21	-5.19	-6.35	-0.032	-0.283	-0.338	-0.032	-0.289	-0.357
11	9.16E-02	1.74E-01	2.08E-01	7.32E-02	1.77E-01	2.01E-01	-3.18	-4.98	-6.35	-1.69	-4.45	-6.14	-0.105	-0.277	-0.327	-0.166	-0.279	-0.351
12	7.93E-02	1.95E-01	2.32E-01	6.10E-02	1.80E-01	2.01E-01	-1.91	-5.29	-6.67	-1.27	-4.55	-6.14	-0.084	-0.283	-0.327	-0.102	-0.294	-0.368
13	9.46E-02	1.77E-01	2.47E-01	7.93E-02	1.92E-01	2.32E-01	-2.75	-6.04	-7.52	-1.91	-4.98	-7.20	-0.116	-0.303	-0.379	-0.144	-0.331	-0.411
14	1.71E-01	1.71E-01	2.41E-01	1.04E-01	1.80E-01	2.41E-01	-3.28	-5.40	-8.05	-2.75	-4.55	-7.52	-0.158	-0.283	-0.395	-0.171	-0.300	-0.438
15	1.89E-01	1.77E-01	2.32E-01	1.77E-01	1.80E-01	2.38E-01	-5.93	-5.19	-7.84	-5.29	-4.55	-7.41	-0.284	-0.283	-0.390	-0.305	-0.289	-0.427
16	1.95E-01	1.65E-01	2.26E-01	2.08E-01	1.80E-01	2.29E-01	-6.57	-5.40	-7.62	-6.35	-4.55	-7.10	-0.338	-0.283	-0.374	-0.337	-0.300	-0.411
17	2.26E-01	1.59E-01	2.23E-01	2.26E-01	1.74E-01	2.26E-01	-6.73	-4.98	-7.31	-6.99	-4.34	-6.99	-0.368	-0.272	-0.369	-0.347	-0.279	-0.400
18	2.44E-01	1.50E-01	2.20E-01	2.38E-01	1.68E-01	2.32E-01	-7.84	-4.77	-7.20	-7.41	-4.13	-7.20	-0.389	-0.262	-0.379	-0.401	-0.269	-0.395
19	3.02E-01	1.53E-01	2.38E-01	2.59E-01	1.59E-01	2.26E-01	-8.47	-4.45	-7.09	-8.15	-3.81	-6.99	-0.426	-0.247	-0.369	-0.401	-0.253	-0.389
20	3.17E-01	1.65E-01	2.41E-01	3.17E-01	1.65E-01	2.41E-01	-10.48	-4.55	-7.73	-10.17	-4.02	-7.52	-0.525	-0.257	-0.395	-0.433	-0.258	-0.422
21	3.30E-01	1.89E-01	2.53E-01	3.27E-01	1.65E-01	2.41E-01	-11.01	-4.98	-8.37	-10.48	-4.02	-7.62	-0.541	-0.257	-0.395	-0.534	-0.279	-0.454
22	2.87E-01	1.77E-01	2.50E-01	3.33E-01	1.89E-01	2.44E-01	-11.44	-5.82	-8.28	-10.70	-4.87	-7.62	-0.552	-0.298	-0.400	-0.561	-0.320	-0.449
23	2.75E-01	1.71E-01	2.47E-01	3.02E-01	1.74E-01	2.38E-01	-9.95	-5.40	-8.15	-9.64	-4.34	-7.41	-0.499	-0.272	-0.390	-0.583	-0.300	-0.443
24	2.81E-01	1.74E-01	2.78E-01	2.99E-01	1.62E-01	2.44E-01	-9.53	-5.19	-8.05	-9.53	-3.92	-7.82	-0.494	-0.252	-0.400	-0.508	-0.300	-0.438
25	2.78E-01	1.62E-01	2.62E-01	3.08E-01	1.74E-01	2.69E-01	-9.74	-5.29	-9.21	-9.85	-4.55	-8.47	-0.510	-0.283	-0.442	-0.486	-0.289	-0.497
26	2.84E-01	1.56E-01	2.62E-01	3.05E-01	1.62E-01	2.62E-01	-9.64	-4.87	-9.11	-9.74	-4.34	-8.26	-0.504	-0.272	-0.431	-0.497	-0.294	-0.492
27	2.56E-01	1.50E-01	3.33E-01	3.02E-01	1.56E-01	2.53E-01	-9.85	-4.66	-8.58	-9.64	-3.81	-7.94	-0.499	-0.247	-0.416	-0.492	-0.274	-0.465
28	2.38E-01	1.46E-01	3.08E-01	2.81E-01	1.50E-01	3.02E-01	-8.90	-4.45	-11.01	-8.90	-3.71	-9.64	-0.462	-0.241	-0.499	-0.502	-0.263	-0.589
29	2.26E-01	1.53E-01	2.84E-01	2.56E-01	1.46E-01	2.75E-01	-8.28	-4.34	-10.17	-8.05	-3.80	-9.64	-0.420	-0.236	-0.499	-0.454	-0.253	-0.546
30	2.23E-01	1.59E-01	2.99E-01	2.59E-01	1.53E-01	2.84E-01	-7.64	-4.55	-9.32	-8.15	-3.81	-8.68	-0.426	-0.247	-0.452	-0.422	-0.248	-0.503
31	2.26E-01	1.92E-01	2.99E-01	2.53E-01	1.59E-01	2.81E-01	-7.73	-5.93	-9.85	-7.94	-4.66	-9.00	-0.415	-0.288	-0.467	-0.401	-0.258	-0.530
32	2.38E-01	1.83E-01	2.47E-01	2.59E-01	1.83E-01	2.81E-01	-7.84	-5.93	-9.85	-8.15	-4.66	-8.90	-0.428	-0.288	-0.462	-0.396	-0.325	-0.530
33	2.29E-01	1.74E-01	2.87E-01	2.59E-01	1.86E-01	2.41E-01	-7.73	-5.40	-9.21	-8.15	-4.45	-8.47	-0.428	-0.277	-0.442	-0.401	-0.300	-0.497
34	2.08E-01	1.62E-01	2.08E-01	2.41E-01	1.83E-01	2.72E-01	-8.28	-5.61	-8.05	-8.15	-4.77	-7.52	-0.426	-0.293	-0.395	-0.422	-0.305	-0.438
35	2.01E-01	1.59E-01	2.75E-01	2.29E-01	1.74E-01	2.87E-01	-7.94	-5.29	-9.42	-7.52	-4.68	-8.58	-0.394	-0.288	-0.447	-0.406	-0.294	-0.508
36	2.01E-01	1.65E-01	1.65E-01	2.29E-01	1.62E-01	2.38E-01	-7.20	-4.87	-10.17	-7.10	-4.45	-9.11	-0.373	-0.277	-0.473	-0.369	-0.274	-0.546
37	1.95E-01	1.86E-01	1.83E-01	2.26E-01	1.68E-01	2.38E-01	-7.10	-4.77	-8.07	-7.10	-4.13	-7.41	-0.388	-0.262	-0.390	-0.358	-0.269	-0.368
38	1.86E-01	2.01E-01	1.98E-01	2.32E-01	1.71E-01	2.59E-01	-7.20	-4.98	-7.62	-7.20	-4.24	-8.15	-0.368	-0.267	-0.426	-0.358	-0.279	-0.416
39	2.04E-01	1.95E-01	1.25E-01	2.26E-01	1.77E-01	3.02E-01	-6.99	-4.98	-9.00	-6.99	-4.45	-9.64	-0.368	-0.277	-0.499	-0.358	-0.279	-0.487
40	2.14E-02	1.89E-01	3.05E-02	2.04E-01	2.04E-01	1.86E-01	-6.78	-6.78	-5.19	-7.10	-5.40	-5.61	-0.373	-0.324	-0.301	-0.347	-0.331	-0.292
41	1.86E-01	2.01E-01	1.83E-01	2.20E-01	2.04E-01	1.77E-01	-6.46	-6.25	-4.77	-6.78	-5.29	-5.29	-0.357	-0.318	-0.286	-0.331	-0.341	-0.270
42	1.86E-01	1.62E-01	2.14E-01	2.32E-01	2.01E-01	2.32E-01	-6.46	-6.25	-6.35	-6.78	-5.40	-7.20	-0.357	-0.324	-0.379	-0.331	-0.341	-0.351
43	2.04E-01	1.65E-01	1.65E-01	2.32E-01	2.01E-01	1.50E-01	-7.09	-6.04	-3.81	-7.20	-5.29	-4.34	-0.378	-0.318	-0.239	-0.363	-0.331	-0.222
44	2.14E-02	1.95E-01	3.97E-02	6.71E-02	2.01E-01	3.97E-02		-6.04			-5.29			-0.318			-0.331	
45	0.00E+00	1.89E-01	2.75E-02	3.36E-02	1.95E-01	2.75E-02		-5.82			-5.08			-0.308			-0.320	
46	6.10E-03	1.83E-01	2.44E-02	3.36E-02	1.89E-01	2.44E-02		-5.61			-4.87			-0.298			-0.310	
47	0.00E+00	1.77E-01	2.14E-02	3.36E-02	1.92E-01	2.44E-02		-5.40			-4.98			-0.303			-0.300	
48	0.00E+00	1.86E-01	2.14E-02	3.36E-01	2.01E-01	2.44E-02		-5.72			-5.29			-0.318			-0.315	

Pa = 30.12 in Hg
Ta = 63 degF

Run Order
A   Tinf = 62 degF
B   Tinf = 64 degF
C   Tinf = 66 degF
C   Tinf = 67 degF
B   Tinf = 69 degF
A   Tinf = 70 degF

Notes:
1) Schmidter: 30 cm H2O = -1.77 V
2) add 0.8 cm H2O to Schmidter pressure reading
3) Run 1 - 10.3 cm speed; Run 2 - 10.3 cm speed
4) 10 msec data read time delay

Test 630.2

Manifold	SDIU (V) +4 AOA / -2.5 SS			SDIU (V) +4 AOA / -5.0 SS			+4 AOA / -2.5 SS			+4 AOA / -5.0 SS			+4 AOA / -2.5 SS			+4 AOA / -5.0 SS		
Port #	A -10 cm	B -10 cm	C -10 cm	A -10 cm	B -10 cm	C -10 cm	A Pg-psi	B Pg-psi	C Pg-psi	A Pg-psi	B Pg-psi	C Pg-psi	A -Cp	B -Cp	C -Cp	A -Cp	B -Cp	C - Cp
1	3.36E-02	3.85E-02	4.27E-02	8.10E-03	6.41E-02	4.27E-02	1.16	1.27	1.48	0.21	2.22	1.48	0.022	0.075	0.075	0.022	0.220	0.081
2	2.44E-02	2.75E-02	3.65E-02	0.00E+00	0.00E+00	3.65E-02	0.32	0.32	0.21	0.21	2.22	0.21	0.000	0.000	0.000	0.000	0.000	0.000
3	-5.22E-01	-5.40E-01	-5.49E-01	-6.22E-01	-5.25E-01	-5.31E-01	19.27	20.01	20.64	18.02	20.44	19.91	0.940	0.840	0.830	0.941	0.941	0.940
4	-1.16E-01	1.31E-01	1.59E-01	-1.68E-01	1.59E-01	1.59E-01	6.04	-3.28	-4.02	4.77	-2.97	-4.02	0.242	-0.172	-0.196	0.303	-0.268	-0.202
5	-1.40E-01	1.53E-01	1.83E-01	-1.31E-01	1.53E-01	1.77E-01	5.40	-4.02	-4.87	3.92	-3.07	-4.66	0.252	-0.212	-0.235	0.193	-0.274	-0.232
6	-1.22E-01	1.56E-01	1.86E-01	-1.07E-01	1.62E-01	1.83E-01	4.65	-4.13	-4.98	3.60	-3.39	-4.87	0.210	-0.217	-0.240	0.176	-0.290	-0.242
7	-9.77E-02	1.13E-01	1.43E-01	-9.77E-02	1.31E-01	1.56E-01	2.97	-2.65	-3.49	2.44	-2.33	-3.92	0.131	-0.141	-0.171	0.116	-0.235	-0.197
8	-5.19E-02	1.59E-01	1.95E-01	-6.41E-02	1.65E-01	1.95E-01	1.16	-4.24	-5.29	0.21	-3.49	-5.29	0.042	-0.248	-0.254	0.000	-0.295	-0.263
9	0.00E+00	1.77E-01	1.95E-01	0.00E+00	1.80E-01	1.95E-01	0.32	-4.87	-5.61	-1.06	-4.02	-5.72	0.000	-0.248	-0.264	-0.066	-0.323	-0.263
10	2.44E-02	1.80E-01	2.04E-01	3.66E-02	1.80E-01	2.08E-01	0.42	-4.98	-5.61	-0.32	-4.02	-5.61	0.005	-0.253	-0.269	-0.028	-0.334	-0.283
11	2.14E-02	1.80E-01	2.01E-01	1.53E-02	1.86E-01	2.04E-01	-0.42	-4.98	-5.51	-1.38	-4.24	-5.61	-0.037	-0.253	-0.284	-0.083	-0.334	-0.283
12	4.58E-02	1.80E-01	2.11E-01	4.58E-02	1.86E-01	2.23E-01	-2.01	-4.98	-5.82	-2.75	-4.24	-6.25	-0.116	-0.268	-0.279	-0.154	-0.317	-0.278
13	9.16E-02	1.89E-01	2.11E-01	8.55E-02	1.77E-01	2.11E-01	-2.97	-5.29	-5.82	-3.49	-3.92	-5.82	-0.163	-0.258	-0.279	-0.193	-0.285	-0.288
14	1.19E-01	1.83E-01	2.11E-01	1.07E-01	1.59E-01	2.14E-01	-3.49	-5.08	-5.72	-3.49	-3.28	-5.93	-0.189	-0.258	-0.274	-0.193	-0.279	-0.293
15	1.34E-01	1.83E-01	2.08E-01	1.07E-01	1.56E-01	2.08E-01	-6.04	-5.08	-5.82	-6.25	-3.18	-5.72	-0.315	-0.273	-0.279	-0.336	-0.279	-0.283
16	2.08E-01	1.92E-01	2.11E-01	1.86E-01	1.59E-01	2.11E-01	-6.88	-5.40	-5.82	-6.88	-3.28	-5.82	-0.357	-0.273	-0.279	-0.369	-0.285	-0.288
17	2.32E-01	1.92E-01	2.11E-01	2.04E-01	1.56E-01	2.04E-01	-7.20	-5.40	-5.93	-7.41	-3.18	-5.61	-0.373	-0.268	-0.284	-0.396	-0.279	-0.278
18	2.41E-01	1.89E-01	2.14E-01	2.20E-01	1.59E-01	2.14E-01	-7.62	-5.29	-5.82	-7.84	-3.28	-5.93	-0.389	-0.253	-0.279	-0.418	-0.285	-0.293
19	2.50E-01	1.80E-01	2.11E-01	2.32E-01	1.50E-01	2.11E-01	-9.32	-4.98	-5.82	-9.85	-2.97	-5.82	-0.478	-0.268	-0.279	-0.523	-0.290	-0.288
20	3.02E-01	1.89E-01	2.11E-01	2.90E-01	1.62E-01	2.14E-01	-9.64	-5.29	-5.93	-10.27	-3.39	-5.93	-0.494	-0.278	-0.284	-0.545	-0.312	-0.288
21	3.11E-01	1.95E-01	2.14E-01	3.02E-01	1.74E-01	2.11E-01	-10.08	-5.51	-6.04	-10.59	-3.81	-5.82	-0.515	-0.268	-0.289	-0.561	-0.279	-0.293
22	3.24E-01	1.89E-01	2.17E-01	3.11E-01	1.56E-01	2.20E-01	-10.00	-5.29	-6.04	-9.74	-3.18	-6.14	-0.478	-0.248	-0.289	-0.517	-0.252	-0.288
23	3.02E-01	1.77E-01	2.17E-01	2.87E-01	1.40E-01	2.20E-01	-9.32	-4.87	-6.07	-9.63	-2.65	-6.14	-0.468	-0.258	-0.308	-0.506	-0.263	-0.303
24	2.96E-01	1.83E-01	2.29E-01	2.81E-01	1.46E-01	2.32E-01	-9.11	-5.08	-6.46	-9.64	-2.88	-6.57	-0.478	-0.258	-0.318	-0.512	-0.274	-0.323
25	3.02E-01	1.89E-01	2.35E-01	2.84E-01	1.53E-01	2.38E-01	-9.42	-5.29	-6.35	-9.64	-3.07	-6.78	-0.483	-0.263	-0.303	-0.512	-0.274	-0.333
26	3.05E-01	1.86E-01	2.26E-01	2.84E-01	1.53E-01	2.29E-01	-9.32	-5.19	-6.14	-9.74	-3.07	-6.46	-0.478	-0.258	-0.352	-0.517	-0.263	-0.318
27	3.02E-01	1.80E-01	2.17E-01	2.87E-01	1.53E-01	2.17E-01	-8.05	-4.98	-7.41	-9.00	-2.86	-6.04	-0.415	-0.263	-0.293	-0.479	-0.279	-0.298
28	2.66E-01	1.83E-01	2.56E-01	2.66E-01	1.56E-01	2.56E-01	-7.94	-5.08	-8.99	-8.05	-3.18	-7.10	-0.410	-0.268	-0.333	-0.429	-0.295	-0.364
29	2.62E-01	1.86E-01	2.44E-01	2.38E-01	1.56E-01	2.47E-01	-7.94	-5.19	-6.78	-8.05	-3.49	-6.67	-0.410	-0.273	-0.323	-0.429	-0.274	-0.349
30	2.62E-01	1.89E-01	2.38E-01	2.38E-01	1.53E-01	2.26E-01	-7.84	-5.29	-6.78	-8.05	-3.07	-6.35	-0.405	-0.268	-0.308	-0.429	-0.268	-0.328
31	2.59E-01	1.92E-01	2.38E-01	2.38E-01	1.53E-01	2.20E-01	-8.05	-5.40	-6.46	-8.05	-3.07	-6.14	-0.405	-0.273	-0.289	-0.429	-0.274	-0.313
32	2.66E-01	1.89E-01	2.29E-01	2.38E-01	1.50E-01	2.14E-01	-7.84	-5.29	-6.04	-8.26	-2.97	-5.93	-0.420	-0.278	-0.289	-0.440	-0.268	-0.313
33	2.59E-01	1.89E-01	2.35E-01	2.44E-01	1.59E-01	2.29E-01	-7.64	-5.40	-6.67	-8.05	-3.28	-6.46	-0.384	-0.278	-0.318	-0.429	-0.285	-0.303
34	2.69E-01	1.92E-01	2.17E-01	2.44E-01	1.59E-01	2.29E-01	-8.15	-5.40	-6.88	-8.05	-3.39	-6.25	-0.347	-0.283	-0.328	-0.380	-0.290	-0.293
35	2.47E-01	1.95E-01	2.35E-01	2.38E-01	1.62E-01	2.23E-01	-7.41	-5.51	-6.25	-7.10	-3.71	-6.07	-0.352	-0.308	-0.298	-0.358	-0.306	-0.318
36	2.26E-01	1.95E-01	2.41E-01	2.11E-01	1.62E-01	2.20E-01	-6.67	-5.51	-6.57	-6.67	-4.24	-5.40	-0.362	-0.293	-0.313	-0.374	-0.334	-0.318
37	2.29E-01	1.95E-01	2.23E-01	1.98E-01	1.71E-01	2.35E-01	-6.78	-5.51	-7.73	-8.99	-3.81	-5.19	-0.378	-0.308	-0.367	-0.380	-0.312	-0.308
38	2.35E-01	2.01E-01	2.66E-01	2.08E-01	1.86E-01	1.98E-01	-6.99	-5.72	-5.19	-7.10	-4.02	-6.25	-0.362	-0.298	-0.249	-0.380	-0.323	-0.303
39	2.44E-01	2.14E-01	2.11E-01	2.11E-01	1.74E-01	1.92E-01	-7.31	-6.14	-4.77	-7.10	-3.81	-4.45	-0.378	-0.308	-0.230	-0.391	-0.312	-0.328
40	2.35E-01	2.14E-01	2.14E-01	2.17E-01	1.80E-01	1.74E-01	-6.99	-5.82	-6.88	-7.31	-4.13		-0.357	-0.293	-0.328	-0.396	-0.323	-0.258
41	2.32E-01	2.14E-01	2.14E-01	2.20E-01	1.74E-01	1.92E-01	-6.88	-6.14	-5.08	-7.41	-3.81		-0.378	-0.323	-0.245	-0.418	-0.312	-0.308
42	2.32E-01	2.08E-01	2.41E-01	2.20E-01	1.80E-01	1.74E-01	-6.88	-5.93		-7.84	-4.55			-0.318			-0.328	-0.222
43	2.44E-01	2.20E-01	1.89E-01	2.32E-01	1.80E-01	2.23E-01	-7.31	-6.35			-4.66			-0.323			-0.339	
44					1.89E-01	1.71E-01		-6.35			-4.87						-0.350	
45					1.95E-01			-6.57			-4.98						-0.356	
46					1.98E-01			-6.46									-0.367	
47					2.04E-01			-6.46									-0.372	
48					2.08E-01													

Pa =	30.12	in Hg
Ta =	63	deg F

Run Order

A	T Inf =	70	deg F
B	T Inf =	72	deg F
C	T Inf =	74	deg F
C	T Inf =	73	deg F
B	T Inf =	75	deg F
A	T Inf =	76	deg F

Notes:
1) Schmidter: 30 cm H2O = -1.77 V
2) add 0.8 cm H2O to Schmidter pressure reading
3) Run 1 - 10.1 cm speed; Run 2 - 10.1 cm speed
4) 10 msec data read time delay

52

Test 607

Port #	SDIU (V) 0 AOA / 0 SS - ANTENNA			0 AOA / 0 SS - ANTENNA			0 AOA / 0 SS - ANTENNA		
	A - 10 cm	B - 10 cm	C - 10 cm	A Pg-psf	B Pg-psf	C Pg-psf	A - Cp	B - Cp	C - Cp
1	6.10E-03	3.36E-02	1.83E-02	-0.21	-1.15	-0.62	-0.021	-0.112	-0.062
2	0.00E+00	0.00E+00	0.00E+00	0.21	1.15	0.62	0.000	0.000	0.000
3	-5.58E-01	-5.62E-01	-5.58E-01	19.26	20.31	19.68	0.940	0.940	0.940
4	-5.80E-02		1.40E-01	2.19	-3.02	-4.17	0.098	-0.204	-0.236
5	-7.02E-02	1.89E-01	1.98E-01	2.60	-5.31	-6.14	0.118	-0.317	-0.334
6	-7.99E-02	1.95E-01	2.14E-01	2.92	-5.52	-6.66	0.134	-0.327	-0.360
7	-3.36E-02	1.74E-01	1.95E-01	1.35	-4.79	-6.04	0.057	-0.291	-0.329
8	0.00E+00	1.89E-01	2.14E-01	0.21	-5.31	-6.66	0.000	-0.317	-0.360
9	3.97E-02	1.98E-01	2.14E-01	-1.15	-5.62	-6.66	-0.067	-0.332	-0.360
10	7.63E-02	1.95E-01	2.11E-01	-2.40	-5.52	-6.56	-0.128	-0.327	-0.355
11	7.63E-02	1.95E-01	2.04E-01	-2.40	-5.52	-6.52	-0.128	-0.327	-0.344
12	7.93E-02	2.01E-01	2.17E-01	-2.50	-5.73	-6.77	-0.134	-0.337	-0.365
13	1.25E-01	1.92E-01	2.20E-01	-4.06	-5.41	-6.87	-0.211	-0.322	-0.370
14	1.53E-01	1.80E-01	2.32E-01	-5.00	-5.00	-7.29	-0.257	-0.301	-0.390
15	1.77E-01	1.83E-01	2.20E-01	-5.83	-5.10	-6.87	-0.298	-0.307	-0.370
16	2.35E-01	1.77E-01	2.23E-01	-7.81	-4.89	-6.98	-0.396	-0.296	-0.375
17	2.72E-01	1.77E-01	2.26E-01	-9.06	-4.89	-7.08	-0.457	-0.296	-0.380
18	2.84E-01	1.71E-01	2.29E-01	-9.48	-4.69	-7.19	-0.478	-0.286	-0.385
19	3.02E-01	1.74E-01	2.23E-01	-10.10	-4.79	-6.98	-0.509	-0.291	-0.375
20	3.57E-01	1.77E-01	2.32E-01	-11.98	-4.89	-7.29	-0.601	-0.296	-0.390
21	3.66E-01	1.83E-01	2.29E-01	-12.29	-5.10	-7.19	-0.617	-0.307	-0.385
22	3.85E-01	1.74E-01	2.38E-01	-12.91	-4.79	-7.50	-0.647	-0.291	-0.401
23	3.33E-01	1.71E-01	2.35E-01	-11.14	-4.69	-7.39	-0.560	-0.286	-0.396
24	3.24E-01	1.68E-01	2.35E-01	-10.83	-4.58	-7.39	-0.545	-0.281	-0.396
25	3.24E-01	1.83E-01	2.41E-01	-10.83	-5.10	-7.60	-0.545	-0.307	-0.406
26	3.33E-01	1.71E-01	2.38E-01	-11.14	-4.69	-7.50	-0.560	-0.286	-0.401
27	3.24E-01	1.68E-01	2.26E-01	-10.83	-4.58	-7.08	-0.545	-0.281	-0.380
28	2.90E-01	1.65E-01	2.72E-01	-9.68	-4.48	-8.04	-0.488	-0.276	-0.457
29	2.62E-01	1.65E-01	2.59E-01	-8.75	-4.48	-8.23	-0.442	-0.276	-0.437
30	2.66E-01	1.62E-01	2.29E-01	-8.85	-4.37	-7.19	-0.447	-0.271	-0.385
31	2.66E-01	1.68E-01	2.29E-01	-8.85	-4.58	-7.19	-0.447	-0.281	-0.385
32	2.72E-01	1.71E-01	2.23E-01	-9.06	-4.69	-6.98	-0.457	-0.286	-0.375
33	2.62E-01	1.77E-01	2.08E-01	-8.75	-4.89	-6.46	-0.442	-0.296	-0.349
34	2.66E-01	1.86E-01	1.95E-01	-8.85	-5.21	-6.04	-0.447	-0.312	-0.329
35	2.50E-01	1.86E-01	2.11E-01	-8.33	-5.21	-6.56	-0.421	-0.312	-0.355
36	2.26E-01	1.77E-01	2.04E-01	-7.50	-4.89	-6.35	-0.380	-0.296	-0.344
37	2.23E-01	1.77E-01	1.92E-01	-7.39	-4.89	-5.94	-0.375	-0.296	-0.324
38	2.29E-01	1.77E-01	1.92E-01	-7.60	-4.89	-5.94	-0.385	-0.296	-0.324
39	2.32E-01	1.83E-01	2.20E-01	-7.71	-5.10	-6.87	-0.390	-0.307	-0.370
40	2.32E-01	1.80E-01	1.46E-01	-7.71	-5.00	-4.37	-0.390	-0.301	-0.247
41	2.23E-01	1.89E-01	1.56E-01	-7.39	-5.31	-4.69	-0.375	-0.317	-0.262
42	2.20E-01	1.86E-01	2.23E-01	-7.29	-5.21	-6.98	-0.370	-0.312	-0.375
43	2.29E-01	1.95E-01	1.86E-01	-7.60	-5.52	-5.73	-0.385	-0.327	-0.313
44		2.01E-01			-5.73			-0.337	
45		1.98E-01			-5.62			-0.332	
46		1.95E-01			-5.52			-0.332	
47		1.92E-01			-5.41			-0.327	
48		1.92E-01			-5.41			-0.322	

Pa = 30.2 in Hg
Ta = 58 deg F

Run Order		
A	T inf =	58 deg F
B	T inf =	60 deg F
C	T inf =	62 deg F

Notes:
1) Schmidter: 30 cm H2O = -1.80 V
2) add 0.8 cm H2O to Schmidter pressure reading
3) Run 1 - 10.1 cm speed
4) 10 msec data read time delay

Test 723

Manifold Port #	X-Position	Full X	SDIU (V) A - 10 cm	Cal & Cor A Pg-psf	A - Cp	Q-bar
1	NA	NA	2.14E-02	-0.74	0.082	
2	NA	NA	0.00E+00	0.74	0.000	
3	NA	NA	-4.88E-01	17.63	0.942	17.98
4	1.27	2.54	-4.94E-01	17.90	0.954	
5	2.3	4.6	-4.30E-01	15.67	0.830	
6	3.5	7	-3.20E-01	11.86	0.618	
7	4.99	9.98	-2.29E-01	8.68	0.442	
8	6.61	13.22	-4.27E-02	2.22	0.082	
9	8.4	16.8	1.74E-01	-5.29	-0.336	
10	10.37	20.74	4.00E-01	-13.13	-0.771	
11	12.35	24.7	2.96E-01	-9.53	-0.571	
12	14.35	28.7	2.56E-01	-8.15	-0.495	
13	16.35	32.7	2.26E-01	-7.10	-0.436	
14	18.35	36.7	2.04E-01	-6.35	-0.395	
15	20.35	40.7	1.68E-01	-5.08	-0.324	
16	22.35	44.7	1.46E-01	-4.34	-0.283	
17	24.35	48.7	1.43E-01	-4.24	-0.277	
18	26.35	52.7	1.65E-01	-4.98	-0.318	
19	28.35	56.7	1.71E-01	-5.19	-0.330	
20	30.35	60.7	1.80E-01	-5.51	-0.347	
21	32.35	64.7	1.68E-01	-5.08	-0.324	
22	34.35	68.7	1.71E-01	-5.19	-0.330	
23	36.35	72.7	1.68E-01	-5.08	-0.324	
24	38.35	76.7	1.56E-01	-4.66	-0.300	
25	40.35	80.7	1.62E-01	-4.87	-0.312	
26	42.35	84.7	1.65E-01	-4.98	-0.318	
27	44.35	88.7	1.53E-01	-4.55	-0.294	
28	46.35	92.7	1.56E-01	-4.66	-0.300	

Reynolds — Test

density	0.00238	slug/ft3	(Based on lab Pa, tunnel Ta)
length	4	ft	(Approx length of fairing)
temp	523.67	deg R	(Tunnel temp)
viscosity	3.77E-07	slug/ft-s	(Sutherland's Eqn)
velocity	122.92	ft/s	(Based on calibrated/corrected qbar)

3107225

Reynolds 5000 ft - 70 KTAS

density	0.002463	slug/ft3	(Standard density at 5kft)
length	8	ft	(Approx actual length of fairing)
temp	500.9	deg R	(Standard Ta at 5kft)
viscosity	3.64E-07	slug/ft-s	(Sutherland's Eqn)
velocity	118.23	ft/s	(Based on 70 KTAS)

6402720

B Section

56

C Section

A Mirror

C Mirror

x	y	Area	1	2	3	4	5	6	7	8	9	10	11	12	13	14	15	16	17	18
3.5	8	0.0087	-0.4690	-0.4116	-0.3464	-0.3464	-0.4618	-0.4075	-0.4748	-0.4531	-0.4871	-0.5900	-0.4797	-0.4646	-0.5224	-0.4222	-0.4203	-0.4098	-0.4293	-0.4419
2	8	0.0122	-0.4475	-0.4003	-0.3574	-0.3574	-0.4567	-0.4076	-0.4435	-0.4485	-0.4724	-0.5408	-0.4647	-0.4598	-0.5380	-0.4009	-0.4255	-0.4098	-0.4293	-0.4470
0	8	0.0152	-0.4475	-0.4149	-0.3513	-0.3513	-0.4567	-0.4127	-0.4695	-0.4578	-0.4674	-0.5558	-0.4647	-0.4153	-0.5380	-0.3955	-0.4150	-0.4045	-0.4293	-0.4470
-2	8	0.0122	-0.4705	-0.4259	-0.3584	-0.3584	-0.4515	-0.4178	-0.4447	-0.4578	-0.4773	-0.5654	-0.5047	-0.4993	-0.5380	-0.3955	-0.4255	-0.4150	-0.4293	-0.4573
-3.5	8	0.0087	-0.4475	-0.4149	-0.3464	-0.3464	-0.4669	-0.4127	-0.4539	-0.4578	-0.4822	-0.5703	-0.4697	-0.4301	-0.5559	-0.3955	-0.4255	-0.4045	-0.4403	-0.4419
3.5		0.0087	-0.3902	-0.3596	-0.3024	-0.3024	-0.3900	-0.3508	-0.4122	-0.3745	-0.4182	-0.5064	-0.4647	-0.4004	-0.3838	-0.3838	-0.3730	-0.3467	-0.3798	-0.3902
2		0.0152	-0.3844	-0.3485	-0.2914	-0.2914	-0.3951	-0.3456	-0.4017	-0.3691	-0.4232	-0.4916	-0.4247	-0.4103	-0.3581	-0.3581	-0.3678	-0.3520	-0.3578	-0.3751
0		0.0213	-0.3730	-0.3651	-0.3079	-0.3079	-0.4002	-0.3663	-0.3913	-0.3850	-0.4182	-0.5015	-0.4597	-0.4153	-0.3703	-0.3703	-0.3703	-0.3625	-0.3743	-0.3854
-2		0.0213	-0.3902	-0.3540	-0.3134	-0.3134	-0.3900	-0.3559	-0.3965	-0.3858	-0.4232	-0.4709	-0.4207	-0.4252	-0.3581	-0.3581	-0.3578	-0.3783	-0.3798	-0.3905
-3.5		0.0152	-0.3844	-0.3596	-0.3079	-0.3079	-0.3951	-0.3951	-0.3965	-0.3978	-0.4182	-0.4867	-0.4097	-0.4153	-0.3474	-0.3314	-0.3474	-0.3625	-0.3798	-0.3751
		0.0087	-0.3787	-0.3540	-0.2969	-0.2969	-0.4105	-0.3508	-0.4017	-0.3745	-0.4232	-0.4816	-0.4097	-0.4301	-0.3572	-0.3314	-0.3572	-0.3572	-0.3908	-0.3699
4.5	4.5	0.0104	-0.3766	-0.2519	-0.2749	-0.2602	-0.3078	-0.3078	-0.3394	-0.2806	-0.2966	-0.3379	-0.3532	-0.3362	-0.3729	-0.3306	-0.2774	-0.2071	-0.2738	-0.3168
3.5	4.5	0.0130	-0.3625	-0.2667	-0.2904	-0.2206	-0.2928	-0.3470	-0.3144	-0.3128	-0.3377	-0.3479	-0.3791	-0.3312	-0.3678	-0.3043	-0.2122	-0.2122	-0.2800	-0.3270
2	4.5	0.0213	-0.3707	-0.2407	-0.2309	-0.2398	-0.2874	-0.3419	-0.2894	-0.2714	-0.2688	-0.2783	-0.3460	-0.3460	-0.3320	-0.2964	-0.2446	-0.2172	-0.2553	-0.2913
0	4.5	0.0243	-0.3863	-0.2651	-0.2969	-0.2653	-0.2876	-0.3074	-0.3294	-0.3036	-0.3428	-0.3628	-0.3688	-0.3460	-0.3831	-0.2841	-0.2825	-0.2172	-0.2855	-0.3168
-2	4.5	0.0213	-0.3883	-0.2631	-0.3134	-0.2398	-0.3074	-0.3074	-0.3294	-0.3128	-0.3573	-0.3777	-0.3638	-0.2904	-0.3633	-0.2892	-0.2825	-0.2475	-0.3228	-0.3221
-3.5	4.5	0.0130	-0.3883	-0.2631	-0.3134	-0.2398	-0.3074	-0.3215	-0.3294	-0.3128	-0.3475	-0.3777	-0.3638	-0.3609	-0.3831	-0.2892	-0.2825	-0.2475	-0.3228	-0.3270
-4.5	4.5	0.0104	-0.4601	-0.2831	-0.2914	-0.2398	-0.3623	-0.3623	-0.3044	-0.3128	-0.3671	-0.3628	-0.3532	-0.3559	-0.3984	-0.2789	-0.2774	-0.2528	-0.3337	-0.3270
5.5	2.5	0.0156	-0.3530	-0.2351	-0.2740	-0.2398	-0.3419	-0.3417	-0.2894	-0.2944	-0.3428	-0.3578	-0.3584	-0.3114	-0.3371	-0.2996	-0.2825	-0.2576	-0.2845	-0.3015
4.5	2.5	0.0195	-0.3648	-0.2407	-0.2584	-0.2104	-0.3317	-0.3317	-0.2795	-0.2898	-0.3328	-0.3379	-0.3428	-0.2917	-0.3474	-0.2892	-0.2825	-0.2576	-0.2790	-0.3066
2	2.5	0.0273	-0.3648	-0.2239	-0.2584	-0.2206	-0.3266	-0.3266	-0.2944	-0.2944	-0.3328	-0.3379	-0.3428	-0.3016	-0.3218	-0.2996	-0.2825	-0.2728	-0.2845	-0.2964
0	2.5	0.0313	-0.3530	-0.2239	-0.2529	-0.2206	-0.3215	-0.3215	-0.2944	-0.2944	-0.3230	-0.3280	-0.3376	-0.2966	-0.3167	-0.2738	-0.2722	-0.2728	-0.2845	-0.2964
-2	2.5	0.0273	-0.3530	-0.2184	-0.2419	-0.2206	-0.3215	-0.3215	-0.3004	-0.2898	-0.3132	-0.3280	-0.3324	-0.3114	-0.3371	-0.2531	-0.2466	-0.2526	-0.2845	-0.2861
-3.5	2.5	0.0195	-0.3471	-0.2295	-0.2309	-0.2245	-0.3215	-0.3215	-0.3044	-0.2806	-0.3083	-0.3230	-0.3376	-0.2917	-0.3474	-0.2531	-0.2446	-0.2526	-0.2881	-0.2913
-5.5	2.5	0.0156	-0.3550		-0.2398	-0.1888	-0.3317	-0.2523	-0.3044	-0.2852	-0.3279	-0.3230	-0.3220	-0.3283	-0.3729	-0.2583	-0.2568	-0.2677	-0.2900	-0.2964
4.5	0	0.0174	-0.3471	-0.2239	-0.2199	-0.2347	-0.3215	-0.2573	-0.2795	-0.2760	-0.3328	-0.3330	-0.3376	-0.3362	-0.3218	-0.2996	-0.2722	-0.2476	-0.2651	-0.2861
3.5	0	0.0217	-0.3471	-0.2127	-0.2920	-0.2194	-0.3266	-0.2371	-0.2645	-0.2760	-0.3328	-0.3230	-0.3324	-0.3312	-0.3116	-0.2892	-0.2517	-0.2576	-0.2736	-0.2810
2	0	0.0347	-0.3589	-0.2351	-0.2529	-0.2347	-0.3215	-0.2573	-0.2795	-0.2898	-0.3428	-0.3280	-0.3272	-0.3411	-0.3269	-0.3044	-0.2625	-0.2677	-0.2738	-0.3066
0	0	0.0304	-0.3354	-0.2254	-0.2740	-0.2092	-0.3215	-0.3266	-0.2795	-0.3036	-0.3181	-0.3181	-0.3260	-0.3460	-0.3269	-0.2738	-0.2625	-0.2677	-0.2845	-0.2661
-2	0	0.0304	-0.3354	-0.2575	-0.2584	-0.2194	-0.3317	-0.3317	-0.2645	-0.2668	-0.3083	-0.3181	-0.3064	-0.3382	-0.2854	-0.2531	-0.2448	-0.2526	-0.2774	-0.2964
-3.5	0	0.0217	-0.3354	-0.2567	-0.2584	-0.1888	-0.3215	-0.3215	-0.2745	-0.2676	-0.3083	-0.3230	-0.2957	-0.2917	-0.2531	-0.2531	-0.2414	-0.2526	-0.2900	-0.2759
-5.5	0	0.0174	-0.3413		-0.2309	-0.2651	-0.3419	-0.2674	-0.3044	-0.2852	-0.3279	-0.3230	-0.2908	-0.3411	-0.3729	-0.2479	-0.2363	-0.2627	-0.2790	-0.2759
4.5	-2.5	0.0156	-0.3589	-0.2799	-0.3024	-0.2529	-0.3215	-0.3215	-0.2795	-0.3002	-0.3377	-0.3230	-0.3460	-0.3609	-0.3474	-0.3254	-0.2678	-0.2677	-0.2881	-0.2861
3.5	-2.5	0.0195	-0.3509	-0.2743	-0.2969	-0.2419	-0.3266	-0.3266	-0.2795	-0.2952	-0.3328	-0.3230	-0.3220	-0.3558	-0.3320	-0.2996	-0.2774	-0.2728	-0.2736	-0.2964
2	-2.5	0.0273	-0.3766	-0.3007	-0.3079	-0.2740	-0.3419	-0.3419	-0.3244	-0.2990	-0.3428	-0.3429	-0.3560	-0.3558	-0.3474	-0.3047	-0.2928	-0.2728	-0.2891	-0.3117
0	-2.5	0.0313	-0.3648	-0.3247	-0.3134	-0.2584	-0.3521	-0.3266	-0.3244	-0.3038	-0.3573	-0.3479	-0.3479	-0.3757	-0.3578	-0.3305	-0.3185	-0.3183	-0.3283	-0.3270
-2	-2.5	0.0273	-0.3589	-0.2867	-0.2969	-0.2347	-0.3189	-0.2876	-0.2994	-0.3128	-0.3573	-0.3479	-0.3324	-0.3757	-0.3474	-0.3183	-0.3185	-0.3183	-0.3392	-0.3372
-3.5	-2.5	0.0195	-0.3883	-0.3079	-0.2969	-0.2594	-0.3201	-0.3076	-0.2994	-0.3128	-0.3611	-0.3479	-0.3324	-0.3393	-0.3474	-0.3202	-0.3002	-0.3284	-0.3502	-0.3321
-5.5	-2.5	0.0156	-0.3942	-0.3023	-0.3189	-0.2602	-0.3464	-0.2674	-0.3144	-0.2898	-0.3769	-0.3578	-0.3272	-0.3344	-0.3933	-0.2996	-0.2979	-0.3233	-0.3558	-0.3219
4.5	-4.5	0.0087	-0.3114	-0.2890	-0.3250	-0.3291	-0.3359	-0.3302	-0.3077	-0.3859	-0.4209	-0.3928	-0.4051	-0.3491	-0.3572	-0.3461	-0.3220	-0.2848	-0.2324	-0.3340
3.5	-4.5	0.0152	-0.2966	-0.2837	-0.2947	-0.3193	-0.3306	-0.3211	-0.2961	-0.3957	-0.4052	-0.3777	-0.3895	-0.3442	-0.3940	-0.3839	-0.3532	-0.2897	-0.2425	-0.3597
2	-4.5	0.0213	-0.3021	-0.2900	-0.2906	-0.3193	-0.3306	-0.3262	-0.2404	-0.3609	-0.4082	-0.3528	-0.3272	-0.3528	-0.3940	-0.3407	-0.3117	-0.1712	-0.1970	-0.3288
0	-4.5	0.0243	-0.3009	-0.2843	-0.3250	-0.3421	-0.3254	-0.3161	-0.2865	-0.3859	-0.3964	-0.3677	-0.3791	-0.3442	-0.3940	-0.4002	-0.3480	-0.2843	-0.2627	-0.3597
-2	-4.5	0.0152	-0.3309	-0.2900	-0.3421	-0.3421	-0.3254	-0.3464	-0.2933	-0.3661	-0.3769	-0.3528	-0.3393	-0.3393	-0.4203	-0.3599	-0.3376	-0.2841	-0.2729	-0.3545
-3.5	-4.5	0.0122	-0.3378	-0.2990	-0.3479	-0.3479	-0.3464	-0.3464	-0.3126	-0.3957	-0.4013	-0.3578	-0.3791	-0.3569	-0.4203	-0.3516	-0.3272	-0.2841	-0.2779	-0.3442

Sea Level - 100 KTAS
q =   33.90   lb/ft^2
p-atm =   2116.8   lb/ft^2

WINDOW - INCREMENTAL PRESSURE INDUCED FORCES

APPENDIX C.   MATLAB GRAPHICS PROGRAMS

This section contains the MATLAB programs that transformed the Microsoft Excel spreadsheet data into the color pressure contour charts. These programs were written by Professor Howard to maximize the visualization of the collected data. A summary of these MATLAB programs follows:

1.   'conplot'.......plots fairing, window & color pressure contours
2.   'dots' ....plots fairing, window & port positions
3.   'fairing_plot' ....data file for fairing plot
4.   'window' .... data file for window plot
5.   'data824' ....data file of C_P's for 'conplot'

The data file (e.g. 'data824') changed periodically as data reduction matured. The '824' portion of the filename referred to the date 24 August 1999, the date of the latest reduced data. The MATLAB codes for the 'conplot' and 'dots' programs are presented in the following two pages.

MATLAB PROGRAM 'CONPLOT'

```
load data824.m -ASCII
a = data824;
x = a(:,1);
y = a(:,2);
for i = 1:18
z = a(:,i+2);
xlin = linspace(min(x),max(x),100);
ylin = linspace(min(y),max(y),100);
[X,Y] = meshgrid(xlin,ylin);
Z = griddata(x,y,z,X,Y,'cubic');
contour(X,Y,Z,15)
caxis([-0.6 0.1])
colorbar
%axis off
%
hold on
load fairing_plot.m -ASCII
b = fairing_plot;
x2 = b(:,1)/2;
y2 = b(:,2)/2;
plot(x2,y2,'k')
xlabel('Model Dimension, inches')
ylabel('Model Dimension, inches')
title('Pressure Coefficients')
load window.m -ASCII
a3 = window;
x3 = a3(:,1);
y3 = a3(:,2);
x3 = x3/2;
y3 = y3/2;
plot(x3,y3,'k')
%axis ([-15 15 -30 25])
%axis equal
axis ([-30 30 -30 30])
hold off
%
%axis off
figure
end
```

MATLAB PROGRAM 'DOTS'

```
load data824.m -ASCII
a = data824;
x = a(:,1);
y = a(:,2);
plot(x,y,'.')
axis ([-30 30 -30 30])
axis equal
%
hold on
load fairing_plot.m -ASCII
b = fairing_plot;
x2 = b(:,1)/2;
y2 = b(:,2)/2;
plot(x2,y2,'k')
xlabel('Model Dimension, inches')
ylabel('Model Dimension, inches')
title('Pressure Port Locations')
load window.m -ASCII
a3 = window;
x3 = a3(:,1);
y3 = a3(:,2);
x3 = x3/2;
y3 = y3/2;
plot(x3,y3,'k')
%%axis equal
hold off
```

LIST OF REFERENCES

1. Komerath, H.M., Ahuja, K.K., and Chambers, F.W., "Prediction and Measurement of Flows Over Cavities – A Survey," AIAA Paper 87-0166, January, 1987.

2. Nestor, Duane E., "Calibration of the Naval Postgraduate School 3.5' X 5.0' Academic Wind Tunnel," Master's Thesis, Naval Postgraduate School, Monterey, California, September 1990.

3. Baldocchi, Robert L., "Modification and Calibration of the Naval Postgraduate School Academic Wind Tunnel," Master's Thesis, Naval Postgraduate School, Monterey, California, December 1992.

4. Bertin, John J., and Smith, Michael L., *Aerodynamics for Engineers*, Third Edition, Prentice Hall, 1998.

5. Greco, Philip A., "Turbine Performance Mapping of the Space-Shuttle Main Engine High-Pressure Fuel Turbopump," Master's Thesis, Naval Postgraduate School, Monterey, California, September, 1995.

6. Pope, Alan, and Rae, William H. Jr., *Low-Speed Wind Tunnel Testing*, Second Edition, Wiley-Interscience, 1984.

INITIAL DISTRIBUTION LIST

No. of Copies

1. Defense Technical Information Center.................................. 2
    8725 John J. Kingman Rd., STE 0944
    Ft. Belvoir, VA 22060-6218

2. Dudley Knox Library 2
    Naval Postgraduate School
    411 Dyer Rd.
    Monterey, CA 93943-5101

3. Department Chairman, Code AA 1
    Department of Aeronautics and Astronautics
    Naval Postgraduate School
    699 Dyer Road, Rm. 137
    Monterey, CA 93943-5107

4. Dr. Richard M. Howard, Code AA/HO................................. 5
    Department of Aeronautics and Astronautics
    Naval Postgraduate School
    Monterey, CA 93943-5107

5. Dr. Garth V. Hobson, Code AA/HG 1
    Department of Aeronautics and Astronautics
    Naval Postgraduate School
    Monterey, CA 93943-5107